

# ESTIMATION OF ABSOLUTE GROUNDWATER TEMPERATURE FROM OXYGEN-18 FRACTIONATION

A thesis submitted to the  
*University of Petroleum and Energy Studies*

For the Award of  
***Doctor of Philosophy***  
in  
Geology

By

**Somenath Ganguly**

February, 2020

SUPERVISOR(S)

Dr. Uday Bhan  
Dr. Saurabh Mittal  
Dr. Santosh K. Rai



UNIVERSITY WITH A PURPOSE

Department of Petroleum Engineering and Earth Sciences  
School of Engineering  
University of Petroleum and Energy Studies.  
Dehradun – 248007. Uttarakhand. India.

ESTIMATION OF ABSOLUTE GROUNDWATER  
TEMPERATURE FROM  
OXYGEN-18 FRACTIONATION

A thesis submitted to the  
*University of Petroleum and Energy Studies*

For the Award of  
***Doctor of Philosophy***  
in  
Geology

*By*

Somenath Ganguly  
(SAP ID: 500041347)

February, 2020

SUPERVISOR(S)

**Dr. Uday Bhan**  
**(Internal supervisor)**

Associated Professor, Department of Petroleum Engineering and Earth Sciences,  
University of Petroleum & Energy Studies, Dehradun, India.

**Dr. Saurabh Mittal**  
**(Internal Co-supervisor)**

Associated Professor, Department of Petroleum Engineering and Earth Sciences,  
University of Petroleum & Energy Studies, Dehradun, India.

**Dr. Santosh K. Rai**  
**(External supervisor)**

Scientist-E, Petrology and Geochemistry Group.  
Wadia Institute of Himalayan Geology, Dehradun, India.



UNIVERSITY WITH A PURPOSE

Department of Petroleum Engineering and Earth Sciences  
School of Engineering  
University of Petroleum and Energy Studies,  
Dehradun – 248007. Uttarakhand. India.

*“Dedicated to my wife and late parents”*

**Declaration**

I declare that the thesis entitled “ESTIMATION OF ABSOLUTE GROUNDWATER TEMPERATURE FROM OXYGEN-18 FRACTIONATION” has been prepared by me under the guidance of Dr. Uday Bhan, Associate Professor of Department of Petroleum Engineering and Earth Sciences, University of Petroleum and Energy Studies, Dehradun, Uttarakhand-248007, India; Dr. Saurabh Mittal, Associate Professor of Department of Petroleum Engineering and Earth Sciences, University of Petroleum and Energy Studies, Dehradun, Uttarakhand-248007, India; and Dr. Santosh K. Rai, Scientist ‘E’, Wadia Institute of Himalayan Geology, Dehradun, Uttarakhand-248001, India. No parts of this thesis has formed the basis for the award of any degree or fellowship previously.

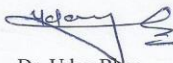
Date: 12 August, 2020

*Somenath Ganguly*  
(Somenath Ganguly)

Place: Dehradun

**THESIS COMPLETION CERTIFICATE**

I certify that Somenath Ganguly (SAP ID: 500041347) has prepared his thesis entitled “ESTIMATION OF ABSOLUTE GROUNDWATER TEMPERATURE FROM OXYGEN-18 FRACTIONATION” for the award of PhD degree of the University of Petroleum & Energy Studies, under my guidance. He has carried out the work at the Department of Petroleum Engineering and Earth Sciences, University of Petroleum & Energy Studies.



Dr. Uday Bhan  
**(Internal Guide)**  
Associate Professor.  
Department of Petroleum Engineering and Earth Sciences.  
School of Engineering, University of Petroleum and Energy Studies (UPES).  
Vill & P.O.-Bidholi, Via Prem Nagar.  
Dehradun.

Place: *Dehradun*

Date: *12 August 2020*

**THESIS COMPLETION CERTIFICATE**

I certify that Somenath Ganguly (SAP ID: 500041347) has prepared his thesis entitled “ESTIMATION OF ABSOLUTE GROUNDWATER TEMPERATURE FROM OXYGEN-18 FRACTIONATION” for the award of PhD degree of the University of Petroleum & Energy Studies, under my guidance. He has carried out the work at the Department of Petroleum Engineering and Earth Sciences, University of Petroleum & Energy Studies.



Dr. Saurabh Mittal  
**(Internal Co-Guide)**  
Associate Professor.  
Department of Petroleum Engineering and Earth Sciences.  
School of Engineering, University of Petroleum and Energy Studies (UPES).  
Vill & P.O-Bidholi, Via Premnagar.  
Dehradun.

Place: *Dehradun*

Date: *12 Aug' 2020*



## WADIA INSTITUTE OF HIMALAYAN GEOLOGY

(An Autonomous Institution of Dept. of Science & Technology, Govt. of India)

33, General Mahadev Singh Road,  
Dehradun (Uttarakhand) - 248001 (INDIA)

Dr. Santosh. K. Rai  
Scientist-E & Coordinator  
Petrology & Geochemistry Group

Phone : +91-0135-2525184  
Fax : +91-0135-2625212  
E-mail: rksant@wihg.res.in

### THESIS COMPLETION CERTIFICATE

I certify that Somenath Ganguly (SAP ID: 500041347) has prepared his thesis entitled "ESTIMATION OF ABSOLUTE GROUNDWATER TEMPERATURE FROM OXYGEN-18 FRACTIONATION" for the award of PhD degree of the University of Petroleum & Energy Studies, under my guidance. He has carried out the work at the Department of Petroleum Engineering and Earth Sciences, University of Petroleum & Energy Studies.

Dr. Santosh K. Rai  
(External Guide)  
Scientist 'E'  
Petrology and Geochemistry Group,  
Wadia Institute of Himalayan Geology,  
33 GMS Road, Dehradun.

Place: DEHRADUN.

Date: 12 Aug, 2020

## Abstract

Stable isotope Hydrology has remained a fascinating branch of science and has attracted many researchers in the field of Earth and Physical Science. It is long reported that the fractionation of different stable isotopes of same element is temperature dependent which is prominent in lighter isotopes. Therefore, this attribute of stable isotopes has long been used as paleo-thermometer to understand the temperature dependent physical processes on earth. These include the processes operating in the hydrosphere involving physical phase change of water-ice-vapor system. Such information is useful to understand the global precipitation pattern, water shed response and hydrograph separation and are elaborated in **Chapter-1**.

Use of the temperature dependent stable isotope fractionation are not only restricted to hydrological processes but are also used for understanding the crystallization of igneous rocks, behavior of hydrothermal systems, water-rock interaction and their kinetic equilibrium, and estimation of mother solution temperature for solution precipitation process etc. These stable isotope geo-thermometers have enabled scientists to estimate paleo-temperature on relative scale. Towards this, the fractionation of hydrogen or oxygen isotopes in water-ice-vapor system may be used to conclude if the past was warmer or cooler than present by calculating their  $\delta$  value (parts per mille ‰).

Apart from these, the other empirical chemical geothermometers are reported like silica ( $\text{SiO}_2$ ), Na/K or Na-K-Ca to understand the thermal equilibrium of the geothermal system, which is also described in **Chapter-2**. However, these chemical



geothermometers for hydrothermal systems and isotopic geothermometers for solution-precipitation reactions are restricted to estimate temperature greater than 100°C. Available lines of investigations show that there is no suitable geothermometer available, that works appropriately at low temperature regime below 100°C for liquid water system to estimate groundwater temperature in absolute scale. This work aims to address this issue by establishing a geothermometer based on temperature dependent  $^{18}\text{O}$  fractionation. It is useful to estimate absolute temperature of groundwater at shallow crustal level when there is no phase change of water involved.

This work attempts to develop a deterministic analytical model to estimate groundwater temperature with reference to 25°C benchmark temperature, when there exists no phase change but a temperature gradient. The geothermometer based on the fact that  $^{18}\text{O}$  fractionation does occur in liquid water system under prevailing temperature gradient with differential bond strengths of heavy and light isotopes. Therefore, the model utilizes the property that heavy isotope tends to concentrate at lower temperature region since it has more bond strength and less vibrational frequency than the light isotopes having affinity to concentrate at higher temperature regime.

**Chapter 3** describe the theoretical derivation of the model coupled with its physical validation supported by laboratory experiment. The proposed model to estimate groundwater temperature in this work is applicable to confined aquifer and it uses the absolute abundance of  $^{18}\text{O}$  (in ppm) rather than the conventional  $\delta$  value (parts

per mille ‰). The derivation starts from one-dimensional approximation of Fick's Law of diffusion, under the assumption that the fractionation of different isotopomers of water are regulated by as thermal diffusion process. It further assumes that the permeable aquifer is a homogenous medium of isotropic nature having similar hydraulic conductivity, structure and diffusive property in all the directions. Here the aquifer boundary is considered as impermeable as the boundary condition of the model. The model also uses the initiation of free unicellular laminar thermal convection due to incremental geothermal heat down dip to a confined aquifer characterized with critical Rayleigh Number ( $Ra_c$ ) less than but close to 40. This convection acts opposite to the direction of natural advection leading to a thermal convection up dip of the aquifer involving no phase change of water. The model compartmentalizes the dipping aquifer into infinitesimal small slices where water remains in isotopic equilibrium with respect to temperature in each slice. This eventually leads to laminar thermal convection up dip due to density gradient and results in  $^{18}\text{O}$  fractionation. It assumes that heavier isotope having more bond strength and less vibrational frequency will tend to concentrate more at low temperature regime than lighter isotope. This implies that  $^{18}\text{O}$  will concentrate at lower temperature end and as moving down  $^{18}\text{O}$  absolute abundance will decrease since exposure to more geothermal heat.

The model assumes that complete mixing of recharge water to aquifer water with homogeneous distribution of all isotopomers of water exists as initial condition. The model further assumes a steady state aquifer condition with negligible effect of pumping. Considering a long residence time of the water in the aquifer, which is

in thermal equilibrium with surrounding isotopomers of water will fractionate in terms of its thermal preference. While deriving the model, 25°C temperature of ocean water has been considered as benchmark temperature at the time of precipitation of Vienna Standard Pee Dee Belemnite (VSMOW) having absolute abundance of  $^{18}\text{O}$  of ocean water 2005.12 ppm. The  $^{18}\text{O}$  geothermometer proposed in this work, can estimate groundwater temperature relative to this benchmark temperature. It means that if the absolute abundance of  $^{18}\text{O}$  is more than 2005.12 ppm then the water temperature is less than 25°C and vice versa.

In addition to the theoretical modeling, an experimental approach was also adopted which involves the fractionation of  $^{18}\text{O}$  in liquid water system with no phase change in controlled laboratory condition. This was required to prove whether the model is applicable to the process that happens in nature. In order to simulate a confined aquifer system with impermeable boundary, a six-inch-long brass tube (Cu 70% and Zn 30%) of  $\approx$  one-inch diameter has been used which has the thermal conductivity of  $\approx$  111.0 W/m K. Throughout the experiment, the Milli-Q water (Resistivity 18.2M $\Omega$ -cm at 25°C and conductivity 0.055  $\mu\text{S}/\text{cm}$ ) was used. At the initial stage of the experiment, an attempt was made to fractionate  $^{18}\text{O}$  in the brass tube filled with natural porous media of well-sorted highly permeable medium to coarse sand of approximately  $\phi$  scale -1.0 to best replicate a confined aquifer. However, it could not yield significant  $^{18}\text{O}$  fractionation for a given temperature gradient of one-day thermal equilibration time, perhaps due to multiple variables which were not considered in the theoretical model.

Therefore, the experimental apparatus was simplified by filling the tube only with Milli-Q water while keeping the entire thermal conditions the same. This experiment yielded significant  $^{18}\text{O}$  fractionation as per theoretical expectation. The experiment was further conducted for the temperature range of  $10^{\circ}\text{C}$  to  $50^{\circ}\text{C}$  with equal interval of  $10^{\circ}\text{C}$ . For all the temperature gradients, “experimentally derived” and “model derived”  $^{18}\text{O}$  absolute abundances were compared and found consistent within the standard deviation of absolute abundance of  $^{18}\text{O}$  of Vienna Standard Pee Dee Belemnite (VPDB) which was  $\pm 2.1$  ppm which is described in **Chapter 4**. In cross plot “experimentally derived” and “model derived”  $^{18}\text{O}$  absolute abundance shows a very strong linearity.

For isotopic analysis of liquid water, a Laser Water Isotope Analyzer (PICARRO of model L1102-i) was used. It takes approximately  $1.9\ \mu\text{ml}$  of water sample in a single suction and evaporate it instantaneously to put it into the gas cell or cavity before its measurement. In the apparatus a symmetrically tuned laser of each 1 Hz cycle pass to generate absorption spectra in near IR spectral range for different isotopomers (e.g.  $^2\text{HO}$ ,  $\text{HDO}$ ) present in the water sample. Since the absorption line intensity is linearly dependent on concentration of different isotopomers of water therefore  $^{18}\text{O}/^{16}\text{O}$  ratio can be calculated accurately. Further the Laser Water Isotope Analyzer evaporates the whole water sample collected in a single suction, and it rejects any salt present in the water and reports  $^{18}\text{O}/^{16}\text{O}$  ratio exclusive to water sample. Therefore, salt effect on isotope fractionation need not to be considered in the deterministic model. In case of non-availability of Laser Water Isotope Analyzer still the model works fine for isotopic analysis with Isotope Ratio

Mass Spectrometer (IRMS), with the help of simple salt rejection technique of water sample before isotopic analysis as describe in **Chapter 2**.

Initial results of laboratory experiments for the  $^{18}\text{O}$  geothermometer was further testified by published field data of  $\delta^{18}\text{O}$  from Sacramento Valley, California, which is presented in **Chapter 4**. Reported data reveals that meteoric water and Holocene groundwater have similar  $\delta^{18}\text{O}$  composition probably due to the frequent meteoric recharge. However,  $\delta^{18}\text{O}$  values may be significantly different for the Pleistocene and Holocene groundwater. To validate the model for the study area it was assumed that Pleistocene groundwater in the formation are deep seated than Holocene groundwater since it is geologically older. Therefore, Pleistocene groundwater is likely to be warmer than Holocene groundwater responding to the geothermal gradient. Flood plain groundwater can be considered geologically as the youngest as well as the coldest. While calculating absolute abundance of  $^{18}\text{O}$  in ppm for waters of different geological age, it was observed a continuous warming trend of groundwater with increasing geological age with respect to  $25^\circ\text{C}$  taken as benchmark temperature. This satisfies the basic postulation that  $^{18}\text{O}$  does fractionate in natural confined aquifer and hence could be used to estimate groundwater temperature. For the reported data of  $\delta^{18}\text{O}$  of Sacramento Valley, California, the “experimentally derived” and “model derived”  $^{18}\text{O}$  abundance of groundwater of different geological age were in agreement with internationally accepted standard of  $^{18}\text{O}$  for VPDB, which is  $\pm 2.1$  ppm. Therefore, the deterministic analytical model proposed in this work describes the physical principle of  $^{18}\text{O}$  isotope fractionation process of liquid water system under imposed

temperature gradient. This  $^{18}\text{O}$  fractionation is attributed to free unicellular laminar thermal subsurface fluid convection along with thermal stratification of different isotopomers of water molecule by thermal diffusion process.

The **Chapter 5** elaborates isotopic fractionation and stratification in liquid water system is not due to the gravitational attraction but heat driven. However, for stable isotopic fractionation of gas in polar region along with temperature; gravity has also been considered as one of the important governing factor for the process. If we consider the scenario in liquid water system, inter molecular attraction is much more prominent in liquid than for gas. Further, the thermal equilibration time in the experimental setting, for each set of temperature gradient, was approximately six hours. In this very small span of time, the effect of gravity to govern the  $^{18}\text{O}$  fractionation and stratification is almost negligible. Since temperature was the only variable in the experimental design and for each temperature gradient  $^{18}\text{O}$  fractionated, therefor experimental approach adopted in this work complements the claim of isotopic stratification in liquid water system with imposed temperature gradient. Therefore, it was found appropriate to neglect any gravity effect in proposed deterministic model to estimate groundwater temperature. This finds further support from the fact that no isotopic stratification of water molecule ( $\text{H}_2^{18}\text{O}$ ,  $\text{H}_2^{16}\text{O}$ ) reported for the Philippine Trench and Lake Baikal.

**Chapter 5** covers the concluding remarks regarding the isotopic stratification of oxygen and hydrogen in aquifers that are widely reported in scientific literature. It is also reported that isotopic signature of groundwater replenished by recent

meteoric water recharge is distinct from that of paleo water of the aquifer. This work identifies the phenomena as an effect of geothermal gradient. For every storm event and associated recharge, gravity driven advection replenishes the aquifer storage. Initially the mixing of recharge water with aquifer water leads to homogenization of all isotopomers of water. While percolating through the porous media, the water is expected to expose to more geothermal heat as moving down. This will onset a temperature dependent density driven thermal convection, resulting a mass transfer process opposite to advection. Considering the long residence time of groundwater in aquifer and thermal equilibration with the surroundings, it is likely that heavy isotopomers of water concentrates at lower temperature region where as the geologically older and warmer water tends to deplete in heavier isotopomers, which will eventually fractionate  $^{18}\text{O}$ . It gets support with the fact that the vibrational frequency of  $^{16}\text{O}-^{18}\text{O}$  is  $1535.57\text{ cm}^{-1}$  which is less than the vibrational frequency of  $^{16}\text{O}-^{16}\text{O}$  that is  $1580.19\text{ cm}^{-1}$ . Therefore, with increasing depth  $^{18}\text{O}$  absolute abundance decreases with increasing groundwater temperature. Therefore, this temperature driven natural fractionation of  $^{18}\text{O}$  provide hope to be used as a geothermometer to estimate groundwater temperature.

The theoretical model proposed in this work successfully demonstrate that  $^{18}\text{O}$  does fractionate in groundwater with imposed geothermal gradient. Therefore, proposition of estimating groundwater temperature with respect to  $25^{\circ}\text{C}$  as a benchmark temperature from its  $^{18}\text{O}$  isotopic signature is realizable.

With the present state of this work, we can only estimate groundwater temperature relative to the benchmark temperature of 25°C with corresponding  $^{18}\text{O}$  absolute abundance of 2005.12 ppm. It restricts to construct a universal linear functional model to estimate any groundwater temperature using its isotopic signature when there is no phase change of water involved. To construct such model, water having initial isotopic concentration of  $^{18}\text{O}$  2005.12 ppm is required which is a characteristic of deep ocean water and difficult to acquire due to logistical constrain. If that water is acquired and exposed to thermal conditions as described in **Chapter 3** for temperature dependent  $^{18}\text{O}$  fractionation then the best-fit linear model to the data, will be able to estimate any groundwater temperature ranging from more than 0°C to less than 100°C which provides the future scope of this research work.

A scientific research secures further appreciation if it is oriented and applicable to resolve real time problems of the society. Energy is the inevitable part of our social life and global economy where the fossil fuel is quite indispensable. However, the modern scientific researchers are focused on Uranium based production of atomic energy. The earth's internal heat particularly at shallow crustal level is the product of heat generated by radioactive decay of radioisotopes like U, Th and  $^{40}\text{K}$ . Therefore, one can predict high concentration of radioactive elements if there is an aberrant behavior of water temperature particularly abnormally high. This work may be an indication of radioactive mineral exploration. In addition, this work may be useful in detecting naturally occurring deuterium ( $^2\text{H}/\text{D}$ ) which is used in atomic



nuclear fusion reactors in atomic power generating station, since it will tend to concentrate at lower temperature.

This work finds applications in petroleum exploration and production, where information on formation fluid temperature is an important factor particularly for determining the maturity of kerogen, making decision on well completion and predicting reservoir dynamics at production stage. At the time of drilling, temperature logging is a very common practice in oil industry. However, there are significant chances of error, particularly estimating temperature of pristine formation fluid due to interference of drilling fluid with formation water. In the field of hydrocarbon industry, this work may be applied for determining formation fluid temperature and construction of geothermal gradient of the sedimentary basin. This is also helpful to determine the hydrocarbon reservoir behavior at the production stage as well as for further hydrocarbon exploration in the basin.

The freeware **Isotemp**, which is a spreadsheet software, associated with this publication does all the calculation as described in **Appendices, A1**.

## **Acknowledgments**

In the process of doing my PhD at University of Petroleum and Energy Studies at Dehradun, India, I want to acknowledge Dr. Santosh Kumar Rai from Wadia Institute of Himalayan Geology, Dehradun, India who is my external supervisor of the research. Dr. Rai taught all the basics of Isotope Ratio Mass Spectrometry in his stable isotope laboratory and helped me throughout the experimental work of my research. My internal supervisors from University of Petroleum and Energy Studies, Dehradun, India Dr. Uday Bhan and Dr. Saurabh Mittal supported me throughout by reading my manuscript and give their valuable feedbacks to improve the quality of my research. I also want to pay my warmest gratitude to Dr. Akshaya Verma and Dr. Rajeev S. Ahluwalia and Mr. Abhimanu Yadav of Wadia Institute of Himalayan Geology, Dehradun, India for supporting me throughout the analytical session. Further, I want to acknowledge Dr. S. J. Chopra, Hon'ble Chancellor of University of Petroleum and Energy Studies, Dehradun, Uttarakhand, India; for a constant source of inspiration to conduct and accomplish this research. I got immense support from my wife Ms. Sanghamitra Ganguly not only supported me morally and logistically, sacrificed her own enjoyment to be with me in this journey. My sister Ms. Barsha Ganguly has always motivated me to complete this work. Last but not the least, I want to pay my gratitude to the Director; Wadia Institute of Himalayan Geology, Dehradun, India for the laboratory facilities to support the experimental work for my thesis. On behalf of our research team, I want to acknowledge J. S. Enterprises and Mr. Tejinder Singh for designing and fabricating the experimental setup for us.

## Table of Contents

Abstract.....	i
Acknowledgements.....	xi
List of symbols.....	xiv
List of abbreviations.....	xvi
List of figures.....	xvii
List of tables.....	xix
List of equations.....	xxi
List of plates.....	xxiii
<b>1. Introduction .....</b>	<b>2</b>
1.1. Water and Hydrologic cycle .....	3
1.2. Isotope Hydrology .....	7
1.3. Isotopomers of water in groundwater reservoir .....	13
<b>2. Background of the present work.....</b>	<b>18</b>
2.1. Internal heat of Earth and geothermal gradient.....	19
2.2. Geothermometers.....	22
2.2.1. Basic principle of stable isotope fractionation .....	23
2.2.2. Isotope Geothermometers .....	25
2.2.3. Geothermal system and chemical geothermometers.....	26
2.3. Heat transport and groundwater flow.....	29
2.4. Groundwater chemistry and its isotopic response.....	33
2.4.1. Dissolved salt effect on isotope fractionation .....	33
2.4.2. Isotope fractionation of water with free convection .....	39
2.5. Scope and significance of present work.....	41
<b>3. The oxygen-18 geothermometer .....</b>	<b>44</b>
3.1. The modeling background .....	45
3.2. The analytical deterministic model.....	46
3.2.1. Conceptual model .....	46
3.2.2. Assumptions and boundary conditions .....	49
3.2.3. Analytical model.....	50
3.3. Laboratory experimental work.....	57

3.3.1.	Experimental set up and design .....	57
3.3.2.	Instrumentation for the isotope analyses.....	63
<b>3.4.</b>	<b>Limitations of the model .....</b>	<b>64</b>
<b>4.</b>	<b>Outcome of the work .....</b>	<b>70</b>
4.1.	Statistical analysis of the data .....	71
4.2.	Validation of the model .....	79
4.3.	Primary findings.....	84
<b>5.</b>	<b>Discussion .....</b>	<b>87</b>
5.1.	Conclusions.....	97
5.2.	Future scope of work .....	99
	<b>References .....</b>	<b>102</b>
	<b>Appendices.....</b>	<b>119</b>
A.1	Manual of Isotemp Freeware .....	119
A.2	Publication details .....	121

## List of symbols

$\Delta H_f^0$  : Standard enthalpy of formation

$S^0$  : Standard entropy

$\Delta G_f^0$  : Standard free energy of formation

$R$  : Isotope ratio/Isotopic ratio

$\delta$  : dell

$P_{sat}$  : Saturation vapor pressure

$P_{sat}^0$  : Saturation vapor pressure at due point temperature

$f$  : Rayleigh fractionation factor

$\text{‰}$  : Per mill

$Q$  : Upward heat flux

$k$  : Thermal conductivity

$Q_r$  : Radioactive heat

$\alpha$  : Equilibrium isotopic fractionation factor

$R$  : Gas constant

$T$  : Temperature

$\nabla$  : Gradient

$\epsilon$  : Proportionality constant of Fourier's law

$D$  : Diffusion constant

$F$  : Material flux

$\nabla^2$  : Laplacian operator

$K$  : Permeability of medium

$g$  : Acceleration due to gravity

$\sigma$  : Volumetric thermal expansion coefficient of the fluid

$(\rho C)_t$  : Volumetric heat capacity of fluid

$\gamma$  : Kinematic viscosity of the fluid

$\lambda^*$  : Effective thermal conductivity of the fluid filled medium

$Y$  : Activity coefficient ratio

$k$  : Hydraulic conductivity

$^{\circ}\text{C}$  : Degree centigrade

$^{\circ}\text{K}$  : Degree kelvin

## List of abbreviations

ITCZ: Intertropical convergence zone

D : Deuterium

cP : Continental polar

cT : Continental tropical

mP : Maritime polar

mT : Maritime tropical

MWL: Meteoric Water Line

LMWL: Local Meteoric Water Line

GMWL: Global Meteoric Water Line

D-excess: Deuterium excess

exp: Exponential

ppm: Parts per million

TDS: Total dissolved solid

VSMOW: Vienna Standard Mean Ocean Water

VPDB: Vienna Standard Pee Dee Belemnite

IRMS: Isotope ratio mass spectrometer/spectrometry

A.S.T.M.: American Society for Testing Materials

K.E. : Kinetic Energy

$Ra_c$  : Critical Rayleigh number

SD : Standard deviation

## List of figures

**Figure 1:** Strong linear relationship of  $\delta^{18}\text{O}$  and  $\delta^2\text{H}$  for a Rayleigh Model assuming pseudo adiabatic cooling model following water saturation at 15°C...12

**Figure 2:** Increment of temperature ( $A < B < C$ ) in an inclined confined aquifer due to normal geothermal gradient. Aquifer boundary is assumed as impermeable. Vertical arrows corresponding to the points A, B, C are indicating increasing depth down dip with reference to horizontal ground surface. Groundwater flow due to convection is marked by red arrow. Regional groundwater flow is marked by green arrow. (Schematic diagram, not according to scale).....31

**Figure 3:** Salt rejection technique for sample preparation for oil field brine temperature estimation.....39

**Figure 4:** Change in  $\alpha$  for  $^{18}\text{O}$  and D with respect to temperature for water vapor-liquid water system. (International Atomic Energy Agency, Vienna, 1981, Technical Reports Series No 210). .....40

**Figure 5:** Temperature induced density gradient in a natural porous media. (Schematic diagram, not according to scale) .....47

**Figure 6:** Increasing temperature in “X” direction (Schematic diagram, not according to scale). .....52

**Figure 7:** Fractionation of  $^{18}\text{O}$  in absolute abundance for the temperature range of 10°C to 20°C. Blue color dots are individual  $^{18}\text{O}$  measured data and orange color dots are mean of each small population. Maximum  $^{18}\text{O}$  fractionation corresponding to mean is 0.168 ppm. ....77



**Figure 8:** Fractionation of  $^{18}\text{O}$  in absolute abundance for the temperature range of 10°C to 30°C. Blue color dots are individual  $^{18}\text{O}$  measured data and orange color dots are mean of each small population. Maximum  $^{18}\text{O}$  fractionation corresponding to mean is 0.748 ppm. ....77

**Figure 9:** Fractionation of  $^{18}\text{O}$  in absolute abundance for the temperature range of 10°C to 40°C. Blue color dots are individual  $^{18}\text{O}$  measured data and orange color dots are mean of each small population. Maximum  $^{18}\text{O}$  fractionation corresponding to mean is 0.205 ppm. ....78

**Figure 10:** Fractionation of  $^{18}\text{O}$  in absolute abundance for the temperature range of 10°C to 50°C. Blue color dots are individual  $^{18}\text{O}$  measured data and orange color dots are mean of each small population. Maximum  $^{18}\text{O}$  fractionation corresponding to mean is 0.638 ppm. ....78

**Figure 11:** Cross correlation of mean of actual (experimentally derived) and predicted (model derived)  $^{18}\text{O}$  absolute abundance for each small sample population. ....79

**Figure 12:** Comparative study of  $^{18}\text{O}$  absolute abundance with respect to the “reference water”. ....84

**Figure 13:** Isotopic stratification in confined aquifer system with incremental geothermal heat down dip, which can be further used to estimate ground water temperature. (Schematic diagram, not according to scale). ....92

**Figure 14:** Estimation of groundwater temperature from  $^{18}\text{O}$  isotopic signature with reference to 25°C benchmark temperature. (Schematic diagram; not according to scale) .....101

## List of tables

<b>Table 1:</b> Selected physical properties of water. Values are at 293K.....	4
<b>Table 2:</b> Natural abundance of oxygen and hydrogen isotopes.. .....	5
<b>Table 3:</b> Origin and characteristics of major air mass types defining the for global precipitation pattern in the Northern Hemisphere. ....	7
<b>Table 4:</b> Thermodynamic data for different isotopomers of water. ....	8
<b>Table 5:</b> Relative volume and $\delta^{18}\text{O}$ and $\delta^2\text{H}$ characteristics values of the different reservoirs of Hydrosphere.....	9
<b>Table 6:</b> Rayleigh Condensation Models for Water-Water Vapor.....	11
<b>Table 7:</b> Average amount of radioactive element present in granitic rock along with its contribution to Earth's internal heat.....	21
<b>Table 8:</b> Thermal conductivity of common aquifer materials.....	22
<b>Table 9:</b> Experimentally derived $\delta^{18}\text{O}$ values and absolute abundance of $^{18}\text{O}$ with their corresponding mean and standard deviation of each small sample population corresponding to a particular temperature. ....	72
<b>Table 10:</b> Detail calculation of model derived absolute abundance of $^{18}\text{O}$ .....	74
<b>Table 11:</b> Model derived $^{18}\text{O}$ absolute abundance with their mean and standard deviation of each small sample population corresponding to a particular temperature. ....	75
<b>Table 12:</b> Groundwater and surface water $\delta^{18}\text{O}$ data of Sacramento Valley, California. Age of water calculated from $^{14}\text{C}$ dating of dissolve inorganic carbon.....	81

**Table 13:** Experimentally derived  $^{18}\text{O}$  absolute abundance of  $\delta^{18}\text{O}$  data of Sacramento Valley, California.....82

**Table 14:** Theoretically derived  $^{18}\text{O}$  absolute abundance in ppm. Values of column “K” is from fourth column of Table 13. ....83

## List of equations

<b>Equation 1:</b> Rayleigh fractionation model for constant fractionation factor ( $\alpha$ ). .10	10
<b>Equation 2:</b> Meteoric water line .....	13
<b>Equation 3:</b> Governing equation of mantle heat flux to lithosphere.....	20
<b>Equation 4:</b> Amount of radiogenic heat production due to distribution of radioactive minerals in crustal material. ....	21
<b>Equation 5:</b> Fractionation factor ( $\alpha$ ) for equilibrium isotopic fractionation.....	24
<b>Equation 6:</b> Equation governing nonequilibrium isotopic fractionation. ....	24
<b>Equation 7:</b> Relation between isotope fractionation factor ( $\alpha$ ) and temperature in °K. ....	25
<b>Equation 8:</b> Silica geothermometer. ....	28
<b>Equation 9:</b> Na/K geothermometer. ....	29
<b>Equation 10:</b> Na-K-Ca geothermometer.....	29
<b>Equation 11:</b> Force balance equation of a fluid in a gravitational field. ....	30
<b>Equation 12:</b> Equation of Rayleigh Number. ....	31
<b>Equation 13:</b> Chemical reaction governing rainwater carbonate interaction. ....	35
<b>Equation 14:</b> Equation governing silica dissolution.....	36
<b>Equation 15:</b> Quantitative expression governing salt effect on activity coefficient.. ....	37
<b>Equation 16:</b> Fourier's Law of thermal conduction.....	45
<b>Equation 17:</b> Fick's Law of diffusion.....	50
<b>Equation 18:</b> One-dimensional approximation of Fick's Law of diffusion.....	51

<b>Equation 19:</b> Initial expression of temperature with isotope concentration. ....	53
<b>Equation 20:</b> Temperature and isotope concentration as VSMOW standard. ....	53
<b>Equation 21:</b> Linear relationship of VSMOW and VPDB. ....	54
<b>Equation 22:</b> Temperature and isotope concentration as VPDB standard. ....	55
<b>Equation 23:</b> Calculation of $^{18}\text{O}$ absolute abundance in ppm from reported $\delta$ value by analysis. ....	56
<b>Equation 24:</b> Relation of permeability and hydraulic conductivity. ....	61

## List of plates

<b>Plate 1</b> : Experimental apparatus kept at an angle of 14° dip.....	66
<b>Plate 2</b> : Experimental brass tube alternately wrapped with aluminum foil and glued plastic tape to minimize radiation heat loss. ....	66
<b>Plate 3</b> : Free circulating water bath adjacent to experimental tube to maintain desired adjacent temperature with the PVC casing.....	67
<b>Plate 4</b> : Experimental apparatus covered by PVC casing to make it thermally isolated from ambient geared with RTD sensors to measure temperature of different components of the apparatus. ....	67
<b>Plate 5</b> : Experimental apparatus in fully functional mode. ....	68

# **Chapter 1**

## **Introduction**

## **1. Introduction**

Isotopic tools are quite useful in scientific studies pertaining to the understanding of different physical processes operating on Earth and Planetary Sciences (Sharp, 2007). These include both stable as well as radiogenic isotopes. Radiogenic isotopes are generally used for radiometric dating of rocks, which gives a comprehensive understanding of absolute time, covering the Geological events and marking its finer subdivisions. Stable isotopes have huge implication in tracing the different physical processes operating on Earth which are temperature dependent. Therefore, stable isotopes may be used as “Geothermometer” to understand thermal history of rocks (Urey et al., 1951; Craig, 1966).

In Earth Science, stable isotope fractionation has been used for in-depth understanding of process of crystallization of igneous rocks and its geochemistry (Friedman et al., 1977; Chiba et al., 1989), understanding of water-rock interaction (Taylor 1977) and hydrothermal system and hydrologic cycle (Craig, 1966; Gregory et al., 1981, 1989; Criss et al., 1983, 1986; Criss et al., 1985).

The water-ice-vapor system best manifests the temperature dependent stable isotope fractionation pattern in the hydrosphere through its oxygen and hydrogen isotope components. Oxygen and hydrogen ratios act as conservative tracer in the hydrologic cycle and are intrinsic to water molecule. These explicate the origin of the water as well as its phase transition and transportation of water (Shiklomanov et al., 1983). Stable isotopes have been used to estimate the aquifer recharge and seasonality effect on the recharge (Darling et al., 1988) and separating the base



flow/surface flow through hydrograph separation (Criss, 1997; Maurya et al., 2011). It has also been used to understand the process of global precipitation pattern (Craig, 1961 (a); Craig, 1961(b)).

Use of isotope based temperature estimation of groundwater origin and flow in the aquifer is gaining momentum in research field. Variation of  $\delta^{18}\text{O}$  and  $\delta\text{D}$  ( $\delta^2\text{H}$ ) has geographic influence, covering variation in temperature, altitude, latitude and longitude effect in terms of precipitation pattern. Therefore, isotopic signature of groundwater can provide rich information regarding its recharge sources and subsurface flow paths. Despite all the complexities, there exist a strong linear variation of  $\delta^{18}\text{O}$  and  $\delta^2\text{H}$  in global precipitation, which is defined by an empirical relation and called the Global Meteoric Water Line or MWL (Craig; 1961, (a)). It can distinguish water of meteoric origin from any other sources. Therefore, a systematic mapping of isotope variation in groundwater can establish the evolution and dynamics of groundwater flow pattern of an aquifer.

Isotopes are important to understand the processes involved in the natural Hydrologic cycle which is described as follows. This research mainly focuses on stable isotope fractionation in groundwater system. Therefore, the discussion is only restricted to stable isotopic fractionation of oxygen and hydrogen in hydrologic cycle mainly focusing to groundwater.

### **1.1. Water and Hydrologic cycle**

Isotope are the atoms of same element having different mass number but same electronic configuration. As the electronic configuration determines the chemical

property of an element, different isotopes of same element are only distinguishable in terms of its physical properties. Chemical formula of water is H<sub>2</sub>O and it consists of two hydrogen atoms bonded covalently with a single atom of oxygen. The covalent bond forming electrons are not equally shared between the hydrogen and oxygen atoms owing to their differential electron affinities and therefore, the electrons in the O–H bond are more attracted to oxygen. Because electrons have a negative charge, the unequal sharing in the O–H bond results in the Oxygen atom acquiring a partial negative charge and the Hydrogen a partial positive charge, which makes H<sub>2</sub>O a polar molecule. The H–O–H bond angle in water is 104.5°. Salient physical properties of water are given in **Table 1** (Sharp, 2001).

**Table 1:** Selected physical properties of water. Values are at 293K. (Sharp, 2001).

Values at 293 K unless indicated.  
a: In the gas phase

Formula	Molecular weight (g mol <sup>-1</sup> )	Density (kg L <sup>-1</sup> )	Boiling point (K)	Molecular volume (nm <sup>3</sup> )	Volume of fusion (nm <sup>3</sup> )	Specific heat (JK <sup>-1</sup> g <sup>-1</sup> )	Heat of vaporization (kJ g <sup>-1</sup> )	Surface tension mN	Viscosity (μPa s)	Dielectric constant	Dipole moment (Cm × 10 <sup>30</sup> ) a
H <sub>2</sub> O	18	0.998	373	0.0299	0.0027	4.18	2.3	72.8	1002	78.6	6.01

For water molecule, it has oxygen and hydrogen as its atomic constituents. **Table 2** gives a comprehensive description of oxygen and hydrogen isotopes in terms of their natural abundances (Dingman, 2002; p 541).

**Table 2:** Natural abundance of oxygen and hydrogen isotopes. (Dingman, 2002).

Isotope	Natural abundance (%)	Natural abundance (ppm)	Stability
<sup>1</sup> H	99.985	999850	Stable
<sup>2</sup> H	0.015	150	Stable
<sup>3</sup> H	Trace	-	Radioactive
<sup>16</sup> O	99.76	997600	Stable
<sup>17</sup> O	0.04	400	Stable
<sup>18</sup> O	0.20	2000	Stable

Water is essential for life and covers about 70% of Earth's surface. It is the only substance that exists naturally on Earth in all three physical states of matter that is gas, liquid, and solid. It is always on the move to exchange among them which defines the Hydrologic Cycle (Shiklomanov et al., 1983). In hydrologic cycle water evaporates from open water body like open ocean or directly from ice which is known as the sublimation. The vapor condenses due to the adiabatic cooling as it rises upward. For dry air with no condensation, dry adiabatic lapse rate is 1°C/100 meter. During condensation moist adiabatic lapse rate is approximately 0.5°C/100 meter and it is dependent on initial temperature and initial vapor pressure. However, average lapse rate of troposphere is about 0.65°C/meter, which is the weighted average of dry and moist lapse rate (Dingman, 2002; p 590).

The process of precipitation brings a part of water stored at atmosphere to land or at open ocean either in the form of water droplets or snow which constitutes a part of the hydrologic cycle. In the global scenario of evaporation and precipitation, different regions are characterized by the different origin of large moist air parcel with relatively higher average precipitation for a particular time of year. This is

generally known as the “rainy season” or the “monsoon”. Along the equatorial region belt, particularly for the Asia, high precipitation occurs due to topography and migration of Intertropical Convergence Zone (ITCZ) which brings monsoon, the “rainy season” generally from July to October in parts of India. **Table 3** summarizes the origin and characteristics of major air mass types defining the global precipitation pattern in the Northern Hemisphere (Barry et al., 1982).

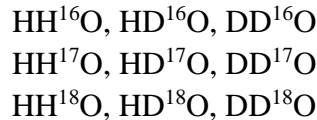
Components of the hydrologic cycle like evaporation, condensation and precipitation etc. which involves continuous phase change of water-vapor then liquid in case of rain and water-snow fall followed by melting of ripe snow and it is temperature dependent. Therefore, temperature dependent fractionation of oxygen and hydrogen can be applied to track these phase transitions for example constructing local meteoric water line, fractionation of isotope in glacial melt water and ice.

**Table 3:** Origin and characteristics of major air mass types defining the for global precipitation pattern in the Northern Hemisphere. (Dingman, 2002; p 96).

Air Mass	Characteristics	Source Regions	
		Winter	Summer
Continental polar (cP)	Cold, dry	Arctic Ocean	Northern Canada
		Canada-northern USA	Northern Asia
		Eurasia	
Continental tropical (cT)	Warm, dry	California-Arizona-Mexico	Nevada-Arizona-northern Mexico
		Northern Africa-Arabia	Northern Africa-Mediterranean
		Northern India	Arabia-central Asia
Maritime polar (mP)	Cold, moist	Northern Atlantic Ocean	Northern Atlantic Ocean
			Arctic Ocean
Maritime tropical (mT)	Warm, moist	Northern Pacific Ocean	Northernmost Pacific Ocean
		Central Atlantic Ocean	Central Atlantic Ocean
		Central Pacific Ocean	Central Pacific Ocean
		Arabian Sea-Bay of Bengal	

## 1.2. Isotope Hydrology

Chemical composition of water (H<sub>2</sub>O) suggests that the two hydrogen atoms bonded with one oxygen atom could be arranged in different configurations. Depending on different combinations of different isotopes of oxygen and hydrogen, water may have the following nine chemical configurations (Criss 1999, p 17)



These different combinations of oxygen and hydrogen isotopes in water are called the “isotopomers” or “isotopologue” of water molecule. For different isotopomers

of water, thermodynamic properties are also different which are presented in **Table 4**.

**Table 4:** Thermodynamic data for different isotopomers of water. (Lide, 1991)

Substance	$\Delta H_f^0$ (kcal/mol)	$S^0$ (cal/mol-deg)	$\Delta G_f^0$ (kcal/mol)
H <sub>2</sub> O (gas)	-57.796	45.104	-54.634
H <sub>2</sub> O (liquid)	-68.315	16.71	-56.687
HDO (gas)	-58.628	47.658	-55.719
HDO (liquid)	-69.285	18.95	-57.817
D <sub>2</sub> O (gas)	-59.56	47.378	-56.059
D <sub>2</sub> O (liquid)	-70.411	18.15	-58.195

Water contains isotopes of oxygen and hydrogen with different combinations and therefore it fractionates depending on temperature at the time of its phase transition. One of the most fundamental characteristics that isotope fractionation of water is only dependent on temperature and has nothing to do with other variables of energy like the etc. The fractionation process does not involve any breaking of O-H bond or any chemical reaction but only the exchange of isotopes among them.

As discussed earlier each change of phase of water in the global hydrologic cycle has its own characteristic isotopic signature and are given in **Table 5**. It shows that the isotope concentration in each reservoir is uniform and deviation is quite conservative. Therefore, it forms the basis that the water of different origin can be distinguished using their isotopic signature.

**Table 5:** Relative volume and  $\delta^{18}\text{O}$  and  $\delta^2\text{H}$  characteristics values of the different reservoirs of Hydrosphere. (Criss, 1999; p 90)

Reservoir	Volume (%)	$\delta^2\text{H}$ (‰)	$\delta^{18}\text{O}$ (‰)
Ocean	97.2	$0 \pm 5$	$0 \pm 1$
Ice caps & glaciers	2.15	$-230 \pm 120$	$-30 \pm 15$
<i>Groundwater</i>	<i>0.62</i>		
Vadose water		$-40 \pm 70$	$-5 \pm 15$
Dilute groundwater		$-50 \pm 60$	$-8 \pm 7$
Brines		$-75 \pm 50$	$0 \pm 4$
Surface waters	0.017		
Fresh water lakes		$-50 \pm 60$	$-8 \pm 7$
Saline lakes & inland seas		$-40 \pm 60$	$-2 \pm 5$
River & stream channels		$-50 \pm 60$	$-8 \pm 7$
Atmospheric water	0.001	$-150 \pm 80$	$-20 \pm 10$

The main focus of this work lies with the dilute groundwater, which accounts for 0.62% of the volume of total Hydrosphere. This small amount of water stored in the soil and rocks is one of the major fresh water source for human being and other living organisms on earth. However, rivers, lakes and springs are also sources of fresh water. With increasing pressure of human population, there is a huge stress on this fresh water reserve which is gradually depleting. However, under favorable conditions nature replenishes it constantly by rain, which is known as recharge of aquifers. Therefore, for a better understanding of dynamics of groundwater flow, oxygen and hydrogen isotopes may be used as tracers. Towards this, first we need to have the understanding of stable isotope fractionation process involved in precipitation. Therefore, the origin of meteoric water can be understood as follows.

A warm moist air front originated at ocean ward side as a result of precipitation and gradually moves towards continental side. Then it rises up and cools adiabatically before its precipitation. As the moisture parcel moves towards the continent its moisture content is used up due to process of continuous precipitation and the intensity of further rainfall gradually decrease from ocean to continental side. This is also called the rainout process.

As a result of the rainout process, the  $\delta^{18}\text{O}$  and  $\delta^2\text{H}$  of the moisture parcel change which cause the heavier isotope to concentrate at lower temperature regime. Since water vapor has more heat content in terms of latent heat of 540 calorie/gram, therefore resulting water droplets formed due to process of condensation will be enriched in  $^{18}\text{O}$  and Deuterium (D or  $^2\text{H}$ ). The moisture present in the air front gradually depletes in  $\delta^{18}\text{O}$  and  $\delta^2\text{H}$  of water as it moves towards continental side with continued precipitation.

This process of stable isotope fractionation can be understood by the Rayleigh Fractionation Model (Rayleigh, 1902) which deals with the process of removal of a fractional increment of a trace substance from a large reservoir under the open system. For our interest, the “trace substance” is heavy isotope of oxygen ( $^{18}\text{O}$ ) and hydrogen (D or  $^2\text{H}$ ) and the large reservoir is moisture parcel. Therefore, the Rayleigh Fractionation Model can be defined by **Equation 1**.

$$\frac{R}{R_i} = f^{\alpha-1}$$

**Equation 1:** Rayleigh fractionation model for constant fractionation factor ( $\alpha$ ).



When  $R_i$  is the isotope ratio of the reservoir at the beginning of the process when  $f = 1$ . Since  $\alpha$  is assumed as a constant, it makes no difference in the case whether  $R$  refers to isotope ratio to the liquid or vapor phase.

Rayleigh fractionation model is very useful to model and understand meteoric precipitation employing the stable isotopes. It assumes the starting reservoir, which can be any major moist air mass responsible for global precipitation pattern originated from the open ocean. Studies following Rayleigh fractionation model, states that variation of  $\delta^2\text{H}$  and  $\delta^{18}\text{O}$  shows a strong linear relationship as shown in **Figure 1** (Criss, 1999; p 113) and in **Table 6** while considering the pseudo adiabatic cooling model following water saturation at 15°C.

**Table 6:** Rayleigh Condensation Models for Water-Water Vapor. (Data from Criss 1999; p 113)

Pseudo adiabatic Cooling Model				
T (°C)	P <sub>total</sub>	<i>f</i>	$\delta^{18}\text{O}$	$\delta^2\text{H}$
15.0	755	1.0000	-1.88	-2.7
10.0	674	0.8040	-3.69	-17
5.0	601	0.6408	-5.68	-33.2
0.0	536	0.5039	-7.9	-51.6
-5.0	480	0.3900	-10.4	-72.7
-10.0	432	0.2960	-13.3	-97
-15.0	393	0.2193	-16.5	-125.3
-20.0	362	0.1579	-20.4	-158.2
-25.0	340	0.1098	-24.8	-196.5

Pseudo adiabatic cooling model is more realistic assumption for the condensation of water droplets from moisture in the hydrologic cycle. At the time of beginning of condensation, the fractionation factor (*f*) remains as a function of saturation

vapor pressure ( $P_{sat}$ ) of water at temperature of given stage, divided by the saturation vapor pressure ( $P^0_{sat}$ ) at the dew point temperature where condensation initiated. Therefore, a hot moist air front moving towards continental side suffers an incremental loss of moisture due to precipitation. However, it remains saturated in moisture content at all times in pressure-temperature trajectory. This saturated adiabatic cooling trend differs from conventional adiabatic cooling trend taking the account of release of latent heat release by condensation of vapor (Criss, 1999; p 112).

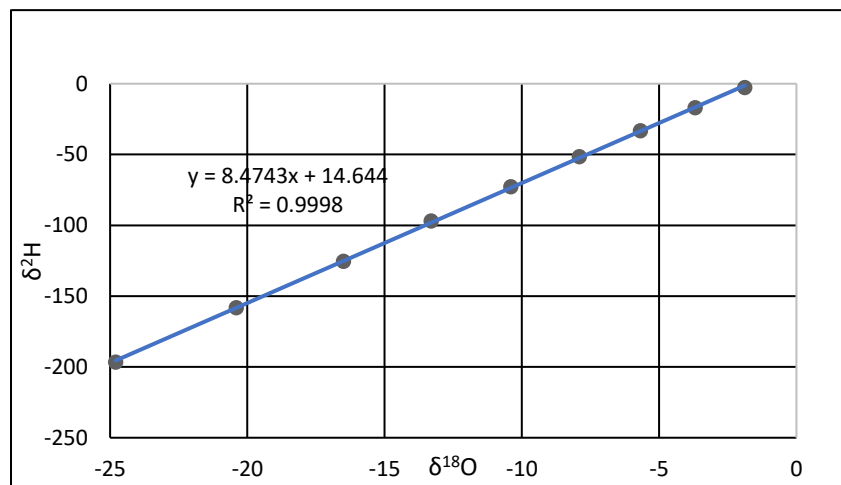


**Figure 1:** Strong linear relationship of  $\delta^{18}\text{O}$  and  $\delta^2\text{H}$  for a Rayleigh Model assuming pseudo adiabatic cooling model following water saturation at 15°C. (Data from **Table 6**).

A large variation in the isotopic ratio of meteoric water has been reported globally which considers the physical processes responsible for generation, transportation and condensation of atmospheric water vapor. Reported range of  $\delta^{18}\text{O}$  is from +4 to -62‰ and for  $\delta^2\text{H}$  it is by the range of +40 to -500‰ in natural precipitation.

However, fractionation of  $\delta^{18}\text{O}$  and  $\delta^2\text{H}$  for any natural precipitation shows a very strong linear relationship governed by Rayleigh fractionation considering the pseudo adiabatic cooling model. This empirical linear relationship leads to the development of “meteoric water line” (MWL) (Craig, 1961; Dansgaard, 1964) which is described by **Equation 2**.

$$\delta^2\text{H} = 8\delta^{18}\text{O} + 10$$

**Equation 2:** Meteoric water line.

Latter investigations with enhanced data set for local precipitation this linear trend was referred as “local meteoric water line” (LMWL). The slope of the line in **Equation 2** remains by and large invariant but the intercept varies from - 2 to values as positive as about + 15 (Sharp, 2007) in meteoric water. This variable intercept is known as “deuterium excess” (D-excess). International Atomic Energy Agency network had established “Global Meteoric Water Line” (GMWL) by analyzing huge data collected throughout the globe which yielded the intercept value of D-excess as 10.35 (Rozanski et al., 1992) for the modern day GMWL. This is in good agreement with the D-excess value reported by Kendall and Coplen (2001) which is 8.99. However, D-excess of 10‰ is still the best approximate of modern worldwide meteoric water line.

### **1.3. Isotopomers of water in groundwater reservoir**

Earlier studies have reported extensive use of stable isotope to delineate the micro-catchment area and to estimate the aquifer recharge (Gat et al., 1991) which was

further extended up to understanding the precipitation pattern in continental scale (Deshpande et al., 2010) is reported. In addition, fractionation process of different isotope species of water has extensively reported when there is phase change involved like for the process of formation of vapor from ice system (Casado et al., 2016); formation of ice from water (Souchez et al., 2000); formation of vapor from water (Cappa et al., 2005; Christopher et al., 2003) etc. Experimental work for detail understanding of temperature dependent stable isotope fractionation of different stable isotope species of water system under supersaturated condition has also been recently reported (Deshpande et al., 2013).

The meteoric water originated from the condensation and precipitation in atmosphere, is the major source that replenishes the groundwater reservoir which accounts for  $\approx 0.62\%$  of hydrosphere. The process of recharge of unconfined aquifers are largely governed by the gravity controlled drainage and hence it retains the isotopic signature very close to local meteoric water. In a storm event, significant amount of precipitation returns back to atmosphere by evaporation (Cappa et al., 2005) and transpiration while rest of the water percolates through the soil profile as gravity drainage to recharge of the aquifer. However, for confined aquifers, the process of recharge is not exclusively governed by simple gravity drainage and it involves hydraulic pressure gradient also. This hydraulic pressure gradient is actually the most important governing parameter along with hydraulic conductivity of the aquifer skeleton material, which determines the amount of water that contributes to the confined aquifer as recharge.

The focus of this work pertains to the distribution of different stable isotopes ( $\delta^{18}\text{O}$  and  $\delta^2\text{H}$ ) of groundwater under varied geothermal gradient. Therefore, attempts are made to confine the scope of the discussion only to the distribution of water isotope composition of the groundwater reservoir.

$\delta^{18}\text{O}$  and  $\delta^2\text{H}$  have proven itself as a very useful tool to evaluate the source and flow paths of groundwater as it retains the pristine isotopic signature of the local precipitation. However, for deep confined aquifers, the relation is a bit complex where the isotopic signature shows a departure from that of the modern-day precipitation of that area (Gat, 1983). This discrepancy is attributed to very slow percolation of water through the confined aquifer system governed by hydraulic gradient and hydraulic conductivity of the aquifer linked with very distal recharge area (Issar et al., 1972; Gat and Issar, 1974). Water present in the confined aquifer is quite old (Sonntag et al., 1978) and formally named as paleo water (Fontes, 1981) which remains in thermal equilibrium with surrounding rocks and soil with different isotopic signatures than that of meteoric water.

Discrepancy of isotopic signature in deep confined aquifer system with modern day precipitation of the area is the “*key information*” which can be addressed from the current work. Considering a closed system approximation for a confined aquifer, (since the recharge area is very distal with respect to the aquifer), this work attributes this discrepancy of isotopic signature to natural geothermal gradient. It demonstrates a deterministic analytical model supported by laboratory experiment and field validation, which will be helpful to estimate groundwater temperature

with respect to 25°C benchmark temperature, where no phase change of water is involved. This is achieved in terms of  $^{18}\text{O}$  fractionation in absolute scale (ppm) which has been elaborated and described in upcoming chapters. Estimating the absolute groundwater temperature is the punch line of this work as limited effort has been made so far in this direction.

## **Chapter 2**

### **Background of the present research**

## **2. Background of the present work**

Use of stable isotope composition ( $\delta^{18}\text{O}$  and  $\delta^2\text{H}$ ) as effective tool to trace the physical processes dates back with Harold Urey's discovery of deuterium (Urey, 1947). This was further contributed by A. O. Nier by developing the sophisticated mass spectrometer to precisely measure the relative abundances of different isotopes (Nier, 1947). Later on, with advancement of technology, precision of isotope measurement improved significantly which enabled it as an indispensable tool in the field of Earth and Planetary Science. These tools are important to understand different geological processes that are being operated from molecular level to global scale. These include geochemistry and cosmochemistry, evolving hard rock geochemistry, rock-fluid interaction, paleoclimatology, ore genesis, oceanography and hydrologic cycle etc.

These isotopic tools have been used for in-depth understanding of the process of crystallization of igneous rocks and its geochemistry (Friedman et al., 1977; Chiba et al., 1989), mineral-water interaction (Taylor, 1977), hydrothermal system (Craig, 1966; Gregory et al., 1981, 1989; Criss et al., 1983, 1986) also. Towards this, understanding of fractionation of stable isotope has significant implication in the field of isotope hydrogeology covering subjects of global meteorology, precipitation patterns and paleoclimate reconstruction. Further, it has facilitated the detail understanding of rain fall-run off dynamics in a watershed, separating base flow from surface flow, estimating the recharge sources for the aquifer etc. Significant work has been reported in the laboratory experimental condition to



separate heavy water from water isotope mixture considering the process of thermal diffusion (Bebbington et al., 1959; Murphy, 1955; Yeh, 1984; Yeh, 2009).

The scope of the current research work is to understand behavior of groundwater and its isotopic response under imposed natural geothermal gradient. The discussion also includes the low temperature aqueous chemistry related to the water and aquifer skeletal material interactions. A discussion on natural geothermal springs with empirical chemical geothermometer has also been made to elucidate the aberrant groundwater temperature due to other geological factors excluding normal geothermal gradient.

### **2.1. Internal heat of Earth and geothermal gradient**

Earth started to cool just after the formation of solar system and evolved for millions of years before it reached its life sustainable thermal stability. However, the outer part of the earth crust, has cooled fast enough to get its rigid configuration while leaving its interior still hot enough to carry molten rocks. Therefore, for the purpose of hydrogeology and related aspects like its response to geothermal gradient, good understanding of thermal zonation of crustal level is required.

Generally, as we go down through outer crust, the temperature increases with depth. The Earth is constantly losing its internal heat which is acquired from several sources namely,

- a) Heat flowing at the base of the lithosphere from the deeper mantle.
- b) Radiogenic heat production in the crust.

Considering the first point that heat flow into the base of the lithosphere from the deeper mantle, the governing equation proposed by Turner and Verhoogen (2004, p 436) given by **Equation 3** is as follows;

$$Q = \frac{k dT}{dh}$$

**Equation 3:** Governing equation of mantle heat flux to lithosphere.

When  $Q$  = Upward heat flux ( $\text{cal/cm}^2\cdot\text{sec}$ );  $k$  = Thermal conductivity ( $\text{cal/cm}\cdot\text{sec}\cdot^\circ\text{C}$ ), and  $T$  &  $h$  stands for temperature and depth respectively. Average value of  $k$  is around  $4 \times 10^{-3} \text{ cal/cm}\cdot\text{sec}\cdot^\circ\text{C}$ . (Turner and Verhoogen, 2004; p 437). Kappelmeyer and Hänel (1974) reported the value of  $2.0\text{-}2.5 \text{ W m}^{-1} \text{ Kelvin}^{-1}$  for the thermal conductivity of Earth's crust, which is very close to other estimates (Turner and Verhoogen 2004; Lawrie 2007; p 231). As the current work is mainly focused on shallow crustal depth up to one to two kilometers, the mantle heat flux may be neglected due to its negligible contribution.

Main source of heat available at shallow crustal level is radiogenic heat produced due to decay of radionuclides of U, Th and  $^{40}\text{K}$ , the radioactive minerals present in the crust. The radioactive heat generated by these elements have an important role on Earth's internal heat at shallow crustal level. This work deals with the heat flow in the shallow continental lithosphere having geochemical composition similar to Granitic family of rocks. These rocks contain the major constituents as orthoclase and plagioclase feldspar with quartz. Orthoclase feldspar contains  $^{40}\text{K}$ , whereas the plagioclase feldspar is rich in U and Th. **Table 7** describes average amount of

radioactive element present in the Granitic rock along with their heat production. (Lowrie 2007; p 228; Rybach, 1976; 1988)

**Table 7:** Average amount of radioactive element present in granitic rock along with its contribution to Earth’s internal heat (Lawrie 2007; p 228).

Characteristic	U	Th	<sup>40</sup> K
Concentration (ppm by weight)	4.6	18	33,000
Heat production 10 <sup>-11</sup> W kg <sup>-1</sup>	43.8	46.1	11.5

For a rock of Granitic family total amount of radioactive heat production can be estimated by following the **Equation 4**. (Lawrie 2007; p 228)

$$Q_r = 95.2 C_U + 25.6 C_{Th} + 0.00348 C^{40}_K$$

**Equation 4:** Amount of radiogenic heat production due to distribution of radioactive minerals in crustal material.

When  $Q_r$  = Total radioactive heat,  $C_U$ ,  $C_{Th}$  and  $C^{40}_K$  are contributions from U, Th & <sup>40</sup>K towards the process (Lawrie 2007; p 228). Earlier studies (Turner and Verhoogen; 2004; p 436) and Lawrie (2007; p 225) have reported the average geothermal gradient of Earth as  $\approx 30$  °C per km for undisturbed crustal material, however, it is not constant worldwide. It may be significantly high near active mid oceanic spreading center, subduction zones to as low as 7°C/km in nearby deep oceanic tranches (Best, 2003).

In addition to the tectonic setting and concentration of radiogenic minerals present in the undisturbed crustal material, thermal conductivity of rocks also affects the

geothermal gradient. It varies with temperature and therefore suitable corrections are required to calculate the heat flow in crustal materials (Lee et al., 1998). The process of thermal conduction is the main mechanism of heat flow through crustal material. **Table 8** summarizes the thermal conductivity of some common aquifer material including the fractured igneous rocks (McCray, 2005; p 55). It is mainly attributed to the lattice conductivity rather than radiative conductivity, which is negligible below 500°C. (Sibbitt et al., 1979). Theoretical models attribute the lattice conductivity as inversely proportional with absolute temperature whereas radiative conductivity is directly proportional with the cube of absolute temperature (Clark, 1969; Schatz and Simmons, 1972; Anderson, 1989; Poirier, 1991). Precambrian cratons may have high geothermal gradient due to their older age and high concentration of radioactive minerals.

**Table 8:** Thermal conductivity of common aquifer materials (McCray, 2005).

Thermal conductivity of rocks (x 10 <sup>3</sup> CGS Units)	
Sandstone	3.0-5.0
Shale	2.0-4.0
Porous Limestone	3.0-5.0
Dense Limestone	5.0-8.0
Granite	5.0-8.0
Basalt	5.0-7.0

## 2.2. Geothermometers

As described earlier, the internal heat source of earth and geothermal gradient are needed to be measured precisely for estimating heat flux in different tectonic settings. Towards this, the mantle heat flux, partial melting of subduction plate at

convergent plate boundary and associated parameters are closely linked with the heat source. The quantification of the internal heat of earth has been attempted by the geophysicist and geochemists which has significantly contributed to the development of a new research field called “geothermics”. Using stable isotope as geothermometer was first reported by Harold Urey in the year 1947 which laid the foundation of the temperature dependent fractionation of stable isotope. Since then it has been extensively used for geothermometry and understanding the reaction kinetics of mineral water interaction at low temperature. Recently few chemical geothermometers have been reported which can be successfully used in geothermal systems for heat quantification (Goff, et al., 2000). A brief of basic principles of isotopic fractionation is summarized as follows.

### **2.2.1. Basic principle of stable isotope fractionation**

Stable isotope fractionation can be classified into two groups, namely the equilibrium fractionation and non-equilibrium/kinetic fractionation. In the equilibrium isotopic fractionation, there is no breakdown of chemical bond whereas the nonequilibrium/kinetic fractionation involves the breaking of chemical bonds and formation of new phases.

Equilibrium isotopic fractionation occur between two phases or molecular species that have a common element (stable isotope of interest) that undergoes a chemical reaction. Chemical reaction always tends to reach equilibrium with respect to two phases or molecular species that are not in isotopic equilibrium (Drever, 2002). In

the equilibrium fractionation the distribution of stable isotope is defined by the fractionation factor ( $\alpha$ ) as given by **Equation 5**.

$$\alpha = \frac{[(A^*/A)]_m}{[(A^*/A)]_n}$$

**Equation 5:** Fractionation factor ( $\alpha$ ) for equilibrium isotopic fractionation.

When  $m$  and  $n$  are two phases or reactants and  $A^*$  is the heavy isotope of interest and  $A$  is the most abundant isotope. At present  $A^*$  is  $^{18}\text{O}$  and  $A$  is  $^{16}\text{O}$ .

In non-equilibrium/kinetic isotopic fractionation process, mainly involves the biological systems like photosynthesis where the isotope fractionation process barely reaches in equilibrium (Drever, 2002). Fundamental principle of this process is fractionation of isotope due to breaking of chemical bonds involving activation energy of the reaction. Considering heavy isotope of an element with respect to lighter one, more activation energy is required to break the heavy isotope bond than light isotope bond. Therefore, the resultant organic material (i.e. glucose for the process of photosynthesis) will be enriched in  $^{12}\text{C}$  than the  $\text{CO}_2$  source. The reaction rate of the process can be defined by **Equation 6**.

$$\text{Rate} = A \exp\left(-\frac{\text{activation energy}}{RT}\right)$$

**Equation 6:** Equation governing nonequilibrium isotopic fractionation.

When  $R$  is Gas constant,  $T$  is absolute temperature and  $A$  is empirical constant. (Drever, 2002).

This work deals mainly with the temperature dependent isotopic fractionation of liquid water system without a phase change and no breakdown of chemical bond. Therefore, only equilibrium isotope fractionation is considered.

### 2.2.2. Isotope Geothermometers

Temperature dependent isotope fractionation between two mineral phases can be understood like the process of element partitioning between two mineral phases with varying chemical composition (Chacko et al., 2001) and crystal structure (Zheng, 1993; Bottinga, 1969). However, reaction kinetics of element partitioning is pressure sensitive whereas the isotopic partitioning is pressure insensitive because of negligible change in volume (Hoefs, 2009). Oxygen isotope fractionation between two anhydrous phases of minerals the fractionation factor ( $\alpha$ ) maintains a linear function with respect to temperature. Bottinga and Javoy (1973) demonstrated that oxygen isotopic fractionation between anhydrous mineral pairs at temperatures more than 500°C, can be expressed by **Equation 7**.

$$1000 \ln (\alpha) = A/T^2 + B$$

**Equation 7:** Relation between isotope fractionation factor ( $\alpha$ ) and temperature in °K.

When “A” is experimentally derived known parameter for calculating temperature of equilibration. Value of “A” varies with mineral pairs considering isotopes of different minerals. For temperature very close to 500°C, in most of the cases, the parameter “B” approximates to zero making the expression simpler.

However, in the case of aqueous solution-precipitation reaction, the modeling scenario is a bit complex where the isotope fractionation factor ( $\alpha$ ) is determined at precipitation temperature using water fugacity (Kohn et al., 1998)(a). Negligible effect of pressure in aqueous solution-precipitation reaction has been observed for oxygen isotope fractionation, however significant influence has been reported for hydrogen isotopes (Driesner, 1997), Horita and Berndt, (1999, 2002), Polyakov et al., (2006). Considering precipitation of epidote from water, Driesner (1997) reported that hydrogen isotope fractionation changed from -90‰ at 1 bar pressure to -30‰ at 4000 bars and at 400°C between the mineral phase and water. Empirical geothermometer to estimate water temperature from  $\delta^{18}\text{O}$  value from precipitated calcite has also been reported at 25°C. (McCrea, 1950; Epstein et al., 1953, a; b). Studies on the equilibrium stable isotopic fractionation have provided with the important information on mineral fractionation to the rock type and minerals under investigation. (Kohn and Valley, 1998)(b); Sharp, 1995; Kitchen and Valley, 1995). However, this work employs the isotopic fractionation of stable isotopes to estimate the water reservoir temperature in varied geothermal gradients.

### **2.2.3. Geothermal system and chemical geothermometers**

Geothermal system manifests the out flow of abnormally high temperature groundwater coming out of the earth surface. For a liquid dominated hydrothermal system the temperature of the water may range from 150°C to as high as 370°C which may be associated the with areas of high heat flow setting thermal convection. This natural superheated water source is commonly called “natural geysers”. Generally, these geothermal systems are distributed along active



continental plate margins including “Black Smokers” of active mid oceanic ridge-rift systems and may also be associated with mantle plume like in Yellowstone National Park of USA. This circulation of water under high heat flow is described as the forced convection (Bear, 1988; p 642). This can be exemplified by thermal convection of regional groundwater flow due to emplacement of an igneous pluton or from other source of mantle heat flux to shallow crustal level. In this case, thermally charged water carries its own heat content and moves up from deeper region towards the surface. In this scenario, there is no density gradient of water and Darcy’s law holds good. A geothermal system may have three components

- a. A high heat source from subsurface.
- b. Adequate supply of water.
- c. A highly permeable reservoir rock for thermal convection of water.

Such geothermal systems are also being used as alternative energy resources in several countries like USA, Iceland, New Zealand etc. for the electricity generation and different engineering applications like space heating. However, this work uses water isotope ( $\delta^{18}\text{O}$  and  $\delta^2\text{H}$ ) of geothermal systems as an empirical chemical geothermometers to estimate the temperature of groundwater.

Geothermal fluids have a wide range of water chemistry with varying salt content having total dissolved solid (TDS) ranging 1000 to more than 350,000 ppm which is higher by ten folds in magnitude than seawater. These highly mineralized geothermal springs forming them economically exploitable hydrothermal mineral deposits. A typical liquid dominated hydrothermal system may contain major ions of Sodium (Na), Potassium (K), Calcium (Ca), Magnesium (Mg) Silica (Si) and

Chlorine (Cl), Bicarbonate ( $\text{HCO}_3^-$ ), Sulphate ( $\text{SO}_4^{2-}$ ). These generally have traces of Arsenic (As), Boron (B), Lithium (Li) and Bromine (Br) and Carbon di oxide ( $\text{CO}_2$ ) and Hydrogen Sulfide ( $\text{H}_2\text{S}$ ) as the common dissolved gases. Methane ( $\text{CH}_4$ ) and ammonia ( $\text{NH}_3$ ) may also be present as dissolved gas if the circulating water encounters any organic derived compound at its flow path (Fournier 1979; Fournier 1982; Fouillac et al. 1981; Arnorsson et al. 1985; Giggenbach et al. 1988; Goff, et al., 2000).

Empirical geothermometers have been developed to estimate temperature of geothermal system (Goff, et al., 2000). These are based on the elemental concentration while few rely on elemental ratios. These geothermometers are calibrated in laboratory under ideal condition with known temperature. Most commonly used one is the silica geothermometer, which uses the absolute abundance of  $\text{SiO}_2$  in the solution covering a temperature range of 150-250°C and is represented by **Equation 8**.

$$T = \frac{1309}{5.19 - \log \text{SiO}_2} - 273.15$$

**Equation 8:** Silica geothermometer.

Na/K is another widely used geothermometer which takes into account of Na/K elemental ratio when water temperature is more than 150°C and described by **Equation 9**.

$$T = \frac{1217}{1.483 + \log Na/K} - 273.15$$

**Equation 9:** Na/K geothermometer.

In addition, the Na-K-Ca geothermometer described by **Equation 10** is useful for calculating water temperature when the temperature is more than 100 °C.

$$T = \frac{1647}{\log \frac{Na}{K} + \frac{1}{3} \left[ \log \left( \frac{Ca^2}{Na} \right) + 2.06 \right] + 2.47} - 273.15$$

**Equation 10:** Na-K-Ca geothermometer.

All the above-mentioned geothermometers consider element concentration in the unit of parts per million (ppm) and report temperature in degree centigrade. Radiometric dating of geothermal waters using Tritium, <sup>14</sup>C, and <sup>36</sup>Cl generally shows that they can be applicable for the system with age range of 1,000 to 100,000 years (Goff et al., 2000). However, these geothermometers have their own limitations in the field in terms of changing water chemistry, mixing with other water, and vigorous boiling of water etc. These geothermometers are applicable to more than 100°C of water temperature in the reservoir at elevated pressure. Therefore, a suitable method is required to deal with temperature ranging below 100°C, which is attempted in this work.

### **2.3. Heat transport and groundwater flow**

Geothermal gradient has significant influence on the groundwater flow which can be traceable through its stable isotope distribution pattern. For an inclined confined

aquifer, there may be increase in temperature moving down dip (**Figure 2**). However, the groundwater flow being the Newtonian type and directed against the temperature gradient it may cause another differential movement to set thermal convection from higher to lower temperature (**Figure 2**). This derives the thermally charged hot water at depth to rise up dip by displacing the cold water. This results in a laminar flow opposite to natural gravity driven advection. This is called free convection which is driven by the density difference of water due to temperature gradient. (Domenico, 1997; p 207). The associated mechanism could be elaborated as follows.

Consider a force balance on a fluid in a gravitational field under hydrostatic equilibrium which may be described by **Equation 11**. (Wood et al., 1982).

$$\nabla\rho \times g = 0$$

**Equation 11:** Force balance equation of a fluid in a gravitational field.

When  $\nabla\rho$  = density gradient due to temperature gradient,  $g$  = local gravity vector.

The phenomenon can be understood as described in **Figure 2**.

Further, the onset of the free convection in naturally occurring porous media can be defined by a dimensionless parameter the Rayleigh Number ( $Ra$ ) which can be defined as follows by **Equation 12** considering geothermal gradient of 25°centigrade/kilometer. (Wood et al., 1982)

$$Ra = \frac{K \cdot g \cdot \sigma \cdot (\rho C)t \cdot H \cdot \Delta t}{\gamma \cdot \lambda^*}$$

**Equation 12:** Equation of Rayleigh Number.

When  $K$  = permeability of medium,  $g$  = acceleration due to gravity,  $\sigma$  = volumetric thermal expansion coefficient of the fluid,  $(\rho C)t$  = volumetric heat capacity of fluid,  $H$  = thickness of the porous layer,  $\Delta t$  = temperature difference across the layer,  $\gamma$  = kinematic viscosity of the fluid,  $\lambda^*$  = effective thermal conductivity of the fluid filled medium.

The Rayleigh Number expresses the transport of energy by free convection. Onset of free convection in porous media occurs at Rayleigh number on the order of  $4\pi^2$  that is  $Ra < Ra_c = 4\pi^2 \cong 40$ , where  $Ra_c$  is the critical number for onset of free convection (Wood et al., 1982). Therefore, the free convection of groundwater is expected if this number is close to the critical number.

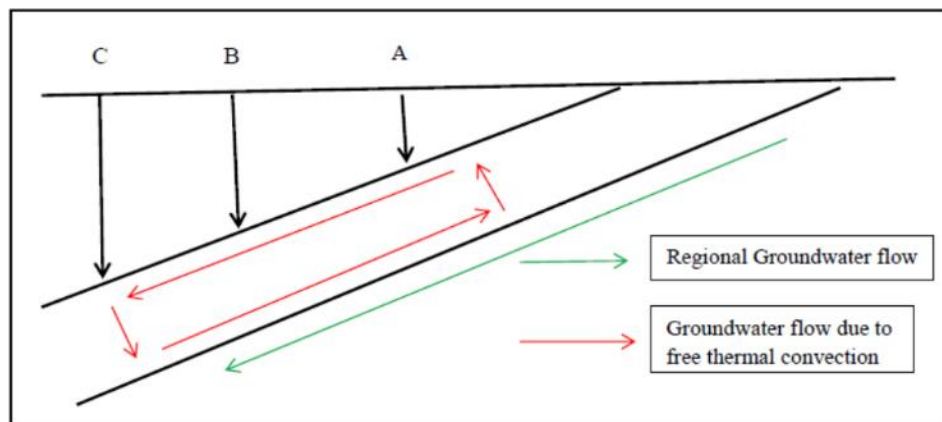


**Figure 2:** Increment of temperature ( $A < B < C$ ) in an inclined confined aquifer due to normal geothermal gradient. Aquifer boundary is assumed as impermeable.

Vertical arrows corresponding to the points A, B, C are indicating increasing depth down dip with reference to horizontal ground surface. Groundwater flow due to convection is marked by red arrow. Regional groundwater flow is marked by green arrow. (Schematic diagram, not according to scale).

If we consider a dipping stratum (**Figure 2**), there is no thermal stability criterion as temperature is increasing down dip and there will always be a free convection due to temperature gradient. For a dip angle  $\theta$ ,  $Ra_c$  needs to be multiplied with  $\cos(\theta)$  to accommodate changed orientation of gravity relative to the stratum. Depending on amount of dip of the stratum and value of  $Ra_c$ , following cases can arise for the different theoretical convection flow pattern of subsurface fluid (Wood et al., 1982).

- a. *Dip angle is less than but close to  $15^\circ$  and  $Ra_c$  is less than but very close to 40.*

The convection flow will be characterized by a steady unicellular motion. Convection current will move up-dip from heated bottom layer turns at the upper extremity of the layer then moves down-dip through upper cold layer forming a continuous convection loop as shown in **Figure 2**.

- b. *Dip angle is less than  $15^\circ$  and  $Ra_c$  is more than 40.*

The convection flow will be upward with approximate geometrical shape of polyhedral cells with roughly hexagonal plan view symmetry.

*c. Dip angle is more than 15° and  $Ra_c$  is more than 40.*

The convection flow will be same as moving upward with approximate geometrical shape of polyhedral cells with roughly hexagonal plan view symmetry but the convection cells will be stretched down-dip into counter rotating longitudinal rolls. Since we are interested in free convection of groundwater with steady unicellular motion, our goal is to select a field area where the dip of the confined aquifer which is less than but close to 15° and  $Ra_c \cong 40$ .

## **2.4. Groundwater chemistry and its isotopic response**

Here we discuss temperature dependent isotopic fractionation of groundwater with free convection considering low temperature mineral water interaction in clastic and carbonate aquifers. Though the groundwater chemistry can be changed with mineral water interaction however the isotopic signature remains unaffected up to 60°centigrade temperature irrespective of aquifer material and water interaction. (Gat, 2010).

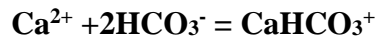
### **2.4.1. Dissolved salt effect on isotope fractionation**

By and large, the isotopic fractionation during precipitation of a solid phase from aqueous mother solution is a temperature dependent process (Zhang et. al., 2001; Zheng, 2011). In low temperature aqueous chemistry, mineral rock interaction may lead to precipitation or dissolution of solid phase depending on temperature and this may be applied to the clastic and carbonate aquifers which may influences the outcome of the present work.

With the suggestion that the rainwater is slight acidic, their recharge in to the carbonate aquifers involves carbonate mineral and water interaction. While rain drops pass through atmosphere, the CO<sub>2</sub> gets dissolved into the water droplets which form a dilute carbonic acid (H<sub>2</sub>CO<sub>3</sub>) at the time of precipitation. Intensity of such acidification is variable both temporally and specially. Earlier work has reported a range of natural rainwater pH covering from 4.8 to 6.9 in different parts of Europe, Australia, North America, Hawaii and some parts of Africa (Barrett and Brodin; (1955). They have also reported a pH value of 5.7 at 25 °C in Northern Europe (Barrett and Brodin; 1955). However, these values have significant variation on local effect of atmospheric condition and associated CO<sub>2</sub> influx due to anthropogenic input. These studies have revealed that the mean pH of rainwater throughout global network stations have temporal variability with acidity greatest in winter and the alkalinity greatest in late spring. It has been demonstrated that after industrial revolution around 1760 AD there is an increasing trend of atmospheric CO<sub>2</sub> gas due to anthropogenic input. The scenario becomes worst at 16<sup>th</sup> December, 2014 when Mauna Loa Observatory reported the highest concentration of atmospheric CO<sub>2</sub> of 399.35 ppm (Ganguly et al., 2015). Solubility of CO<sub>2</sub> in the rainwater increases with partial pressure of CO<sub>2</sub> in the atmosphere under open system condition like an open surface water body (Rosenbaum, 1997). However, for a closed system like confined aquifer with impermeable boundary as proposed in this research the scenario is little different. Once the meteoric water infiltrates to recharge the confined aquifer, its connection with open atmospheric CO<sub>2</sub> detaches or cuts off. Therefore, the very dilute carbonic acid of rainwater is



consumed by dissolution of carbonate minerals at shallow subsurface with no replenishment of atmospheric CO<sub>2</sub>. In addition, a significant amount of rainwater with dissolving carbonate minerals will go through the process of evaporation leading to carbonate mineral precipitation. It may be described by **Equation 13**; with log  $K_{25}$  1.11 (Equilibrium constant at 25°C) and  $\Delta H^0_R$  of 22.64 kJ/mole (Drever, 2002; p 420)

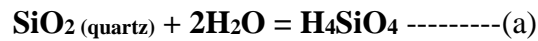


**Equation 13:** Chemical reaction governing rainwater carbonate interaction.

The above-mentioned chemical reaction significantly precipitates carbonate minerals in upper A-Horizon of soil profile. This type of carbonate mineral dissolution and precipitation has been reported by Criss (1999, p 131) from basinal fluids from the California Coast Ranges with no deviation of  $\delta^{18}\text{O}$  and  $\delta^2\text{H}$  values from normal meteoric water values. As the temperature increases solubility for carbonate minerals decreases. For example, Solubility Product ( $K_{sp}$ ) of calcite decreases from  $10^{-8.38}$  to  $10^{-8.51}$  if the temperature increases from 0°C to 30°C (Langmuir, 1997). It has been shown for the carbonate mineral dissolution/precipitation process that bicarbonate ( $\text{HCO}_3^-$ ) solubility greatly decreases with increasing temperature as bicarbonate ( $\text{HCO}_3^-$ ) solubility is 74 mg/L at 10 °C which reduces to 58 mg/L at 25 °C (Parkhurst et al., 1990). It is observed that when groundwater saturated with dissolved carbonate, is pumped to the surface and quickly heated, the carbonate minerals precipitates out from the original solution (Jenne, 1990).

In this way most of the dilute carbonic acid gets neutralized or consumed reacting with carbonates at the topsoil which further precipitates out due to evaporation of meteoric water at the top soil. As a part of the water percolates down into the aquifer, the ambient temperature increases down dip and thereby reduces the carbonate solubility. Therefore, as a precaution, the water sample collected from carbonate aquifer may be heated in a closed system to avoid minimum residual carbonate in the water before measuring  $^{18}\text{O}$  isotope ratio.

Considering the pH of a rainwater in which silica dissolution may be governed by **Equation 14 (a & b)**.



**Equation 14:** Equation governing silica dissolution.

For **Equation 14 (a)**  $\log K_{25} -3.98$  (Equilibrium constant at  $25^\circ\text{C}$ ) and  $\Delta H^0_{\text{R}}$  of  $25.06 \text{ kJ/mole}$  and for **Equation 14 (b)**  $\log K_{25} -2.71$  (Equilibrium constant at  $25^\circ\text{C}$ ) and  $\Delta H^0_{\text{R}}$  of  $14.00 \text{ kJ/mole}$  (Drever, 2002).

Since dissolution rate of silica is extremely low and can be considered negligible influence on analytical results. With this background discussion on fresh water aquifers, the model proposed in this work may be applied to estimate the temperatures of oil field brines and associated mineralized groundwater with high salt contents.

Salt effect on isotopic fractionation is a contested issue and have been widely debated. Feder et al., (1952) and Googin et al., (1957) reported effect of salt and its influence on activity coefficient. Sofar et al., (1972, 1975) quantitatively reported the salt effect on activity coefficient ratio for  $H_2^{18}O$  and  $HD^{16}O$  at 25 °C in a mixture of Na, K, Ca, Mg along with Cl as anion. The quantitative expression is given by **Equation 15 (a & b)**.

For  $^{18}O$  the expression is

$$(1/Y-1) 10^3 = 1.11 M_{Mg} + 0.47 M_{Ca} - 0.16 M_K \text{-----(a)}$$

For deuterium ( $^2H$ ) the expression is

$$(1-1/Y) 10^3 = 6.1 M_{CaCl_2} + 5.1 M_{MgCl_2} + 2.4 M_{KCl} + 0.4 M_{NaCl} \text{-----(b)}$$

**Equation 15:** Quantitative expression governing salt effect on activity coefficient. When  $M$  = Molality of the solution and  $Y$  = Activity coefficient ratio.

Epstein et al., (1953) found that isotope variation of surface waters of North Atlantic showing significant correlation with variations in salinity which was contested with counter arguments. Craig et al (1965) have ruled out the salt effect on isotopic fractionation ( $^{18}O$ ) of ocean water having no influence of NaCl in the process. However, Stewart et al., (1975) reported that NaCl salts could influence on deuterium ( $^2H$ ) fractionation significantly and therefore present work has not used deuterium ( $^2H$ ) fractionation.

The issue of salt effect problem, if any may be overcome by adopting a salt rejection technique during analysis. Keeping these precaution, the oil field brine sample may be collected from pristine formation for isotope analysis, or water sample

containing significant dissolved carbonate mineral need to be preserved in a temperature resistant container with a tube at the top of it. The other end of the tube may be connected to another temperature resistant container to make it a closed system. Such a configuration is shown in **Figure 3** where the brine sample is put in an empty container “A” which is interconnected with container “B” by a tube (**Figure 3**) to maintain a closed system. Container “A” is maintained at  $\approx 100\text{ }^{\circ}\text{C}$  with the help of a hot water bath while the container “B” is put in a cold bath. Therefore, the water kept in the hot container, “A” starts evaporating and subsequently condenses in container “B”. The process of complete evaporation of water from container “A” rejects the salt under a closed system ensuring the complete evaporation and condensation without a change of the isotopic signature of the sample. Water sample collected from container “B” has no salt in it but having same isotopic signature of sample in container “A”. Water sample taken from container “B” can be analyzed in Isotope Ratio Mass Spectrometer (IRMS) and the data can give a good estimate of the oil field brine temperature.

However, for isotopic analysis of liquid water, an alternative method, using Laser Water Isotope Analyzer is preferred. It takes approximately  $1.9\text{ }\mu\text{ml}$  of water sample in a single suction and completely evaporates the suction water instantaneously before it put it into the gas cell or cavity to measure the ratios of different isotopomers (e.g.  $^2\text{HO}$ ,  $\text{HD}^{18}\text{O}$ ) of water present in the sample. In the process of complete evaporation, it rejects any salt present in the sample and thereby eliminating the possibility of salt related fractionation effects.

Here it is important to note that the mineral water interaction has minimal effect on the isotope ratio measurements. Further, silica dissolution can be neglected owing to its very low solubility in aqueous system at low temperature. While deriving the deterministic analytical model to estimate groundwater temperature, salt effect has been excluded in the final expression of the mathematical model.

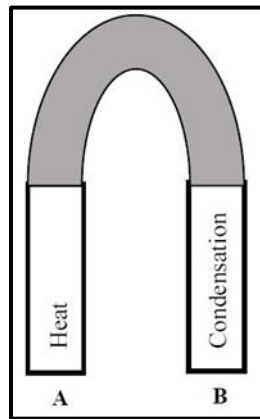


**Figure 3:** Salt rejection technique for sample preparation for oil field brine temperature estimation.

#### 2.4.2. Isotope fractionation of water with free convection

This discussion is about the response of oxygen and hydrogen isotope fractionation to a small compartment of hydrologic cycle, which simulates the conditions of the groundwater and its isotopic response under imposed geothermal gradient.

The International Atomic Energy Agency, (Vienna, 1981) reported an experimental work on temperature dependent stable isotopic fractionation of vapor-liquid water system. This shows a strong inverse linear relationship for  $^{18}\text{O}/^{16}\text{O}$  in vapor phase with increasing temperature, resulting (**Figure 4**) the residual water enriched in  $^{18}\text{O}$ .

As proposed in this work, a gently dipping (Dip amount  $\cong 15^\circ$ ) aquifer manifests a free unicellular laminar convection maintained under temperature dependent density gradient as a result of downward incremental geothermal heat. Since water in the confined aquifer remains in equilibrium with ambient geothermal gradient, it may be close to the equilibrium isotope fractionation.

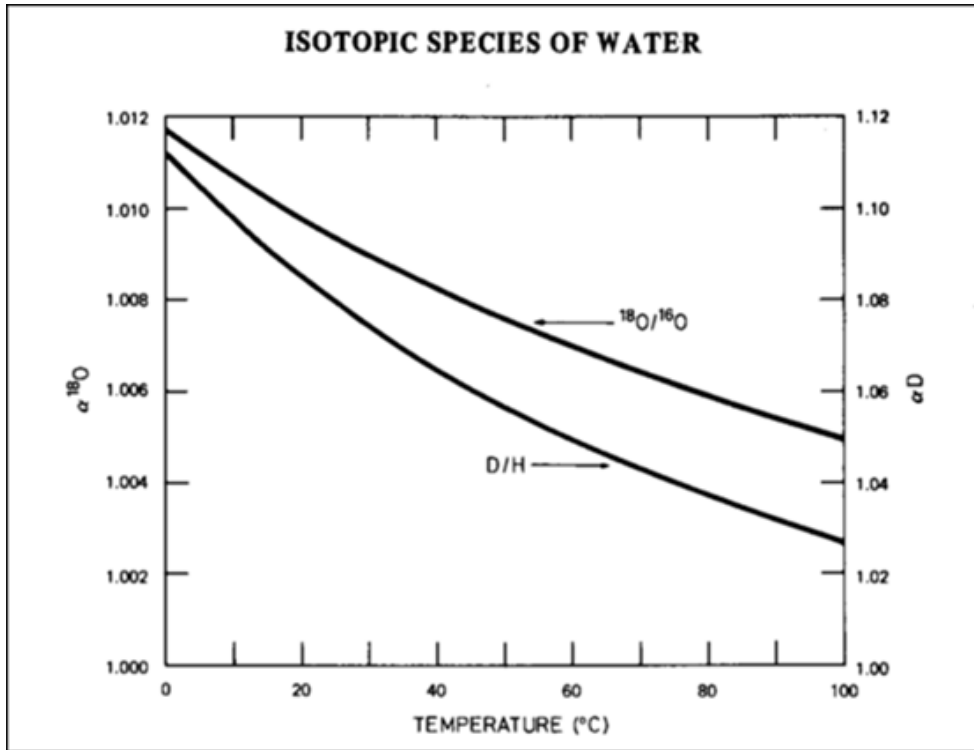


**Figure 4:** Change in  $\alpha$  for  $^{18}\text{O}$  and D with respect to temperature for water vapor-liquid water system. (International Atomic Energy Agency, Vienna, 1981, Technical Reports Series No 210).

Spectroscopic data for the vibrational frequencies ( $^{16}\text{O}-^{16}\text{O}$  is  $1580.193\text{ cm}^{-1}$ ,  $^{16}\text{O}-^{18}\text{O}$  is  $1535.57\text{ cm}^{-1}$ , H-H is  $4401.213\text{ cm}^{-1}$  and H-D is  $3813.15\text{ cm}^{-1}$ ) suggest that

it decreases with increasing bond strength (Huber et al., 1979). Therefore, for a confined aquifer system the heavier isotope tends to concentrate at lower temperature regime when it is subjected to a temperature gradient. A detail discussion of derivation of deterministic analytical model supported by conceptual model with their initial and boundary condition coupled with the limitations is provided in **Chapter 3**.

### **2.5. Scope and significance of present work**

As described earlier the fractionation of different stable isotopic species of water involving a phase change have been studied extensively. The isotopic and chemical geothermometers to estimate temperature of geothermal system are restricted to higher temperature regime of more than 100°C. Towards this, the  $^{18}\text{O}$  geothermometer is attempted to estimate the temperature of mother solution from its calcite precipitate is and reported in the literature.

However, limited studies are reported which involve the temperature dependent fractionation of  $^{18}\text{O}$  in liquid water without phase change but under a temperature gradient. Also, there is no chemistry based geothermometer reported for low temperature regime below 100°C to estimate groundwater temperature. *Present work is exclusively focused on this aspect to bridge the gap in the field of stable isotope hydrogeology based geothermometry.* It demonstrates that temperature dependent isotopic fractionation of  $^{18}\text{O}$  in liquid water system can be useful to estimate absolute temperature of groundwater.

This work finds application in the geothermal energy sector, which is the inevitable part of our life and economy. It may provide clue for radioactive mineral exploration in terms of high water temperature anomaly despite no emplacement of pluton nearby. This work may also be helpful to identify concentrated deuterium ( $^2\text{H}$ ) used in atomic nuclear fusion reactor as it tends to concentrate at lower temperature region.

This work is also relevant in hydrocarbon exploration and production sector where it can be used in estimating formation fluid temperature which is required during the well drilling and predicting reservoir dynamics for production stage. This makes an important information for decision making of hydrocarbon well completion. There are significant chances of error in temperature logging, particularly estimating the temperature of pristine formation fluid, due to mud cake invasion during drilling. However, by sidewall coring pristine formation fluid sample can be obtained overcoming the mud cake invaded zone. This can provide very good estimate of formation fluid temperature by its isotope signature.



## **Chapter 3**

### **The Oxygen-18 geothermometer**

### **3. The oxygen-18 geothermometer**

Towards the estimation of groundwater temperature using the stable isotope fractionation ( $^{18}\text{O}$ ) an analytical working model was evolved with its boundary and initial condition. Analytical model starts with Fick's Law of diffusion and obeying Fourier's Law of thermal conduction. This is represented by an one-dimensional first order, first degree differential equation and solved by analytical method. Variables have been rearranged for the one-dimensional Fick's Law of diffusion to fit the analytical model in the modeling scenario.

This model makes the use of absolute abundance of  $^{18}\text{O}$  in ppm and is able to give good estimate of groundwater temperature with reference to  $25^\circ\text{C}$ . The reference temperature ( $25^\circ\text{C}$ ), is thought to be the equilibrium temperature of precipitation of VPDB from VSMOW at which the absolute abundance of  $^{18}\text{O}$  in the ocean water is 2005.12 ppm. The model estimates the absolute abundance of  $^{18}\text{O}$  with respect to this reference value (2005.12 ppm) and simultaneously calculates the groundwater temperature in absolute scale with respect to  $25^\circ\text{C}$ . Experimental work demonstrates that the proposed  $^{18}\text{O}$  geothermometer is not only theoretically viable but it is also realizable under imposed temperature gradient where there is no phase change of water is involved.

Utilizing the basic principle of isotope fractionation, basic proposition of the model stands on the fact that the preferential enrichment of heavier isotopes is likely in the lower temperature region in a confined aquifer which lies under the geothermal temperature gradient. After testifying the theoretical feasibility of the  $^{18}\text{O}$

geothermometer, it was cross-checked in the controlled laboratory conditions to fractionate  $^{18}\text{O}$  under incremental temperature gradient where no phase change of water involved. In addition, the  $^{18}\text{O}$  geothermometer was also testified in field conditions by published  $\delta^{18}\text{O}$  data of Sacramento Valley, California, which is elaborated in **Chapter 4**. The deterministic analytical model was able to estimate groundwater temperature in the field condition with its  $^{18}\text{O}$  isotopic signature and hence are useful in the field of reservoir thermometry and research.

### **3.1. The modeling background**

Towards the principle aim to derive a model of  $^{18}\text{O}/^{16}\text{O}$  fractionation of water in natural porous media maintained under normal geothermal gradient was used and the associated requirements has been already described in **Chapter 2** which is based on the random molecular motion and vibration.

The methodology starts with mathematical approximation of stable isotope fractionation of water due to normal geothermal gradient and can be best understood by Fourier's Law. It is described by **Equation 16**.

$$H = - \epsilon \text{ grad } T$$

**Equation 16:** Fourier's Law of thermal conduction.

When  $H$ =Heat flux,  $T$ =Temperature,  $\epsilon$ = Proportionality constant. Negative sign of the equation denotes that heat will flow from higher temperature to lower temperature (Domenico et al.1997, p 192).

The aquifer as described in (**Figure 2**) contains three points A, B, C having temperature increasing along down dip, where  $^{18}\text{O}$  of natural water is expected to fractionate as per the temperature gradient. Such fractionation will attain the state of equilibrium involving no breakdown of chemical bonds and therefore it may be close to “Equilibrium Isotope Fractionation”.

### **3.2. The analytical deterministic model**

Initial modeling is a basic step towards better understanding of any physical process. It not only helps to quantify and simulate the process but also estimates the associated uncertainties. It assumes many simplifications, which may be very close to reality. This work involves the establishment of a deterministic analytical model which starts from conceptual model, boundary and initial conditions and analytical solution of partial differential equation for simplified Fick’s law of diffusion. It enables  $^{18}\text{O}$  as an isotope geothermometer at shallow crustal level to estimate groundwater temperature with respect to  $25^{\circ}\text{C}$ .

Earlier studies conducted under laboratory experimental condition to separate heavy water from water isotope mixture considering it as a process of thermal diffusion (Bebbington et al., 1959; Murphy, 1955; Yeh, 1984; Yeh, 2009). Therefore, the derivation of the proposed deterministic model is briefed as follows.

#### **3.2.1. Conceptual model**

This conceptual model attempts to understand the process of free unicellular laminar convection of groundwater in a porous media. It is manifested in terms of a gently dipping confined aquifer where the temperature is increasing down dip

(**Figure 5**). It has the temperature dependent density gradient ( $D$ ) when  $D_2 > D_1$ . In this set up, a warmer and less dense (High temperature;  $D_1$ ) water tends to move up where as the denser (Low temperature;  $D_2$ ) water sinks down. This results the onset of the free unicellular laminar convection of groundwater flow marked by the Rayleigh Number ( $Ra_c$ ) very close to  $\leq 40$ ; and may be described by **Equation 12**.

As illustrated in **Figure 5** one can divide the aquifer into infinitesimal equal length ( $X_n$ ) compartments depending on temperature dependent density such that  $X_1 = X_2 = \dots (X_n)$ ; when  $X \rightarrow 0$  (**Figure 5**). Each compartment will have the definite temperature and associated stable isotope concentration owing to its thermal preference. In this regard the  $^{18}\text{O}/^{16}\text{O}$  ratio is expected to decrease down dip under the increasing temperature.

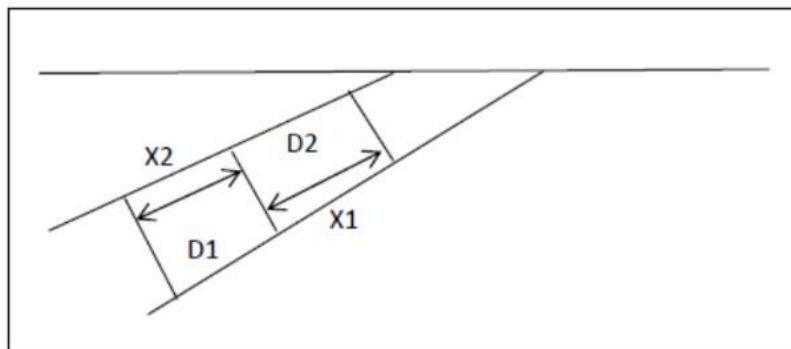


**Figure 5:** Temperature induced density gradient in a natural porous and permeable media. (Schematic diagram, not according to scale)

Since water has different isotopomers with varying combinations, it is expected to undergo temperature dependent stable isotope fractionation during its flow through a porous free flowing media. Such isotope fractionation for fluid is only dependent

on temperature and has no other energy variables which is further elaborated in upcoming **Chapter 4**. As the fractionation process does not involve any breaking of O-H bond or any chemical reaction, the concept of free energy in the process may not be applicable. However, it only involves differential kinetic energy (*K.E*) which may be presented as follows.

$$K.E = \frac{m_1 v_1^2}{2} = \frac{m_2 v_2^2}{2}$$

When  $m_1$  and  $m_2$  are mass of different isotopes of same element ( $m_1 < m_2$ ) and  $v_1$  and  $v_2$  are corresponding vibrational frequencies. Above equation can be rearranged by following

$$\frac{v_1}{v_2} = \frac{\sqrt{m_2}}{\sqrt{m_1}}$$

This shows that, the vibrational frequency increases with increasing temperature. If it is considered that  $m_2 > m_1$  and for both  $m_1$  and  $m_2$  are constant, the right-hand side of the above equation becomes constant. Therefore, it can be further rearranged as following.

$$v_1 = K v_2$$

When  $K$  is a constant and greater than one. The value of “ $K$ ” is defined by  $\sqrt{m_2}/\sqrt{m_1}$  since the value of  $m_2$  and  $m_1$  are constant.

Since  $K$  is always greater than 1, it implies  $v_1 > v_2$ . This work pertains to the vibrational frequency of oxygen and hydrogen as the two components of water. The spectroscopic data suggests that the vibrational frequency of  $^{16}\text{O}-^{16}\text{O}$  is 1580.193  $\text{cm}^{-1}$  whereas  $^{16}\text{O}-^{18}\text{O}$  is 1535.57  $\text{cm}^{-1}$ . For H-H the vibrational frequency is

4401.213  $\text{cm}^{-1}$  and  $\text{H-}^2\text{H}$  vibrational frequency is 3813.15  $\text{cm}^{-1}$  (Criss 1999; p53). Vibrational frequency decreases with increasing bond strength which is consistent with the fact that the bond strength of  $^{16}\text{O-}^{18}\text{O}$  and  $\text{H-}^2\text{H}$  is greater than the bond strength of  $^{16}\text{O-}^{16}\text{O}$  and  $\text{H-H}$ .

However, it increases for both the isotopes with addition of heat to the system. In excited state ( $v_1 > v_2$ ) as the frequency increases, both  $m_1$  and  $m_2$  will differentially deviate from its equilibrium state. This will cause  $m_1$  (the lighter isotope) to concentrate at higher temperature region and  $m_2$  (the heavier isotope) towards the lower temperature region. This model satisfies the real-life analogy of stable isotope fractionation particularly during the process of open water evaporation, where the residual water becomes isotopically enriched in heavier isotope. In this process it is obvious that the water vapor has more heat content than corresponding water at same temperature as latent heat of 40.657 KJ/mol (Kestin et al., 1984). Therefore, for a given liquid water system, the heavier isotope will tend to concentrate at lower temperature regime subjected to a temperature gradient in the system, under following assumptions.

### **3.2.2. Assumptions and boundary conditions**

As shown in **Figure 5**, the boundaries of the natural porous media have been assumed to be impermeable. The possibilities of isotopic fractionation of soil gases by diffusion (Severinghaus et al., 1995) for unconfined aquifer system is not probable while considering the impermeable confined aquifer boundary. Further, the aquifer is subdivided to infinitesimal compartments ( $X_1, X_2, \dots, X_n$ ) with the

boundaries of individual compartments are by and large isothermal but considering the finite length of the aquifer, temperature increases down dip. The porous media has been assumed highly permeable and it is homogenous and isotropic in nature having hydraulic conductivity, structure and diffusive property same in all directions. Therefore, for a gently dipping confined aquifer it is assumed that the area of recharge is very distal and water within the aquifer remains in thermal equilibrium with surrounding having minimal effect of pumping. Therefore, this work assumes a steady state aquifer condition to start with.

### **3.2.3. Analytical model**

Diffusion is a key process through which matter is transported from one part to another part of the system of its random molecular motion and concentration gradient. Thermal diffusion and related fractionation of  $^{18}\text{O}$  in liquid water system with temperature gradient may be best represented by Fick's Law of diffusion (Crank, 1993) which is described by **Equation 17**.

$$F = -D\nabla C$$

**Equation 17:** Fick's Law of diffusion.

When  $F$ =Material flux (g/cm),  $D$ =Diffusion coefficient ( $\text{cm}^2/\text{s}$ ) and  $C$ =Spatial gradient in concentration. Negative sign signifies that the transport is in the direction of decreasing concentration (Criss 1999).

If we restrict the above equation for only one-dimensional transport then the above equation simplifies to following which is described by **Equation 18**.



$$F = -D \frac{\partial C}{\partial x}$$

**Equation 18:** One-dimensional approximation of Fick's Law of diffusion

This work assumes that there exist a steady state aquifer condition and thermal flux, therefore it is not required to apply Laplacian operator ( $\nabla^2$ ) on Fick's Law of diffusion to estimate divergence of the flux through time with respect to concentration in the reference volume.

Now for **Equation 18**, we may replace the variables of one-dimensional Fick's Law of diffusion to fit it in our modeling scenario. In the present modeling scenario, particularly for the initial condition, the distribution of all isotopomers of water are homogeneously distributed before imposing the thermal gradient. Therefore, with this analogy, we can ignore the negative sign of Fick's Law of diffusion for our modeling scenario. Now let us replace " $F$ " by " $I$ " when " $I$ " is heavy isotope concentration. " $\partial C$ " can be replaced by " $\partial C *$ " when " $\partial C *$ " is infinitesimal change of concentration of diffusing heavy isotope. " $I$ " is a function of " $C *$ ". Now only constrain with replacing " $\partial x$ " by " $\partial T$ " (when " $T$ " is temperature) lies with the fact that in the original Fick's Law " $x$ " is a vector quantity whereas " $T$ " which is temperature is a scalar quantity which could be overcome conceptually by means of **Figure 6** with points A, B, C as increasing temperature down dip. Alternately we can also assume that temperature is increasing along " $X$ " axis, where small increment of " $X$ " in positive direction implies an increase in " $T$ ". Therefore, one can substitute " $X$ " by " $T$ ". Now " $D$ " (diffusion constant) can be substituted by

absolute abundance of  $^{18}\text{O}$  ( $2005.12 \pm 0.45$  ppm) reported in VSMOW (Vienna Standard Mean Ocean Water) (Craig, 1961,(b); Baertschi, 1976; O’Neil, 1986). We can use the notation of  $I_{VSMOW}$  for replacing “ $D$ ” as it has been demonstrated that temperature dependent  $^{18}\text{O}$  fractionation could be used as geo-thermometer with respect to  $^{18}\text{O}$  absolute abundance of VSMOW with respect to the reference temperature of  $25^\circ\text{C}$ .

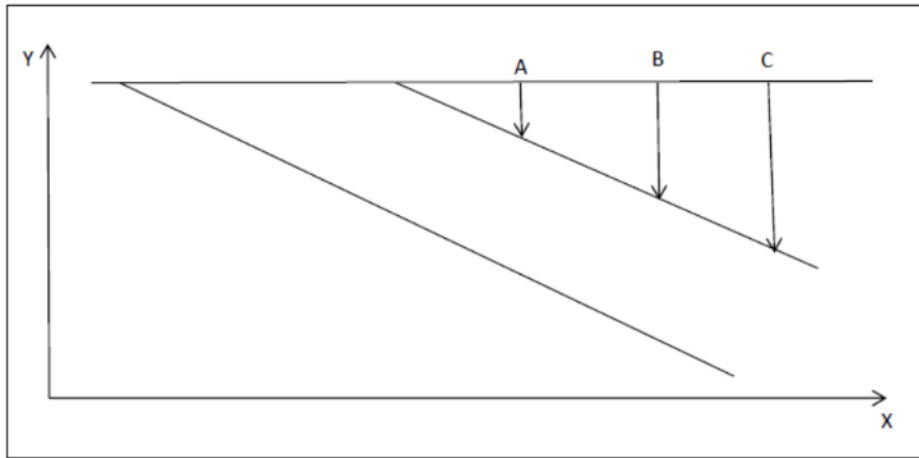


**Figure 6:** Increasing temperature in “X” direction (Schematic diagram, not according to scale).

After rearranging the Fick’s Law of diffusion in one-dimensional transport for stable isotope fractionation due to diffusion becomes

$$I = I_{VSMOW} \frac{\partial C^*}{\partial T}$$

Separating the variables in the above equation, it reduces to

$$\partial T = I_{VSMOW} \frac{\partial C^*}{I}$$

Taking the integral

$$\int \partial T = I_{VSMOW} \int \frac{\partial C^*}{I}$$

Solving it

$$I_{VSMOW} \ln (I) = T + K$$

When, K = Constant

Rearranging the constant the above equation can be written as **Equation 19**.

$$I_{VSMOW} \ln (I) + K^* = T$$

When  $K^* = -K$

**Equation 19:** Initial expression of temperature with isotope concentration.

Concentration of desired heavy isotope is normally expressed in ratio with reference to some international standard which is VSMOW for this work. Therefore, we can replace “ $T$ ” by  $I/I_{VSMOW}$ . For the value of “ $K^*$ ” we can put the absolute value of  $I_{VSMOW}$ ; since it is a constant.

Therefore, the **Equation 19** becomes as follows;

$$I_{VSMOW} \ln (I/I_{VSMOW}) + I_{VSMOW} = T$$

**Equation 20:** Temperature and isotope concentration as VSMOW standard.

Therefore this (**Equation 20**) shows that how a change in temperature may lead to the fractionation of the heavy stable isotope with respect to VSMOW with a corresponding  $^{18}\text{O}$  absolute abundance is  $2005.12 \pm 0.45$  ppm (Craig, 1961; Baertschi, 1976; O'Neil, 1986). The definition of VSMOW do not include any associated temperature with it. Therefore, the reference of VSMOW of **Equation 20** needs to be replaced by VPDB, which incorporates  $25^\circ\text{C}$  benchmark temperature of ocean water at the time of precipitation of carbonate material of *Belemnitella americana* fossil (Coplen et al., 1983; Clark 1997 et al., p 11).

The VPDB is a carbonate material from *Belemnitella americana* fossil of Cretaceous Pee Dee Formation in South Carolina. It is an international reference material of  $^{18}\text{O}/^{16}\text{O}$  ratio used for marine carbonate. It was assumed that the internal calcite structure of the fossil was precipitated from sea water with  $\delta^{18}\text{O}$  very close to VSMOW at  $25^\circ\text{C}$  (Coplen et al., 1983; Clark 1997 et al., p 11). The relation between  $\delta^{18}\text{O}$  of VSMOW and VPDB is linear and described by **Equation 21**.

$$\delta O_{VSMOW}^{18} = 1.03091\delta O_{VPDB}^{18} + 30.91$$

**Equation 21:** Linear relationship of VSMOW and VPDB.

Rearranging the equation, we can write

$$\frac{\delta O_{VSMOW}^{18}}{1.03091} - 29.98 = \delta O_{VPDB}^{18}$$

Now we can rewrite **Equation 20** by replacing VSMOW by VPDB as described by **Equation 22**.

$$I_{VPDB} \ln (I/I_{VPDB}) + I_{VPDB} = T$$

**Equation 22:** Temperature and isotope concentration as VPDB standard.

Reported value of  $^{18}\text{O}/^{16}\text{O}$  for VPDB is  $(2067.1 \pm 2.1) \times 10^{-6}$  (Urey et al., 1951; Cuna et al., 2001; Werner et al., 2001) at  $25^\circ\text{C}$  which may be translated to the absolute abundance of  $^{18}\text{O}$  in VPDB is  $2067.1 \pm 2.1$  ppm at that temperature. However, we are dealing with water and reported absolute  $^{18}\text{O}$  absolute abundance in ocean water was  $2005.12 \pm 0.45$  ppm at  $25^\circ\text{C}$  at the time of precipitation of VPDB. Therefore, it can be assumed that absolute abundance of  $^{18}\text{O}$  at  $25^\circ\text{C}$  for liquid water system is 2005.12 ppm. As the VSMOW values are changed to VPDB standard, it has been considered a standard deviation corresponding to absolute abundance of  $^{18}\text{O}$  at  $25^\circ\text{C}$  which is  $\pm 2.1$  ppm and not  $\pm 0.45$  ppm. It is important to note that changing the reference from VSMOW to VPDB, the absolute abundance of  $^{18}\text{O}$  (in ppm) in the water sample will remain unchanged. This conversion of standard is only required to put a benchmark temperature which is  $25^\circ\text{C}$  corresponding to absolute abundance of  $^{18}\text{O}$  2005.12 ppm in the proposed deterministic analytical model.

For a given water sample, we can get  $\delta^{18}\text{O}_{VSMOW}$  by stable isotope mass spectrometry (either IRMS or Laser Water Isotope Analyzer) and can convert it to  $\delta^{18}\text{O}_{VPDB}$  from the above-mentioned linear relation of **Equation 21**. Considering the basic equation of  $\delta$  (‰) the calculation of absolute abundance of  $^{18}\text{O}$  in ppm may be expressed by **Equation 23**.

$$\delta_x = 1000 \left( \frac{x}{R_{std}} - 1 \right)$$

**Equation 23:** Calculation of  $^{18}\text{O}$  absolute abundance in ppm from reported  $\delta$  value by analysis.

When “ $\delta_x$ ” is the value reported in per-mill (‰). “ $R_{std}$ ” refers to the isotopic ration in the standard which is VPDB with absolute abundance of  $2067.1 \pm 2.1$  ppm at  $25^\circ\text{C}$  and “ $x$ ” is the ratio of  $^{18}\text{O}/^{16}\text{O}$ . Now the only unknown quantity is “ $x$ ” in the **Equation 23**, which can be solved to give the absolute abundance of  $^{18}\text{O}$  in ppm. Towards these conversion, the spreadsheet software “Isotemp” associated with this publication was used.

**Equation 22** shows that all the parameters at left hand side are known in which the  $\frac{I}{I_{VPDB}}$  term may have three possible outcomes. The ratio will be either greater than 1 or less than 1 or equal to 1. Taking under consideration of three possible outcomes; if  $(I/I_{VPDB})$  is greater than 1 ( $I/I_{VPDB} > 1$ ) then;  $\ln(I/I_{VPDB})$  is a positive fraction which will give absolute abundance of  $^{18}\text{O}$  greater than the benchmark of 2005.12 ppm. It means that it will indicate temperature lower than  $25^\circ\text{C}$ . If  $(I/I_{VPDB})$  is less than 1 ( $I/I_{VPDB} < 1$ ) then;  $\ln(I/I_{VPDB})$  is a negative fraction which will give absolute abundance of  $^{18}\text{O}$  lesser than the benchmark of 2005.12 ppm. It implies that it will indicate the temperature higher than  $25^\circ\text{C}$ . Considering the last scenario if the expression  $(I/I_{VPDB})$  is equal to 1 ( $I/I_{VPDB} = 1$ ) then; absolute abundance of  $^{18}\text{O}$  will be 2005.12 ppm and will indicate the temperature equal to  $25^\circ\text{C}$ .

Therefore, we can get a number in terms of  $^{18}\text{O}$  absolute abundance corresponding to a particular temperature “ $T$ ” with reference to the benchmark temperature of

25°C. The  $^{18}\text{O}$  geothermometer will work in such a way that how much the water is warmer or cooler in absolute temperature scale with respect to 25°C. Therefore, with varied scenarios of  $I/I_{VPDB}$  we get  $^{18}\text{O}$  absolute abundance either greater or lesser or equal to 2005.12 ppm. This will indicate temperature either lesser or greater or equal to 25°C respectively.

An attempt was made to validate the theoretical model by fractionating  $^{18}\text{O}$  in liquid water system with imposed temperature gradient in controlled laboratory setup with satisfying the required initial and boundary conditions. The experimental details are described in **Section 3.3** as follows.

### **3.3. Laboratory experimental work**

Earlier studies on isotope fractionation of water for multiphase system i.e. water-vapor, or ice-vapor suggest that fractionation of  $\delta^{18}\text{O}$  is 0.7 per mil per °C and 6 per mill per °C for  $\delta^2\text{H}$  6. (Masters et al., p 506). The experimental approach adopted in this work is designed to fractionate  $^{18}\text{O}$  in controlled laboratory condition in liquid water system with imposed temperature gradient undergoing no phase change of water. A brief description of the same is as follows.

#### **3.3.1. Experimental set up and design**

The set-up attempts to simulate a confined aquifer system satisfying the boundary conditions and initial conditions of  $^{18}\text{O}$  geothermometer. It ensures to make it thermally isolated and closed system from the ambient as well as minimize radiation heat loss. The experimental apparatus has **(Plate 1 to 5)** fabricated

components which are custom made for the purpose in the local workshop (J.S. Enterprises).

To replicate a confined aquifer system with impermeable boundary condition a six-inch-long brass tube (Cu 70% and Zn 30%) has been used. It has the diameter of approximately one-inch having thermal conductivity of nearly 111.0 W/m K. It is kept gently dipping ( $\approx 15^\circ$ ) with help of standing clamp and is wrapped with alternate aluminum foil and glued transparent plastic tape to minimize the heat loss (**Plate 1** and **Plate 2**) providing with thermal isolation.

A desired temperature gradient was maintained at the two ends of the brass tube using free circulating water bath through conduit (**Plate 2**). Further, to maintain ambient temperature adjacent to the brass tube another water bath of small open water tank within the plastic casing was used (**Plate 3**). The entire experimental setup was covered by six millimeters thick transparent plastic Polyvinyl chloride (PVC) casing for thermal isolation (**Plate 4**).

Therefore, in this set-up, the heat exchange with air and free circulating water maintains the desired temperature in the small open tank within the casing after certain time. For a desired water bath temperature at two ends of the brass tube and the water bath controlling the casing air temperature it took approximately six hours to get everything thermally equilibrated. Quantity of water was kept constant for all water bath tanks (**Plate 5**) at approximately five liters which was a mixture solution of 1:1 ratio of ethaline glycol and water. Microprocessor based temperature indicator was used to digitally display all the temperatures of different components



of the experimental apparatus. To sense the temperature, three wire resistance temperature detector (RTD) input of PT 100 sensor (make MULTISPAN) were used with 220 Volt operating voltage (**Plate 4**). Once the desired temperature equilibrium is achieved, (6 Hrs)  $\approx$ 2 ml water sample was collected by removing the PVC casing and perforating the septa as documented by **Plate 2** with the help of a clinical syringe from either ends for their  $^{18}\text{O}$  analysis. During the water sample collection from up dip, the septa was perforated first to avoid the possibility of isotopic mixing of water within the apparatus. The entire assembly of the experimental set-up was put together with **Illustration** as (1-10) in **Plate 1-5**.

**Plate 1** documents  $14^\circ$  dip of the experimental tube measured by Brunton Compass.

**Plate 2** documents brass tube wrapped by alternate aluminum foil and glued plastic tape to minimize radiation heat loss (**Illustration 1**). **Plate 2** also documents conduit to circulate water bath of desired temperature at two ends of the brass tube to make desired temperature gradient (**Illustration 2**). Septa attached at two ends of brass tube to collect water sample perforated by clinical syringe has been documented by **Plate 2 (Illustration 3)**. **Plate 3** documents small water tank with continuous flow of water of desired temperature to control the ambient temperature adjacent to brass tube within the casing of experimental apparatus (**Illustration 4**).

**Plate 4** documents experimental apparatus covered by PVC casing (**Illustration 5**).

In addition, **Illustration 6** and **Illustration 7** of **Plate 4** document RTD sensors attached to experimental apparatus to measure temperature of its different components and digital thermometer to monitor room temperature respectively.

**Plate 5** is the photographic documentation of the experimental apparatus in fully

functional mode. **Illustration 8** of the plate document programmable microprocessor based temperature controlling and displaying switch to main desired temperature in the main water bath tanks. **Illustration 9** and **Illustration 10** of the same plate documents main water bath tanks and digital temperature display panel of different components of experimental apparatus.

Throughout the experiment, the Milli-Q water of Resistivity 18.2M $\Omega$ -cm at 25°C and conductivity 0.055  $\mu$ S/cm was used. The main purpose of the experiment was just to fractionate  $^{18}\text{O}$  with imposed temperature and therefore for keeping other parameters constant and therefore the initial  $^{18}\text{O}$  absolute abundance of Milli-Q water was not an imperative information. Initially the experiment was conducted by filling the brass tube with highly porous and permeable sand of approximately  $\phi$  scale of -1.0 and saturated with Milli-Q water to replicate a highly porous confined aquifer system justifying  $Ra_c \approx 40$  to onset free unicellular thermal convection. Towards these following values were assumed for different parameters of **Equation 12** to calculate permeability ( $K$ ).

When,  $K$ = permeability of medium,  $g$  = acceleration due to gravity (9.8m/sec<sup>2</sup>),  $\sigma$  = volumetric thermal expansion coefficient of the fluid (2.0 x 10<sup>-4</sup> K<sup>-1</sup>),  $(\rho C)t$  = volumetric heat capacity of fluid(4x10<sup>6</sup> Watt-sec/m<sup>3</sup>;Pryor 1971),  $H$  = thickness of the porous layer (0.0254 m; which is equivalent to one inch),  $\Delta t$  = temperature difference across the layer (10°C),  $\gamma$  = kinematic viscosity of the fluid (4x10<sup>-7</sup> m<sup>2</sup>/sec),  $\lambda^*$  = effective thermal conductivity of the fluid filled medium (1.4Watt/m<sup>2</sup>.K) (Combarous; 1975).

All those parameters were put into **Equation 12** and taking  $Ra_c$  of 39, which is less than but very close to 40 the permeability of the medium, ( $K$ ) was  $8 \times 10^{-10}$  meter<sup>2</sup> which is quite similar to the unconsolidated well sorted highly permeable medium to coarse sand of  $\phi$  scale -1.25 to +1. It is within the range of permeability reported by Freeze et al., (1979; p 29) for clean coarse sand with permeability range from  $10^{-8}$  meter<sup>2</sup> to  $10^{-12}$  meter<sup>2</sup>.

Considering the value of  $8 \times 10^{-10}$  meter<sup>2</sup> for permeability ( $K$ ) for the porous media of unconsolidated highly pervious very coarse sand of  $\phi$  scale -1.25 to +1 hydraulic conductivity is calculated for the porous media under consideration by **Equation 24**.

$$K = k \frac{\mu}{\rho g}$$

**Equation 24:** Relation of permeability and hydraulic conductivity.

When  $K$ = Permeability,  $k$ =Hydraulic conductivity,  $\mu$ =Dynamic viscosity of the fluid,  $\rho$ =Density of the fluid,  $g$ =Acceleration due to gravity.

Now putting the corresponding values of  $K= 8 \times 10^{-10}$  meter<sup>2</sup>,  $\mu = 0.001002$  kg/meter.second,  $\rho = 1000$ kg/meter<sup>3</sup>,  $g = 9.8$  meter/second<sup>2</sup> (all the reported values are of general agreement) in **Equation 24**, corresponding hydraulic conductivity ( $k$ ) yielded to  $0.8 \times 10^{-2}$  centimeter/second. It is quite consistent within the upper range of reported values of hydraulic conductivity for unconsolidated highly pervious coarse sand (Bear, 1988; p 136, Fetter, 2001; p85). Therefore, choice of well-sorted very coarse sand of  $\phi$  scale -1.0; having grain diameter of

approximately 2.0 millimeter to 1.7 millimeter is realistic to make the hydraulic conductivity of the experimental apparatus consistent as per **Equation 12**. Therefore, this water saturated pervious porous media when subjected to the external temperature gradient it is likely to onset the free laminar convection and eventually results in isotope fractionation.

Earlier studies (Wood et al., 1982) suggested that the feasibility of unicellular laminar convection is better met for the dip of the strata very close to  $15^\circ$ . Therefore, throughout the experiment, the dip of the brass tube was kept constant at  $14^\circ$ . Considering value of  $\text{Cos}(14^\circ)$  which is 0.97 the  $Ra_c$  comes to 38, which is quite close to  $\approx 40$  and is suitable to initiate free laminar convection.

Experiment was conducted for the temperature range of  $10^\circ\text{C}$  to  $50^\circ\text{C}$  with  $10^\circ\text{C}$  equal incremental interval; that is  $10\text{-}20^\circ\text{C}$ ,  $10\text{-}30^\circ\text{C}$  and so on. Justification behind selecting this temperature range was to void the higher temperature regime to minimize the chances of water-vapor phase change. Moreover, considering  $25^\circ\text{C}/\text{km}$  geothermal gradient (Turner and Verhoogen., 2004); (Lawrie, 2007) this temperature range can accommodate  $^{18}\text{O}$  fractionation up to the depth of two kilometer, which covers the depth of availability of fresh groundwater in shallow subsurface. The first temperature gradient was maintained between  $10^\circ\text{C}$  to  $20^\circ\text{C}$ , which approximately six hours for equilibration. After that the water samples ( $\approx 2$  ml) were collected from two ends of the experimental brass tube by perforating the septa. After the sampling, water within the apparatus was drained and the brass tube were dried so that there is no water inside into the apparatus. For next temperature

gradient, with fresh Milli-Q water and sand was put under the gradient of 10°C to 30°C and same procedure was performed to collect corresponding samples. The experiment was further extended to 10°C to 50°C gradient. For each and individual temperature gradient, the ambient temperature of the casing as well as the room temperature were kept approximately 25°C. This helped to maintain the required temperature gradient at the two ends of the brass tube.

While controlling ambient temperature the basic principle stands on the fact that there will be constant adiabatic heat exchange between free circulating water bath and air of the apparatus casing. Since specific heat of water (1 calorie/gram) is quite high than the specific heat of dry air (0.24 calorie/gram) therefore heat capacity of water is also very high with respect to dry air. Therefore, in the process of heat exchange between water bath and apparatus casing air the water bath will gain or lose insignificant amount of heat, which can be neglected.

### **3.3.2. Instrumentation for the isotope analyses**

A state of the art Laser Water Isotope Analyzer (PICARRO make model L1102-i) was used for isotope analysis. The apparatus takes 1.9 µml of water sample for isotope analysis in a single suction. Then it evaporates the whole sample instantaneously before putting it into the gas cell/cavity. In the gas cavity, symmetrically tuned laser of each 1 Hz is pass to generate absorption spectra in near IR spectral range for different isotopomers (e.g. H<sub>2</sub>O, H<sup>2</sup>HO) of water present in the sample. The absorption line intensity or area under the peak is linearly dependent on concentration of different isotopomers of water present in the gas cell

or cavity. Therefore,  $^{18}\text{O}/^{16}\text{O}$  ratio can be calculated with sufficient accuracy and precision. This instrument rejects any salt present in the water sample by the process of evaporation and reports  $^{18}\text{O}/^{16}\text{O}$  ratio exclusive to water sample. Therefore, salt effect on isotope fractionation may not be considered at the time of reporting the data generated from this experiment. Alternately, one can adopt simple salt rejection technique as explained in **Section 2.4.1** to prepare water sample for isotope analysis by IRMS.

### **3.4. Limitations of the model**

Limitations of this model lie with the assumptions that are made particularly in terms of material property and associated boundary conditions. Here it assumes that the aquifer is homogeneous and is highly permeable with skeleton structure, hydraulic conductivity and similar diffusive property in all directions along with impermeable boundary. However, despite a good portrayal of natural set up, these assumptions may not hold good in the field conditions leading to considerable uncertainties in temperature estimation of groundwater.

The model works fine in confined aquifer condition to estimate groundwater temperature but it is not suitable for unconfined aquifer or water table condition, which remains prone to an open surface evaporation. Therefore, groundwater in unconfined aquifer or water table condition will constantly be enriched in heavy isotope ( $^{18}\text{O}$ ). In addition, every storm event may add water from precipitation to the unconfined aquifer, which will change the isotopic composition due to simple mixing of rainwater with aquifer water. This makes the isotopic composition of

unconfined aquifer is quite similar to the isotopic composition of local precipitation.

In principle, it is also limited by the cases where considerable recharge alters the isotopic composition of confined aquifer system. However, contribution of water as recharge to confined aquifer is a very slow process and mainly dependent on hydraulic conductivity of the aquifer material. Considering the recharge, which is a very slow process along with long residence time of water, it is assumed that aquifer system will be in thermal equilibrium with the surrounding. This will lead to fractionation of  $^{18}\text{O}$  in the liquid water of aquifer as per its thermal stability region. Further, this model assumes a steady state aquifer condition with minimal and negligible effect of pumping which may not hold good in the field condition. Here we cannot ignore the effect of pumping at the time of taking the water sample from aquifer for isotopic analysis. It needs to make sure that all the pumping wells are shut down and the aquifer is given enough time to recover the pumping effect. In addition, adequate time should be given to the aquifer water to become equilibrated with ambient geothermal gradient assuming temperature dependent isotopic fractionation is an instantaneous process.

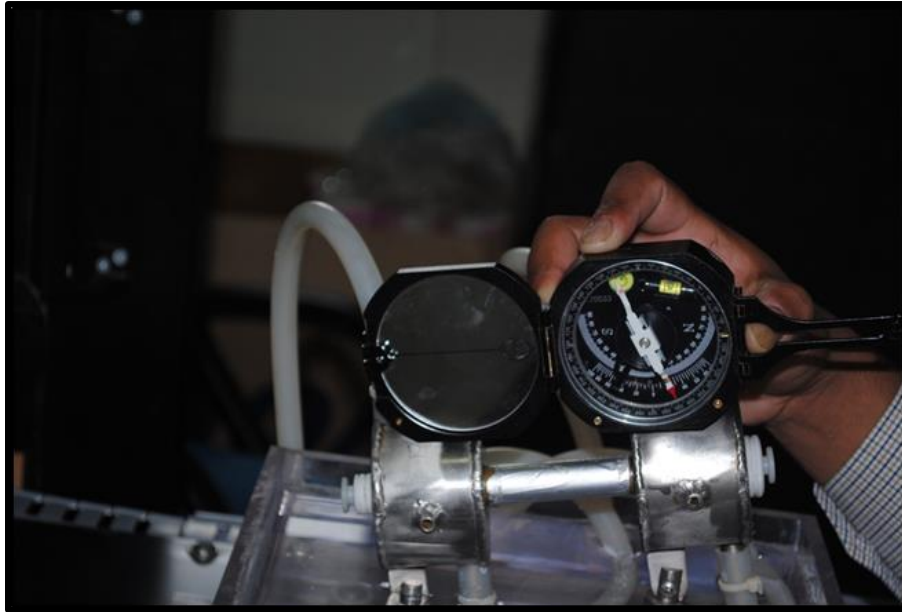


**Plate 1 :** Experimental apparatus kept at an angle of  $14^\circ$  dip.

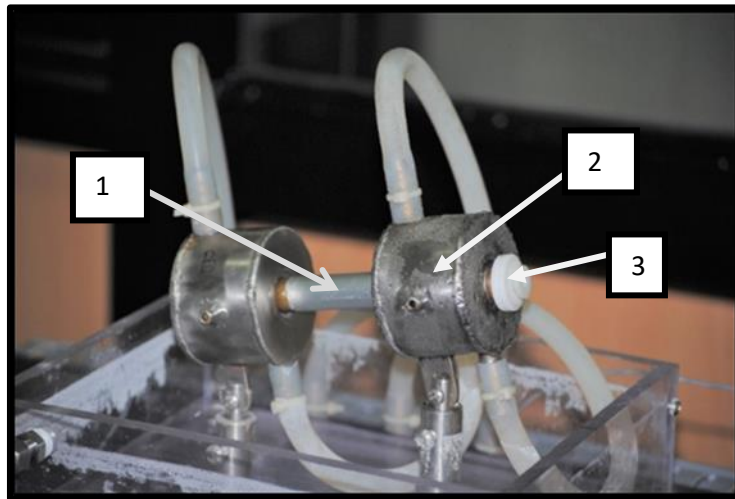


**Plate 2:** Experimental brass tube alternately wrapped with aluminum foil and glued plastic tape to minimize radiation heat loss.





**Plate 3:** Free circulating water bath adjacent to experimental tube to maintain desired adjacent temperature with the PVC casing.

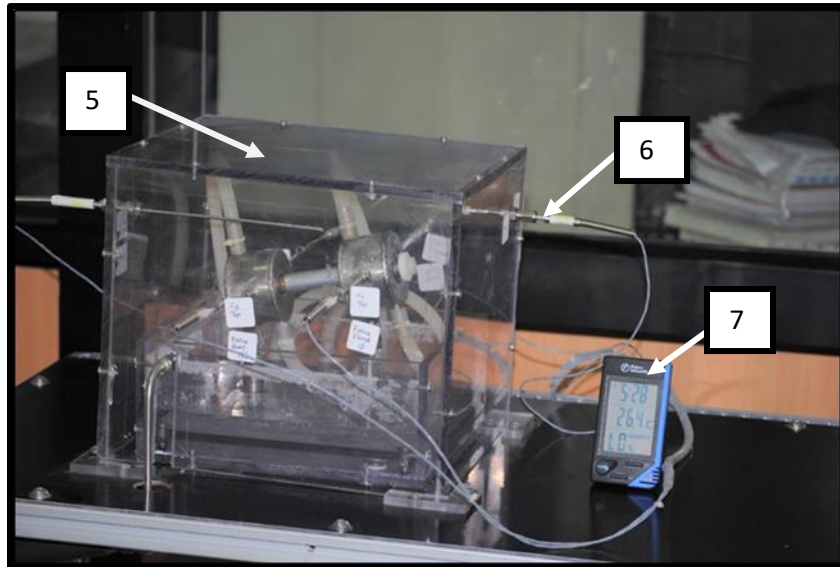


**Plate 4:** Experimental apparatus covered by PVC casing to make it thermally isolated from ambient geared with RTD sensors to measure temperature of different components of the apparatus.

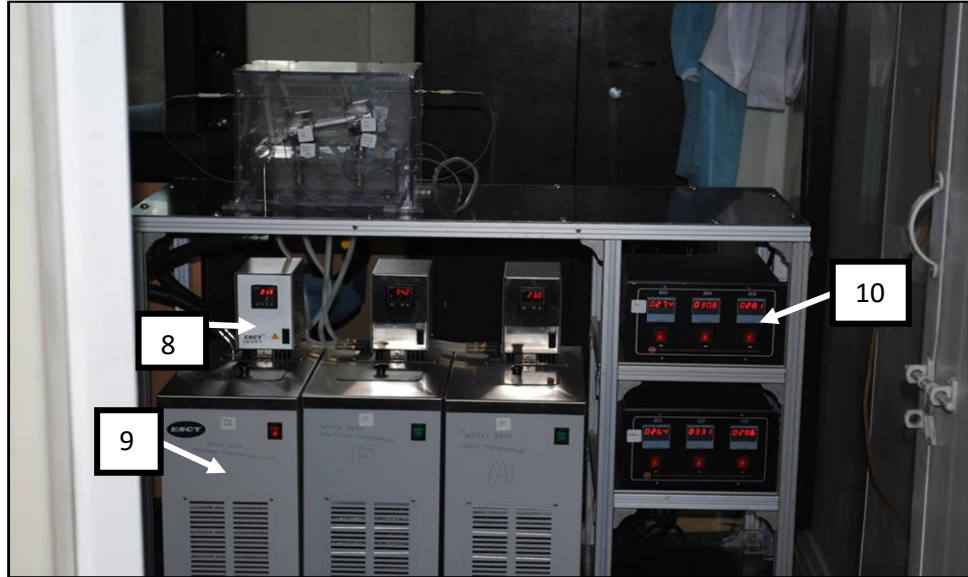


**Plate 5:** Experimental apparatus in fully functional mode.

## **Chapter 4**

### **Research outcome**

#### 4. Outcome of the work

The proposed deterministic analytical model aims to estimate groundwater temperature using the isotopic fractionation ( $^{18}\text{O}$ ) under imposed temperature gradient simulating a gently dipping confined aquifer system in laboratory condition. The experimental work is carried out to supplement the proposed theoretical model for estimating groundwater temperature in confined aquifers under field condition. The experimental work has been able to generate a good dataset, which satisfies the physical fractionation of  $^{18}\text{O}$  in liquid water system with a temperature gradient below  $100^\circ\text{C}$ . Thus, it provides the basis for the proposition that for a gently dipping confined aquifer system,  $^{18}\text{O}$  stratification occurs owing to heat as the primary cause. Further, this temperature dependent  $^{18}\text{O}$  fractionation in liquid water system can also be extended to estimate the groundwater temperature of subsurface reservoir.

However, initial attempt to fractionate  $^{18}\text{O}$  with experimental apparatus filled with coarse sand (approximately  $\phi$  scale of -1.0) and saturated with Milli-Q water, the experimental apparatus could not able to fractionate  $^{18}\text{O}$  for any temperature gradient and thermal equilibration time of one day.

To overcome the initial difficulty the experiment was conducted by removing porous sand where the brass tube of the experimental apparatus was only filled with Milli-Q water, keeping all the thermal conditions same as discussed in **Section 3.3.1**. Now this experimental set up represents a simplified version of a confined aquifer. Under these conditions, the system was allowed to equilibrate and  $^{18}\text{O}$  was

fractionated for each temperature gradient for thermal equilibration time of six hours. In the first part of the experimental work, significant fractionation of  $^{18}\text{O}$  was first noted at 10°C-20°C temperature interval. The analytical protocols are briefly given as follows.

#### **4.1. Statistical analysis of the data**

Individual water sample corresponding to a particular temperature was analyzed using a Laser Water Isotope Analyzer (PICARO, USA) following the principals of cavity ring down spectroscopy. It made five measurements for every water sample for a better statistical analysis which were done with the help of spreadsheet software (EXCEL © Microsoft). The data was reported in ( $\delta^{18}\text{O}$ ) in VSMOW standard which was converted to VPDB standard (**Equation 21**) as per the proposed deterministic model, without any change the  $^{18}\text{O}$  absolute abundance (ppm) in the water samples. **Table 9** represents the experimentally derived  $\delta^{18}\text{O}$  values and absolute abundance of  $^{18}\text{O}$  with mean and standard deviation of each sample population corresponding to a particular temperature. Maximum fractionation of  $^{18}\text{O}$  recorded for the temperature gradient of 10°C-30°C which was found to be 0.7 ppm. **Table 10** represents systematically model derived absolute abundance of  $^{18}\text{O}$  for the same temperature. In **Table 10**, values of column “K” were taken from seventh column of **Table 9**. **Table 11** represents mean and standard deviation of model derived  $^{18}\text{O}$  absolute abundance of each small sample population corresponding to a particular temperature. The major finding indicates that the “experimentally derived” and “model derived”  $^{18}\text{O}$  absolute abundance are

within the internationally accepted standard deviation of absolute abundance  $^{18}\text{O}$  of VPDB that is  $\pm 2.1$  ppm for the temperature range covered in this experimental work.

**Table 9:** Experimentally derived  $\delta^{18}\text{O}$  values and absolute abundance of  $^{18}\text{O}$  with their corresponding mean and standard deviation of each small sample population corresponding to a particular temperature.

Sl No	Temp (°C)	$\delta^{18}\text{O}$ VSMOW	Mean	$\pm$ SD ( $\delta$ VSMOW)	$\delta^{18}\text{O}$ (VPDB)	$^{18}\text{O}$ absolute abundance (ppm)	Mean	$\pm$ SD
<i>10°C to 20°C temperature interval</i>								
1	10	-6.487	-6.668	0.113	-36.276	1992.114	1991.752	0.228
2	10	-6.720			-36.502	1991.647		
3	10	-6.710			-36.492	1991.667		
4	10	-6.639			-36.423	1991.810		
5	10	-6.784			-36.564	1991.519		
6	20	-6.575	-6.752	0.112	-36.361	1991.938	1991.583	0.224
7	20	-6.753			-36.534	1991.581		
8	20	-6.764			-36.544	1991.559		
9	20	-6.884			-36.661	1991.318		
10	20	-6.784			-36.564	1991.519		
<i>10°C to 30°C temperature interval</i>								
11	10	-5.624	-5.680	0.050	-35.439	1993.845	1993.732	0.100
12	10	-5.673			-35.486	1993.747		
13	10	-5.696			-35.508	1993.701		
14	10	-5.756			-35.567	1993.580		
15	10	-5.653			-35.467	1993.787		
16	30	-6.477	-6.054	0.249	-36.266	1992.135	1992.983	0.500
17	30	-6.074			-35.875	1992.943		
18	30	-5.953			-35.758	1993.185		
19	30	-5.892			-35.699	1993.308		
20	30	-5.872			-35.679	1993.348		
<i>10°C to 40°C temperature interval</i>								
21	10	-6.726	-6.746	0.047	-36.508	1991.635	1991.596	0.095
22	10	-6.818			-36.597	1991.451		
23	10	-6.743			-36.524	1991.601		
24	10	-6.754			-36.535	1991.579		

25	10	-6.688			-36.471	1991.711		
26	40	-6.845	-6.848	0.051	-36.623	1991.397	1991.391	0.102
27	40	-6.790			-36.570	1991.507		
28	40	-6.861			-36.639	1991.365		
29	40	-6.819			-36.598	1991.449		
30	40	-6.925			-36.701	1991.236		
<i>10°C to 50°C temperature interval</i>								
31	10	-6.718	-6.776	0.048	-36.500	1991.651	1991.535	0.096
32	10	-6.771			-36.551	1991.545		
33	10	-6.770			-36.550	1991.547		
34	10	-6.770			-36.550	1991.547		
35	10	-6.851			-36.629	1991.385		
36	50	-7.260	-7.094	0.097	-37.026	1990.565	1990.897	0.195
37	50	-7.085			-36.856	1990.915		
38	50	-7.079			-36.850	1990.927		
39	50	-7.023			-36.796	1991.040		
40	50	-7.024			-36.797	1991.038		

The experimental work of temperature dependent  $^{18}\text{O}$  fractionation is a bivariate system where temperature remains independent variable. It needs to be plot along abscissa (X-axis) while  $^{18}\text{O}$  absolute abundance is dependent variable represented along ordinate (Y-axis) in the scatter plot (Mendenhall et al., 2002). The results are presented in the **Figure 7 to 10** showing  $^{18}\text{O}$  fractionation pattern for different temperature intervals. Blue dots in the graph represents individual  $^{18}\text{O}$  measurements (in ppm) with their standard error bar; whereas orange dots represent the arithmetic mean of each small sample population. **Figure 11** represents cross correlation of arithmetic mean of “experimentally derived” and “model derived” small sample population of  $^{18}\text{O}$  absolute abundance corresponding to different temperature interval adopted in this experimental work. The cross correlation shows a strong linear relationship.

**Table 10:** Detail calculation of model derived absolute abundance of <sup>18</sup>O.

	J	K	L	M	N	O	P
Sl No	VPDB	Absolute abundance( <sup>18</sup> O) in ppm	(K/J)	Ln(K/J)	VPDB*M	Theoretical <sup>18</sup> O abundance in ppm(VPDB+N)	Temp(°C)
<i>10°C to 20°C temperature interval</i>							
1	2067.1	1992.114	0.964	-0.037	-76.379	1990.721	10
2	2067.1	1991.647	0.963	-0.037	-76.864	1990.236	10
3	2067.1	1991.667	0.964	-0.037	-76.843	1990.257	10
4	2067.1	1991.810	0.964	-0.037	-76.696	1990.404	10
5	2067.1	1991.519	0.963	-0.037	-76.997	1990.103	10
6	2067.1	1991.938	0.964	-0.037	-76.563	1990.537	20
7	2067.1	1991.581	0.963	-0.037	-76.933	1990.167	20
8	2067.1	1991.559	0.963	-0.037	-76.956	1990.144	20
9	2067.1	1991.318	0.963	-0.037	-77.206	1989.894	20
10	2067.1	1991.519	0.963	-0.037	-76.997	1990.103	20
<i>10°C to 30°C temperature interval</i>							
11	2067.1	1993.845	0.965	-0.036	-74.585	1992.515	10
12	2067.1	1993.747	0.965	-0.036	-74.687	1992.413	10
13	2067.1	1993.701	0.964	-0.036	-74.734	1992.366	10
14	2067.1	1993.580	0.964	-0.036	-74.859	1992.241	10
15	2067.1	1993.787	0.965	-0.036	-74.645	1992.455	10
16	2067.1	1992.135	0.964	-0.037	-76.359	1990.741	30
17	2067.1	1992.943	0.964	-0.037	-75.520	1991.580	30
18	2067.1	1993.185	0.964	-0.036	-75.269	1991.831	30
19	2067.1	1993.308	0.964	-0.036	-75.142	1991.958	30
20	2067.1	1993.348	0.964	-0.036	-75.100	1992.000	30
<i>10°C to 40°C temperature interval</i>							
21	2067.1	1991.635	0.963	-0.037	-76.877	1990.223	10
22	2067.1	1991.451	0.963	-0.037	-77.068	1990.032	10
23	2067.1	1991.601	0.963	-0.037	-76.912	1990.188	10
24	2067.1	1991.579	0.963	-0.037	-76.935	1990.165	10
25	2067.1	1991.711	0.964	-0.037	-76.798	1990.302	10
26	2067.1	1991.397	0.963	-0.037	-77.124	1989.976	40
27	2067.1	1991.507	0.963	-0.037	-77.010	1990.090	40
28	2067.1	1991.365	0.963	-0.037	-77.158	1989.942	40
29	2067.1	1991.449	0.963	-0.037	-77.070	1990.030	40
30	2067.1	1991.236	0.963	-0.037	-77.291	1989.809	40
<i>10°C to 50°C temperature interval</i>							
31	2067.1	1991.651	0.964	-0.037	-76.860	1990.240	10



32	2067.1	1991.545	0.963	-0.037	-76.970	1990.130	10
33	2067.1	1991.547	0.963	-0.037	-76.968	1990.132	10
34	2067.1	1991.547	0.963	-0.037	-76.968	1990.132	10
35	2067.1	1991.385	0.963	-0.037	-77.137	1989.963	10
36	2067.1	1990.565	0.963	-0.038	-77.988	1989.112	50
37	2067.1	1990.915	0.963	-0.038	-77.624	1989.476	50
38	2067.1	1990.927	0.963	-0.038	-77.612	1989.488	50
39	2067.1	1991.040	0.963	-0.037	-77.495	1989.605	50
40	2067.1	1991.038	0.963	-0.037	-77.497	1989.603	50

**Table 11:** Model derived  $^{18}\text{O}$  absolute abundance with their mean and standard deviation of each small sample population corresponding to a particular temperature.

SI No	Temp(°C)	$^{18}\text{O}$ absolute abundance (ppm)	Mean	$\pm$ SD
<i>10°C to 20°C temperature interval</i>				
1	10	1990.721	1990.344	0.236
2	10	1990.236		
3	10	1990.257		
4	10	1990.404		
5	10	1990.103		
6	20	1990.537	1990.169	0.232
7	20	1990.167		
8	20	1990.144		
9	20	1989.894		
10	20	1990.103		
<i>10°C to 30°C temperature interval</i>				
11	10	1992.515	1992.398	0.104
12	10	1992.413		
13	10	1992.366		
14	10	1992.241		
15	10	1992.455		
16	30	1990.741	1991.622	0.519
17	30	1991.580		
18	30	1991.831		
19	30	1991.958		

20	30	1992.000		
<i>10°C to 40°C temperature interval</i>				
21	10	1990.223	1990.182	0.099
22	10	1990.032		
23	10	1990.188		
24	10	1990.165		
25	10	1990.302		
26	40	1989.976	1989.969	0.106
27	40	1990.090		
28	40	1989.942		
29	40	1990.030		
30	40	1989.809		
<i>10°C to 50°C temperature interval</i>				
31	10	1990.240	1990.119	0.099
32	10	1990.130		
33	10	1990.132		
34	10	1990.132		
35	10	1989.963		
36	50	1989.112	1989.457	0.202
37	50	1989.476		
38	50	1989.488		
39	50	1989.605		
40	50	1989.603		

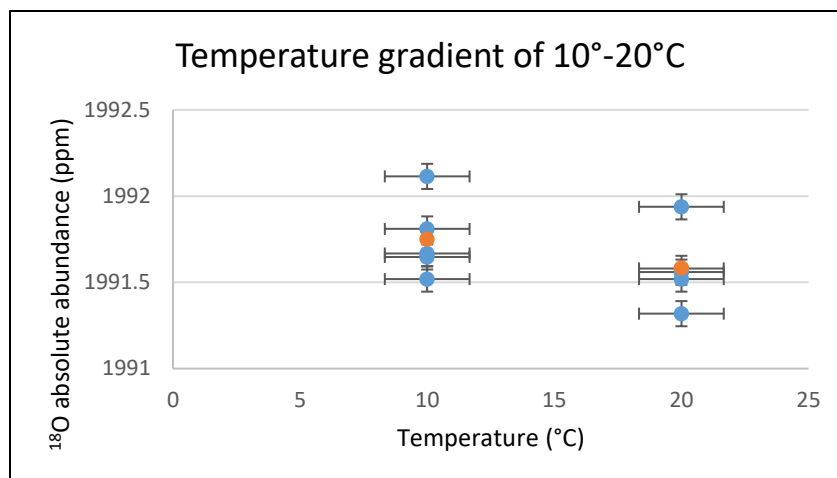


**Figure 7:** Fractionation of  $^{18}\text{O}$  in absolute abundance for the temperature range of 10°C to 20°C. Blue color dots are individual  $^{18}\text{O}$  measured data and orange color dots are mean of each small population. Maximum  $^{18}\text{O}$  fractionation corresponding to mean is 0.168 ppm.

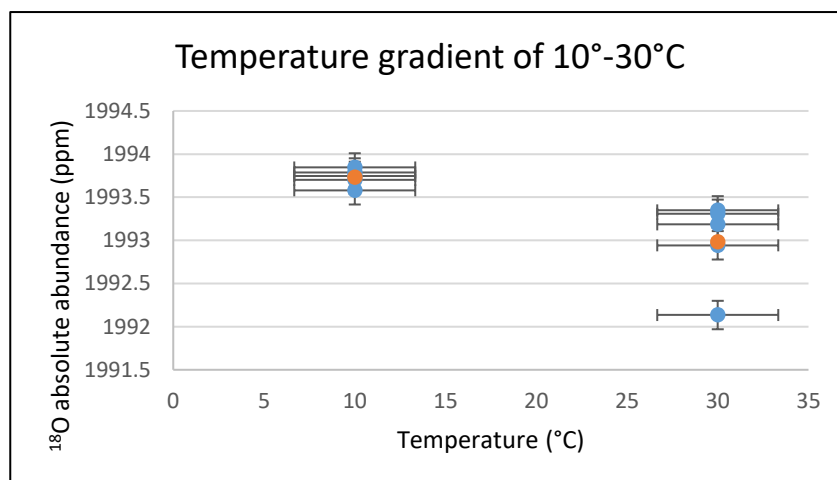


**Figure 8:** Fractionation of  $^{18}\text{O}$  in absolute abundance for the temperature range of 10°C to 30°C. Blue color dots are individual  $^{18}\text{O}$  measured data and orange color dots are mean of each small population. Maximum  $^{18}\text{O}$  fractionation corresponding to mean is 0.748 ppm.

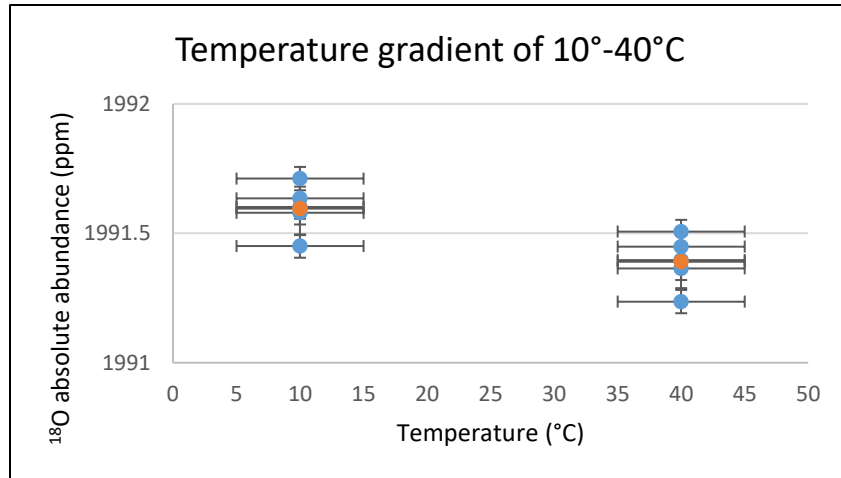


**Figure 9:** Fractionation of  $^{18}\text{O}$  in absolute abundance for the temperature range of  $10^{\circ}\text{C}$  to  $40^{\circ}\text{C}$ . Blue color dots are individual  $^{18}\text{O}$  measured data and orange color dots are mean of each small population. Maximum  $^{18}\text{O}$  fractionation corresponding to mean is 0.205 ppm.

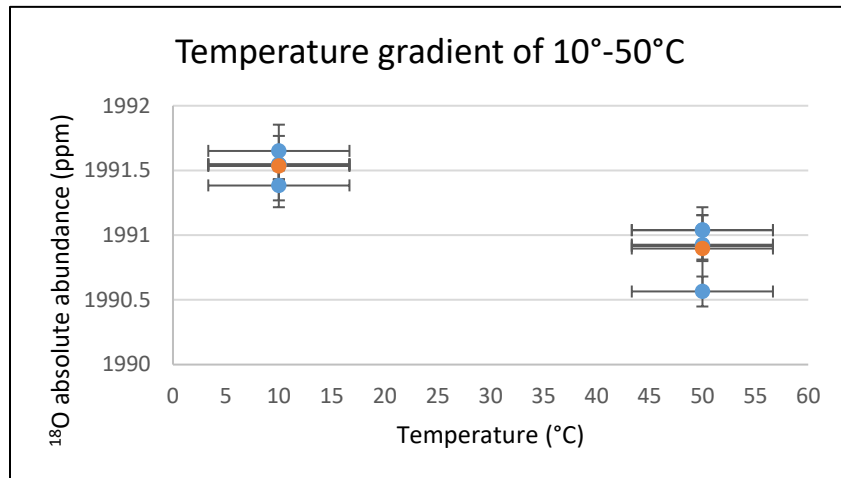


**Figure 10:** Fractionation of  $^{18}\text{O}$  in absolute abundance for the temperature range of  $10^{\circ}\text{C}$  to  $50^{\circ}\text{C}$ . Blue color dots are individual  $^{18}\text{O}$  measured data and orange color dots are mean of each small population. Maximum  $^{18}\text{O}$  fractionation corresponding to mean is 0.638 ppm.

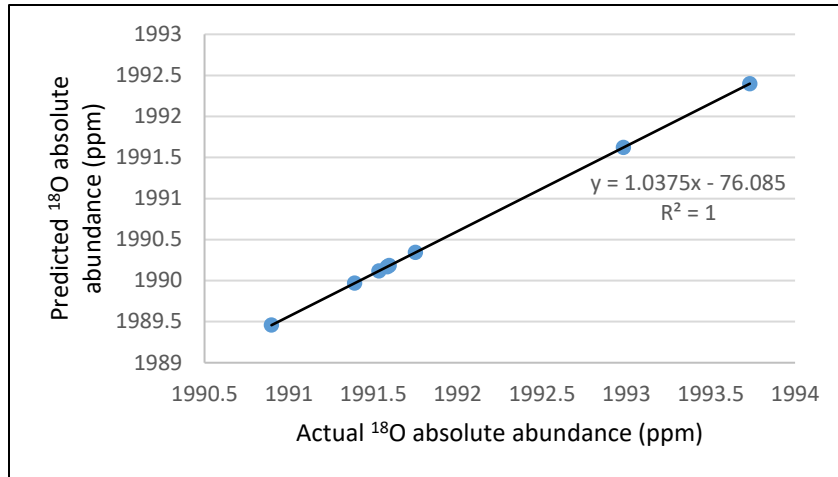


**Figure 11:** Cross correlation of mean of actual (experimentally derived) and predicted (model derived)  $^{18}\text{O}$  absolute abundance for each small sample population.

#### 4.2. Validation of the model

Validation of the proposed model is the basic requirement before its utility. Towards this, the finding of the work was testified with the published  $\delta^{18}\text{O}$  data of groundwater by Criss et al., (1995) from Sacramento Valley, California was considered. **Table 12** represents the  $\delta^{18}\text{O}$  values published by Criss et al., (1995) of aquifers with different geological age of groundwater obtained from  $^{14}\text{C}$  dating of dissolve inorganic carbon. From the data furnished in **Table 12**, it is evident that meteoric water and Holocene groundwater have same kind of isotopic signature ( $\delta^{18}\text{O}$ ) probably due to frequent recharge. However, considering Pleistocene and Holocene groundwater  $\delta^{18}\text{O}$  values are significantly different. Therefore, it can be assumed that Pleistocene groundwater in the formation is deep seated than Holocene groundwater since it is geologically older. With this analogy, Pleistocene


groundwater is likely to be warmer than Holocene groundwater due to incremental geothermal heat. In this regard the Flood plain groundwater can be considered as the geologically youngest and coldest. **Table 13** summarizes the “experimentally derived”  $^{18}\text{O}$  absolute abundance in ppm for Flood plain, Pleistocene and Holocene groundwater with reference to  $25^{\circ}\text{C}$  benchmark temperature by **Equation 23**. In addition, the data furnished in **Table 13** depicts a decreasing trend of  $^{18}\text{O}$  absolute abundance in ppm for geologically older and likely to be warmer groundwater. This trend is consistent with the basic postulation of this work.

**Table 14** summarizes systematic solution in spreadsheet computational environment of **Equation 22**. A comparative observation of **Table 13** and **Table 14** suggests that  $^{18}\text{O}$  absolute concentration for Flood plain, Pleistocene and Holocene groundwater; the “experimentally derived” and “model derived”  $^{18}\text{O}$  absolute abundance values are quite consistent and within the standard deviation of  $^{18}\text{O}$  absolute abundance of VPDB ( $\pm 2.1$  ppm). **Figure 12** represents a comparative study of absolute abundance of  $^{18}\text{O}$  of different geological age with respect to the “reference water” which definitely shows a decreasing  $^{18}\text{O}$  trend with increasing geological age. Considering more exposure time to geothermal heat, groundwater of older geological age shows decrease in  $^{18}\text{O}$  absolute abundance with is consistent with the finding of this work, both in terms of theory as well as in laboratory simulation.

**Table 12:** Groundwater and surface water  $\delta^{18}\text{O}$  data of Sacramento Valley, California. Age of water calculated from  $^{14}\text{C}$  dating of dissolve inorganic carbon (Criss et al., 1995).

Type	$\delta^{18}\text{O} \pm \text{SD}$	Age
Meteoric water	$-7.5 \pm 3.0$	Modern
Putah Creek	$-4.0 \pm 1.0$	Modern
Cache Creek	$-5.0 \pm 3.0$	Modern
Sacramento River	$-10.8 \pm 0.2$	Modern
Holocene groundwater	$-7.5 \pm 0.5$	2.7-4 k years
Flood Plain groundwater	$-5.0 \pm 0.5$	4-8 k years
Pleistocene groundwater	$-8.7 \pm 0.5$	8-16 k years
Formation water	$+3.3 \pm 1.5$	Cretaceous

**Table 13:** Experimentally derived  $^{18}\text{O}$  absolute abundance of  $\delta^{18}\text{O}$  data of Sacramento Valley, California.

Type	$\delta$ VSMOW	$\delta$ VPDB	Absolute abundance ( $^{18}\text{O}$ ) in ppm	Temperature ( $^{\circ}\text{C}$ )
Pleistocene groundwater	-8.7	-38.4224	1987.67	Temperature increasing 
Holocene groundwater	-7.5	-37.2583	1990.08	
Flood plain groundwater	-5	-34.8333	1995.09	
<i>Reference water</i>	0	-29.9832	2005.12	25 $^{\circ}\text{C}$



**Table 14:** Theoretically derived  $^{18}\text{O}$  absolute abundance in ppm. Values of column “K” is from fourth column of **Table 13**.

	J	K	L	M	N	O
Type	VPDB	Absolute abundance ( $^{18}\text{O}$ ) in ppm	(K/J)	$\ln(\text{K/J})$	VPDB*M	Theoretical $^{18}\text{O}$ abundance in ppm(VPDB +N)
Pleistocene groundwater	2067.1	1987.67	0.961578	-0.03918	-80.988926	1986.11
Holocene groundwater	2067.1	1990.08	0.962742	-0.03797	-78.488149	1988.61
Flood plain groundwater	2067.1	1995.09	0.965167	-0.03545	-73.287895	1993.81
<i>Reference water</i>	2067.1	2005.12	0.970017	-0.03044	-62.926469	2004.17

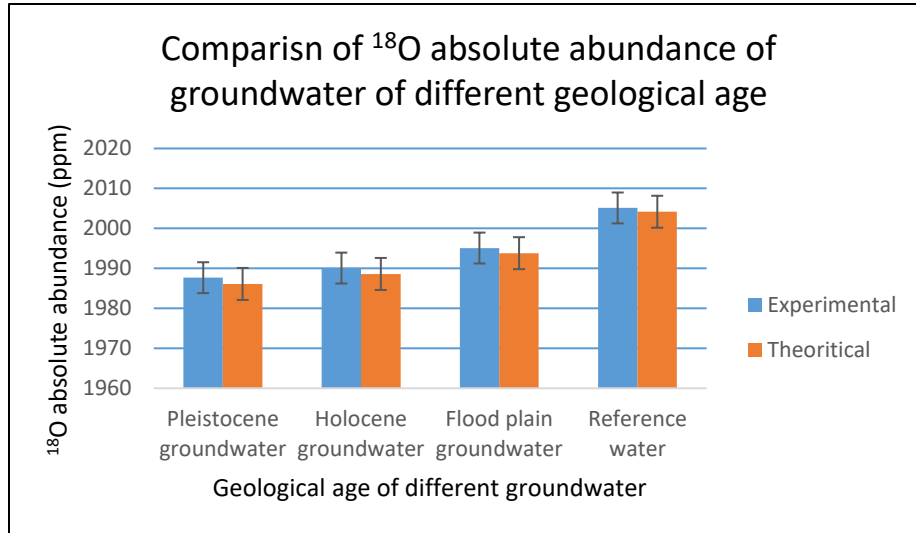


**Figure 12:** Comparative study of <sup>18</sup>O absolute abundance with respect to the “reference water”. Data from column “K” and “O” of **Table 14**.

### 4.3. Primary findings

It was imperative to fractionate <sup>18</sup>O in simulated laboratory condition with no phase change of water to put the theoretical <sup>18</sup>O geothermometer on real life stability. As discussed earlier, that the experimental set up was designed to simulate a simplified version of a real aquifer satisfying the initial and boundary conditions assumed in the theoretical model and its isotopic response ( $\delta^{18}\text{O}$ ) with imposed temperature gradient. However, with initial difficulty to fractionate <sup>18</sup>O with experimental set up brass tube filled with porous sand ( $\phi$  scale of -1.0) and saturated with Milli-Q water keeping  $Ra_c \approx 40$ , experiment was further conducted by removing porous sand from the experimental set up brass tube and only filled with Milli-Q water. For all the temperature gradients considered for the experiment  $\delta^{18}\text{O}$  was measured for corresponding temperature. <sup>18</sup>O fractionated for all the temperature gradients

with maximum fractionation recorded at 10°C-30°C temperature gradient of 0.7 ppm. Further, the theoretical model was testified with published groundwater  $\delta^{18}\text{O}$  data of Sacramento Valley, California to validate it in the field condition. From the field  $\delta^{18}\text{O}$  data it was quite evident that  $^{18}\text{O}$  absolute abundance decreased with increasing geological age of water and exposure time to geothermal heat, which is quite consistent with the basic postulation of the  $^{18}\text{O}$  geothermometer as proposed in this work. The primary finding of the experiment and validation of the model with field  $\delta^{18}\text{O}$  data, it is quite encouraging to apply the proposed  $^{18}\text{O}$  geothermometer successfully in different field conditions to estimate subsurface reservoir temperature which is discussed in **Chapter 5**.

## **Chapter 5**

### **Discussion and conclusions**

## 5. Discussion

Temperature dependent fractionation of stable isotopes find application as a geothermometer in several fields of Earth Sciences. These include the understanding of different physical processes which pertain to hydrology, weathering, geochemistry and crystallization of igneous rocks (Friedman et al., 1977; Chiba et al., 1989); mineral fluid interaction (Taylor 1977) and recharge mechanism of hydrothermal system etc. (Craig, 1966; Gregory et al., 1981, 1989; Criss et al., 1983, 1986; Criss et al., 1985).

Among these, stable isotopes have been extensively used to understand the dynamics of the Hydrosphere which involves the physical phase change of water-ice-vapor system. Water-ice-vapor system best exemplifies the temperature dependent stable isotope fractionation pattern in the hydrosphere in terms of oxygen ( $^{18}\text{O}$ ,  $^{16}\text{O}$ ) and hydrogen (H,  $^2\text{H}$ ) isotope ratios (Souchez et al., 2000; Christopher et al., 2003; Cappa et al., 2005; Deshpande et al., 2013; Casado et al., 2016). These isotopic ratios act as conservative tracer, which are intrinsic to water molecule, and reveal the origin of the water, phase transition and moisture transportation in the hydrologic cycle. These are also used to estimate the aquifer recharge and associated seasonality effect on recharge (Darling et al., 1988), as well as separating base flow from overland flow in hydrograph separation (Criss, 1997, Mouraya 2011, Ahluwalia et al., 2013). Further studies have successfully demonstrated to trace the process of global precipitation pattern and their relation to local meteoric water line. (Craig, 1961, Kumar et al., 2010, Rai et al., 2014). Global precipitation patterns are linked with the, geographic influence like temperature, altitude and

latitude which affect the variation of  $\delta^{18}\text{O}$  and  $\delta^2\text{H}$ . Therefore, under certain assumptions, the isotopic signature of groundwater can provide characteristic information of its origin and flow paths. Despite all the complexities, strong linear variation of  $\delta^{18}\text{O}$  and  $\delta^2\text{H}$  ( $\delta H^2 = 8\delta O^{18} + 10$ ) in precipitation have led researchers to establish empirical Meteoric Water Line or MWL. This may be used to distinguish water of other parentage than of meteoric origin.

Marine carbonates have been proved promising to reconstruct the paleo environment and paleo-temperature in relative scale with reference to the present. (Epstein et al. 1953; Erez et al., 1983; Bemis et al., 1988; McGuffie et al; 2005). The empirical chemical geothermometers are among the basic tools which are reported to estimate temperature of geothermal system considering a range of  $\approx 100^\circ\text{C}$  to  $250^\circ\text{C}$  and associated with a phase change of water (Fournier 1979; Fournier 1982; Fouillac et al. 1981; Arnorsson et al. 1985; Giggenbach et al. 1988; Goff, et al., 2000). However, limited isotopic studies are available which deal with estimating the absolute groundwater temperature in confined aquifer system where there is no phase change of water involved. Therefore, this work makes an attempt to estimate the groundwater temperature from its isotopic response under imposed natural geothermal gradient.

This work proposes an analytical deterministic model to estimate the groundwater temperature which is built on a theoretical model based on the earlier studies related to the subsurface fluid convection and mass transfer due to normal geothermal gradient of  $25^\circ\text{C}/\text{km}$  (Wood et al., 1982). It derives different subsurface fluid

convection models containing varying heat flux and geometry (Dip) of the stratum. It further justifies their thermal convection models for different Rayleigh numbers ( $Ra_c$ ) which signifies the onset of different free thermal convection patterns of subsurface fluid. The main parameters governing the onset of different thermal fluid convection patterns in subsurface are differential heat budget and geometric orientation of the stratum (Dip). These models (Wood et al., 1982) have proposed that the onset of thermal convection in subsurface fluid due to incremental heat budget down dip and resulting in density difference, may take years to generate in any geological setting. Therefore, it is considered a very slow process where the hydraulic conductivity of the porous media may regulate the process.

Considering the gentle dip of the strata (Dip amount  $\cong 15^\circ$ ) and  $Ra_c$  close to  $\leq 40$  it may onset a density difference of subsurface fluid leading to a free unicellular laminar thermal convection down dip which eventually leads to the isotopic stratification. However, for a higher Rayleigh number, particularly for the higher value of the parameter  $\Delta t$  at numerator of **Equation 12**, there will be a rapid thermal convection in the aquifer. This may set up vigorous thermal convection of subsurface fluid restricting the molecular diffusion of the regime resulting no isotopic stratification. However, with the minimum dip angle ( $\approx 15^\circ$ ) the free unicellular laminar convection starts opposite to the gravity driven advection under a normal geothermal gradient of  $25^\circ\text{C}/\text{km}$ .

In general, the regional groundwater flow is expected to be gravity driven advection, however, on micro scale, different isotopomers of groundwater may

fractionate as per its thermal stability regime. Such fractionation of different isotopomers of groundwater may be attributed to different bond strengths and vibrational frequency of lighter and heavier isotope of oxygen and hydrogen and their preferential thermal regime. As the vibrational frequency of a molecule decreases with increasing bond strengths therefore heavier isotope will concentrate at lower temperature regime and vice versa.

This attribute of stable isotope fractionation may be used as geothermometer. However, the proposed geothermometer may be applied to the confined aquifer system and not for the unconfined aquifers where frequent recharge and evapotranspiration could be a possibility. Towards this, one can divide the aquifer to infinitesimally small thermal compartments with increasing temperature down dip, where the boundary of the aquifer can be considered impermeable as proposed in the deterministic model. It is important to note that the possibilities of isotopic fractionation of soil gases diffusion (Severinghaus et al., 1995) is not considered under the assumption of impermeable confined aquifer boundary.

The gently dipping ( $\cong 15^\circ$ ) confined aquifer system may be considered to have an ideal medium which is highly permeable, homogeneous and isotropic in terms of hydraulic conductivity and diffusivity in all the directions. These properties support the unicellular laminar thermal convection, which will eventually fractionate the  $^{18}\text{O}$  in the groundwater. In a steady state the residence time of the water in the aquifer is long enough and therefore ensures a thermal equilibrium with surrounding. However, recharge of confined aquifer involving the gravity driven



advection through long residence time leads to the complete mixing of recharge water in the aquifer. Now considering normal geothermal gradient, where we compartmentalize the aquifer into infinitesimal compartments, it is obvious that as moving down dip the temperature will increase for two successive compartments (**Figure 5**). This leads to initiation of temperature dependent density gradient resulting in unicellular laminar thermal convection up dip when  $Ra_c$  (critical Rayleigh number) is close to  $\leq 40$  (**Figure 2**). This mass transfer process, mobilized by unicellular thermal convection, is in the opposite direction with respect to regional advection direction.

This results in the thermal diffusion of different isotopomers of water leading to isotopic stratification of  $^{18}\text{O}$ , subjected to their differential vibrational frequency of  $^{16}\text{O}-^{16}\text{O}$  which is  $1580.193\text{ cm}^{-1}$  and  $^{16}\text{O}-^{18}\text{O}$  which is  $1535.57\text{ cm}^{-1}$  (Huber et al., 1979). Therefore, it is likely that  $^{16}\text{O}-^{18}\text{O}$  will fractionate more where  $^{18}\text{O}$  will tend to concentrate at lower temperature regime and  $^{16}\text{O}$  will tend to concentrate at higher temperature regime (Grew et al., 1952) which is evident from the **Figure 13**.

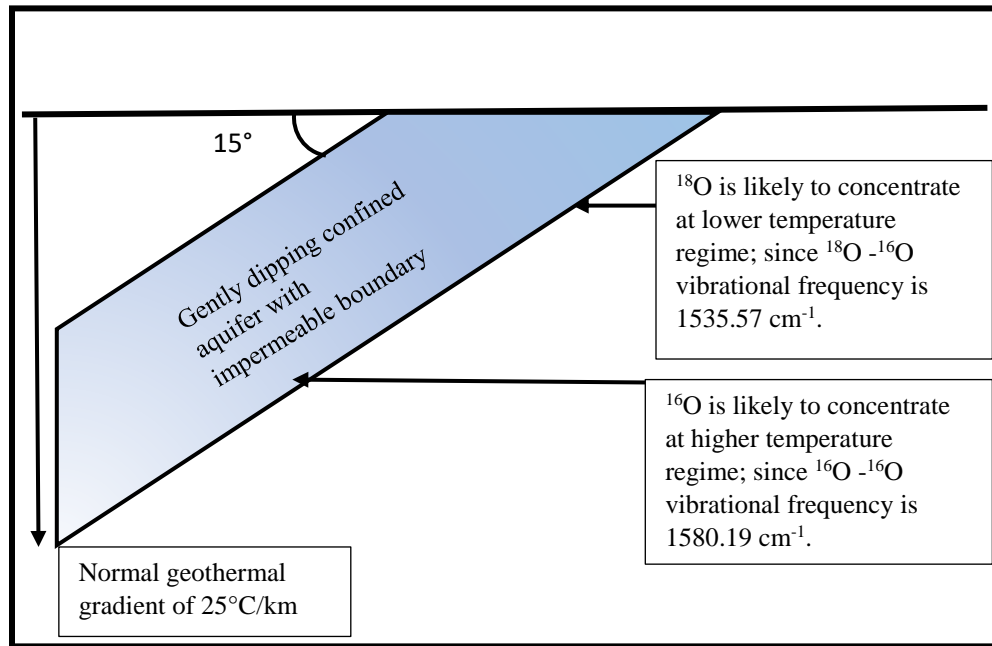


**Figure 13:** Isotopic stratification in confined aquifer system with incremental geothermal heat down dip, which can be further used to estimate ground water temperature. (Schematic diagram, not according to scale).

Therefore, based on these properties, it is possible to use the water isotopes to estimate groundwater temperature. Further, if  $^{18}\text{O}$  absolute abundance is known for a water sample, then its temperature can be estimated relative to absolute abundance of  $^{18}\text{O}$  at  $25^\circ\text{C}$  that is 2005.12 ppm (Urey et al., 1951; Cuna et al., 2001; Werner et al., 2001) with respect to VSMOW standard. The VSMOW may be converted to VPDB (**Equation 21**) which is an international reference material for  $^{18}\text{O}/^{16}\text{O}$  ratio established in marine carbonate. Here it is assumed that at the time of precipitation of VPDB, global ocean temperature was very close to  $25^\circ\text{C}$  with absolute abundance of  $^{18}\text{O}$  is 2005.12 ppm in the global ocean (Coplen et al., 1983; Clark

1997, p 11). Therefore, it is assumed that  $^{18}\text{O}$  absolute abundance of water at  $25^\circ\text{C}$  is 2005.12 ppm and it is termed as “reference water”. Changing the standard from VSMOW to VPDB will not change the absolute abundance of  $^{18}\text{O}$  in the water sample. Now, if for a given water sample if  $^{18}\text{O}$  absolute abundance is less than 2005.12 ppm then its temperature is higher than  $25^\circ\text{C}$  and vice versa.

This deterministic analytical model was tested for its physical validation by fractionating  $^{18}\text{O}$  in controlled laboratory condition under imposed temperature gradients. Earlier studies have demonstrated the fractionation of heavy isotope from a water isotope mixture considering it by thermal diffusion process, which provides a basis for the theoretical model (Murphy 1955; Bebbington et al., 1959; Yeh et al., 1984; 2009). In this regard a suitable experimental set up was designed to fractionate  $^{18}\text{O}$  in liquid water system with imposed temperature as elaborated by **Plate 1-5**.

In this set up, the temperature range selected from  $10^\circ\text{C}$  to  $50^\circ\text{C}$  with  $10^\circ\text{C}$  equal incremental temperature interval, which is similar to the temperature range of shallow crustal level aquifers. The experimental set up by and large, fulfills all the initial and boundary conditions of the proposed deterministic analytical model to estimate groundwater temperature.

Throughout the experiment the brass tube was kept at a dip angle close to  $14^\circ$  which corresponds  $Ra_c$  close to  $\leq 40$  (**Plate 1**). It simulates a gently dipping confined aquifer system with impermeable boundary. The induced temperature gradient was maintained between the two ends of the brass tube by circulating water bath of

desired temperature, while keeping the ambient temperature constant around 25°C (Plate 2 and 4). It is assumed that all the isotopomers of water are uniformly distributed before imposing temperature gradient satisfies the initial condition of the model.

Initially an attempt was made to fractionate  $^{18}\text{O}$  in brass tube filled with porous coarse-grained sand ( $\phi$  scale of -1.0) saturated with Milli-Q water keeping  $Ra_c$  close to but less than  $\leq 40$ . However, this initial attempt to fractionate  $^{18}\text{O}$  was ended with disappointment for thermal equilibrium time of one day and for any temperature gradient. This justifies one of the fundamental assumptions of different subsurface fluid convection theoretical models proposed by Wood et al., (1982) that in natural setting it will take long time to happen. Overcoming the initial disappointment, further the experiment was carried out with brass tube kept empty with porous and permeable sand and only filled with Milli-Q water. This ensures the ease of the process of unicellular laminar thermal convection happen under the imposed temperature gradient and hence leading to isotopic stratification.

Considering the experimental design, the thermal equilibration time for each set of temperature gradient was approximately six hours. In this very small span of time, the gravity effect to fractionate  $^{18}\text{O}$  due to molecular mass difference of different isotopomers of water can be neglected. The temperature was the only variable in the experimental design and for each and individual temperature gradient  $^{18}\text{O}$  fractionated. Therefore, this experiment also complements the claim that for isotopic stratification in liquid water system with imposed temperature gradient

heat is the primary cause. It rules out the gravity induced isotopic fractionation reported for gas in polar ice cap (Craig et al., 1988) considering intermolecular attraction of liquid is way more than gas. The claim of heat as primary cause of isotopic stratification in liquid water can be further justified by no isotopic stratification of water molecule ( $\text{H}_2^{18}\text{O}$ ,  $\text{H}_2^{16}\text{O}$ ) at Philippine Trench and Lake Baikal as reported by Dansgaard (1960). In addition, Laser Water Isotope Analyzer PICARRO of model L1102-i (At Wadia Institute of Himalayan Geology, Dehradun, India) was used for the  $^{18}\text{O}$  measurement. which excludes any possible dissolved salt effect on stable isotope ratio measurement (Craig et al., 1965); (Sofar et al., 1972, 1975); (Mayo et al., 1995).

The experimental apparatus was found to be sensitive where the first significant  $^{18}\text{O}$  fractionation registered at  $10^\circ\text{C}$ - $20^\circ\text{C}$  temperature gradient after thermal equilibration time of approximately six hours. The experiment was further carried out for other temperature ranges of  $10^\circ\text{C}$ - $30^\circ\text{C}$ ;  $10^\circ\text{C}$ - $40^\circ\text{C}$  and  $10^\circ\text{C}$ - $50^\circ\text{C}$  temperature gradient keeping the thermal equilibration time same. For each set of temperature gradient significant  $^{18}\text{O}$  fractionation recorded and the maximum fractionation recorded at  $10^\circ\text{C}$ - $30^\circ\text{C}$  temperature gradient at the level of 0.7 ppm. Therefore, the experimental apparatus and experimental design adopted in this research successfully demonstrate that  $^{18}\text{O}$  does fractionate in the liquid water system with imposed temperature gradient where no phase change of water is involved. These results justify the fundamental proposition of using  $^{18}\text{O}$  as a geothermometer in natural confined aquifer and the suitability of the theoretical

deterministic analytical model to estimate groundwater temperature with reference to benchmark temperature of 25°C.

The experimental results were compared with theoretically derived values of  $^{18}\text{O}$ , where it is observed that “experimentally derived” (**Table 9**) and “model derived” (**Table 10**)  $^{18}\text{O}$  absolute abundance at corresponding temperature where within the internationally accepted standard deviation of absolute abundance of  $^{18}\text{O}$  of VPDB that is  $\pm 2.1$  ppm. Further, “experimentally derived” and “model derived”  $^{18}\text{O}$  absolute abundance shows a strong linearity in cross correlation plot (**Figure 11**) which further demonstrates the consistency of the experimental and theoretical conclusions.

After successful demonstration of  $^{18}\text{O}$  fractionation in controlled laboratory condition, the proposed  $^{18}\text{O}$  geothermometer was further testified by the field  $\delta^{18}\text{O}$  data of Sacramento Valley, California (Criss et al., 1995). While validating, it was assumed that  $\delta^{18}\text{O}$  data of groundwater is from a continuous aquifer system with varying Geological age ( $^{14}\text{C}$  dating) obtained from dissolve inorganic carbon. Despite that  $^{14}\text{C}$  dating of groundwater from dissolve inorganic carbon has certain complexities and controversy, we can assume that for the study area, Pleistocene groundwater was warmer than Holocene groundwater due to incremental geothermal gradient. This is tenable under the analogy that it is geologically older and likely to be deep seated into the formation than Holocene groundwater. The Flood plain groundwater was considered as the geologically youngest and coldest. The assumption was quite consistent and justified with the groundwater model map

of the study area as published by Criss et al., (1995). Considering Flood plain groundwater, Holocene groundwater and Pleistocene groundwater, it reveals a steady decline of  $\delta^{18}\text{O}$  and  $^{18}\text{O}$  absolute abundance (ppm) with increasing geological age. This  $^{18}\text{O}$  isotopic signature depicts a continuous warmer trend of groundwater with increasing geological age with respect to the benchmark temperature of  $25^\circ\text{C}$  and corresponding  $^{18}\text{O}$  absolute abundance of 2005.12 ppm. This also satisfies the basic postulation of this work in field condition. It is important to note that “experimentally derived” (**Table 13**) and “model derived” (**Table 14**)  $^{18}\text{O}$  absolute abundance for waters of different geological age were also within the internationally accepted standard deviation of absolute abundance of  $^{18}\text{O}$  for VPDB ( $\pm 2.1$  ppm).

As the results show a good consistency of “experimentally derived” and “model derived”  $^{18}\text{O}$  absolute abundance (**Figure 11 and 12**) therefore, it can be assumed that the deterministic analytical model proposed in this work describes the physical principle of  $^{18}\text{O}$  isotope fractionation process of liquid water system with imposed temperature gradient. This  $^{18}\text{O}$  fractionation is attributable to the free unicellular laminar thermal subsurface fluid convection model proposed by Wood et al., (1982) and thermal stratification of different isotopomers of water molecule under thermal diffusion process.

### **5.1. Conclusions**

The present work is an attempt to estimate the temperature of groundwater using  $^{18}\text{O}$  fractionation where there is no phase change of water involved. It provides the

experimental support to the proposed deterministic analytical model by using stable isotope fractionation to estimate absolute groundwater temperature by  $^{18}\text{O}$  fractionation with reference to  $25^\circ\text{C}$  benchmark temperature.

The theoretical model was first testified in controlled laboratory condition to fractionate  $^{18}\text{O}$  in liquid water system with imposed temperature gradient. With successful demonstration of significant  $^{18}\text{O}$  fractionation (maximum  $\approx 0.7$  ppm) in liquid water with imposed temperature gradient it was observed that “experimentally derived” and “model derived”  $^{18}\text{O}$  absolute abundance are well within the internationally accepted standard deviation of absolute abundance of  $^{18}\text{O}$  of VPDB that is  $\pm 2.1$  ppm. Further, the “experimentally derived” that is actual and “model derived” that is predicted  $^{18}\text{O}$  absolute abundance shows a strong linearity in cross plot and hence validates the suitability of the method to estimate the groundwater temperature.

With successful demonstration of the model in laboratory condition, the model was further testified by published  $\delta^{18}\text{O}$  data of Sacramento Valley, California to validate it in the field condition. A distinct warmer trend of groundwater was observed from its  $^{18}\text{O}$  isotopic signature with increasing geological age of the water of Sacramento Valley, California with reference to  $25^\circ\text{C}$  benchmark temperature. While validating the model in field condition again it was again observed that “experimentally derived” and “model derived”  $^{18}\text{O}$  absolute abundance in ppm for water samples of different geological age from Sacramento Valley, California are quite similar to each other and well within the standard deviation of  $^{18}\text{O}$  absolute abundance of



VPDB ( $\pm 2.1$  ppm). This trend is consistent with respect to groundwater model map and regional geology of Sacramento Valley, California. Therefore, it satisfies the basic proposition of the deterministic analytical model proposed in this research  $^{18}\text{O}$  does fractionate in liquid water system, which can be further extended to estimate groundwater temperature in absolute scale. This work also identifies that it is not the gravity but heat is the primary cause for isotopic fractionation and stratification in liquid water system. It helps to conclude that  $^{18}\text{O}$  does fractionate in liquid water system with increasing geothermal heat with depth and finding of warming trend of groundwater with increasing geological age.

Along with applying the  $^{18}\text{O}$  geothermometer to estimate groundwater temperature with reference to  $25^\circ\text{C}$  benchmark temperature, this work may be helpful as indirect evidence of exploration of radioactive minerals which accumulate heat inducing warmer groundwater. It is also applicable in hydrocarbon exploration and production, to estimate formation fluid temperature and establishing geothermal gradient of a hydrocarbon province. Such information is very important to understand hydrocarbon reservoir dynamics at production stage. Further, it can also be used to detect concentrated heavy water for deuterium ( $^2\text{H}$ ) which is required in atomic nuclear fusion reactors in atomic power generating stations.

## **5.2. Future scope of work**

This work has been able to demonstrate that  $^{18}\text{O}$  does fractionates in liquid water system with imposed temperature gradient when there is no phase change involved in controlled laboratory condition. This fractionation is evident in reported field

data of  $\delta^{18}\text{O}$  of Sacramento Valley, California depicting a warmer trend of groundwater with increasing geological age with reference to  $25^\circ\text{C}$  having absolute concentration of  $^{18}\text{O}$  of 2005.12 ppm. The way geothermometer will work is that if absolute abundance of  $^{18}\text{O}$  is more than 2005.12 ppm will indicate groundwater temperature less than  $25^\circ\text{C}$  and vice versa. **Figure 14** graphically represents the core finding of the work so far. Further, the major limitations include that the method works only for groundwater temperature estimation of confined aquifer and not for unconfined aquifer.

As per the scope and facilities available for this work, it was not possible to develop a universal linear model, which could estimate any groundwater temperature from its  $^{18}\text{O}$  isotopic signature when there is no phase change of water involved. That linear model is likely to show a strong negative correlation for liquid water in terms of  $^{18}\text{O}$  absolute abundance in ppm with increasing temperature. To develop that linear model, we need to start fractionating water whose initial  $^{18}\text{O}$  concentration is 2005.12 ppm. The physical existence of that water is deep ocean water with  $\delta^{18}\text{O}$  is zero. Due to logistical constrain that water could not be acquired and as a part of this work it has been kept for future work.

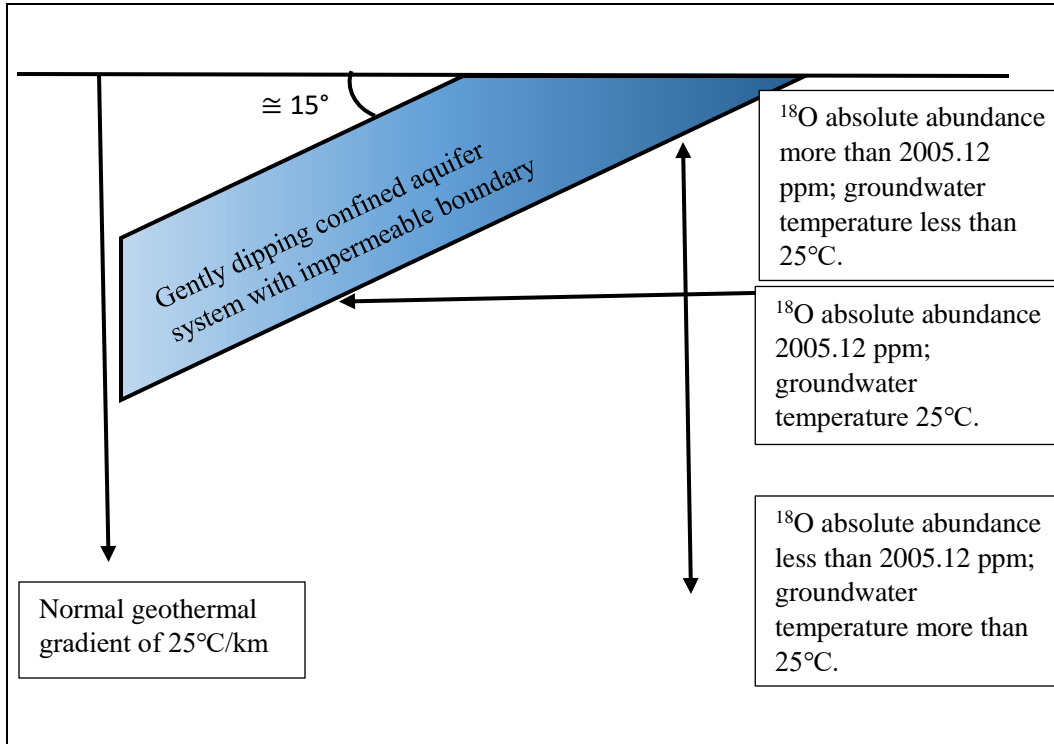


**Figure 14:** Estimation of groundwater temperature from  $^{18}\text{O}$  isotopic signature with reference to 25°C benchmark temperature. (Schematic diagram; not according to scale)

## References

1. Anderson, D. L., (1989) "Theory of the Earth". 366 pp., Blackwell Sci., Cambridge Massachusetts.
2. Arnorsson, S., and Gunnlaugsson, E., (1985): "New gas geothermometers for geothermal exploration - calibration and application". *Geochim. Cosmochim. Acta*, 49, 1307-1325.
3. Ahluwalia, R. Saran., Rai, S.P., Jain, S., Kumar, B., Dobhal, D. P., (2013) "Assessment of snowmelt runoff modeling and isotope analysis: a case study from the western Himalaya, India". *Annals of Glaciology*, vol 54(62) doi: 10.3189/2013AoJ62A133, 299-304.
4. Baertschi, P., (1976) "Absolute  $^{18}\text{O}$  content of standard mean ocean water". *Earth Planet Sci Lett* 31: 341–344.
5. Bottinga, Y., Javoy. M., (1973) "Comments on oxygen isotope geothermometry". *Earth Planet Sci Lett* 20: 250–265.
6. Bottinga, Y., (1969) Carbon isotope fractionation between graphite, diamond and carbon dioxide. *Earth Planet Sci Lett* 5: 301–307.
7. Bebbington, W. P., Thayer, V. R., (1959) "Production of Heavy Water," *Chem. Eng. Prog.*, Vol. 55, p. 70.
8. Bemis, B. E., Spero. H. J., Bijma J., Lea D, W., (1988) "Reevaluation of the oxygen isotopic composition of planktonic foraminifera: Experimental results and revised paleotemperature equations". *Paleoceanography*, Vol. 13, NO. 2, pages 150-160.

9. Bear, J., (1988) "Dynamics of fluids in porous media." Dover Publications, Inc (NY). ISBN: 0-486-65675-6.
10. Barry, R. G., Chorley R. J., (1982) "Atmosphere, Weather, and Climate". New York. NY: Methuen & Co.
11. Barrett, E., Brodin, G., (1955), "The acidity of Scandinavian precipitation", *Tellus*, v. 7, p. 251-257.
12. Best, M. G., (2003) "Igneous and Metamorphic Petrology". (2nd Edition). Blackwell Science Ltd. ISBN 1-40510-588-7.
13. Combarous, M.A., Bories, S.S., (1975) "Hydrothermal convection in saturated porous media". *Advances in Hydrosience* 10, 231-306, Academic Press. NY.
14. Coplen, T. B., Kendall, C., Hopple J., (1983) "Comparison of stable isotope reference samples". *Nature* 302: 236–238.
15. Cappa, C. D., Drisdell W., Smith J. D., Saykally R. J., Cohen R. C., (2005) "Isotope fractionation of water during evaporation without condensation". *J. Phys. Chem. B* 109, 24391–24400.
16. Criss, R. E., Davisson, M. L., (1995) "Isotopic imaging of surface water/groundwater interactions, Sacramento Valley, California. *J. Hydrol.*, 178/1-4, 205-222.
17. Casado, M., Cauquoin, A., Landais, A., Israel, E. D., Ors, Ai., Edouard Pangui, G. E., Landsberg, J., Kerstel, E., Frederic Prie, F., Doussin, J.F., (2016) "Experimental determination and theoretical framework of kinetic fractionation at the water vapour–ice

- interface at low temperature.” *Geochimica et Cosmochimica Acta* 174 (2016) 54–69.
18. Crank, J., (1993) “The mathematics of diffusion”. 2nd Edition. Clarendon Press. Oxford University Press. ISBN: 0-19-853411-6.
  19. Craig, H., (1961),(a) “Isotope variations in meteoric waters”. *Science*, 133, 1702-1703.
  20. Craig, H., (1961),(b) “Standard for reporting concentrations of deuterium and oxygen-18 in natural waters”. *Science* 133, 1833-1834.
  21. Craig, H., (1966) “Isotopic composition and origin of the Red Sea and Salton Sea geothermal brines”. *Science*, 154, 1544-1548.
  22. Criss, R. E., Taylor, H. P., Jr., (1983) “An  $^{18}\text{O}/^{16}\text{O}$  and D/H study of Tertiary hydrothermal systems in the southern half of the Idaho batholith”. *Bull. Geol. Soc. America*, 94, 640-663.
  23. Criss, R. E., Taylor, H. P., Jr., (1986) “Meteoric-hydrothermal systems”. *Rev. Mineral.*, 16, 373-424.
  24. Criss, R. E., Champion, D. E., McIntyre, D. H., (1985) “Oxygen isotope, aeromagnetic and gravity anomalies associated with hydrothermally altered zones in the Yankee Fork Mining District, Custer County, Idaho”. *Econ Geol* 80: 1277–1296.
  25. Chacko, T., Cole, D. R., Horita, J., (2001) “Equilibrium oxygen, hydrogen and carbon fractionation factors applicable to geologic systems”. *Rev Miner Geochem* 43: 1–81.

26. Christopher, D. C., Melissa, B. H., Donald, J. D. P., Ronald, C. C., (2003) "Isotopic fractionation of water during evaporation". *Journal of Geophysical research*, Vol. 108, No. D16, 4525, doi: 10.1029/2003JD003597, 2003.
27. Criss, R. E., (1997) "New formulation for the hydrograph, time constants for stream flow and the variable character of "baseflow". *Trans. Am. Geophys. Union*, 78, 317.
28. Craig, H., Gordon, L. I., (1965) "Duterium and oxygen-18 variations in the ocean and the marine atmosphere", *Stable Isotopes in Oceanographic Studies and Paleotemperatures*".(TONGIORGI, E., Ed), Consiglio Nazionale delle Ricerche, Laboratorio di Geologia Nucleare Pisa, p. 9.
29. Chiba, H. T., Chacko, T., Clayton, R. N., Goldsmith, J. R., (1989) "Oxygen isotope fractionation involving diopside, forsterite, magnetite and calcite: application to geochemistry". *Geochim. Cosmochim. Acta*, 53, 2985-2995.
30. Cuna, C., Pop, D., Hosu A., (2001) "Carbon and oxygen isotope ratios in Rona Limestone, Romania". *Studia Universitatis Babes-Bolyai, Geologia*, XLVI, 1.
31. Criss, R. E., (1999) "Principles of Stable Isotope Distribution." Oxford University Press (NY). ISBN: 978-0-19-511775-2.
32. Clark, I., Fritz, P., (1997) "Environmental Isotopes in Hydrogeology." CRS Press. ISBN: 1-56670-249-6.

33. Craig , H., Horibe, Y., Sowers, T., (1988) “Gravitational separation of gases and isotopes in polar ice caps”. *Science* 242,1675-1678.
34. Clark, S. P., Jr., (1969) “Heat conductivity in the mantle, in *The Earth's Crust and Upper Mantle*”. *Geophys Monogr. Ser.*,vol. 13, edited by P. J. Hart, pp. 622-626, AGU., Washington D, C.
35. Driesner, T., (1997) “The effect of pressure on deuterium-hydrogen fractionation in high-temperature water”. *Science* 277: 791–794.
36. Dansgaard, W., (1964) “Stable isotopes in precipitation”. *Tellus*, 16, p 436-468.
37. Deshpande, R. D., Maurya A.S., Kumar.B., Sarkar. A., Gupta S.K., (2013) “Kinetic fractionation of water isotopes during liquid condensation under super-saturated condition”. *Geochimica et Cosmochimica Acta*. 100 (2013) 60–72.
38. Deshpande, R. D., Maurya A. S., Kumar B., Sarkar A., Gupta S. K., (2010) “Rain–vapor interaction and vapor source identification using stable isotopes from semi-arid western India”. *J. Geophys. Res.* 115, D23311.
39. Dansgaard, W., (1960) *Deep Sea Res.* 6, 346.
40. Darling, W.G., Bath, A. H., (1988) “A stable isotope study of recharge processing in the English Chalk”. *Journal of Hydrology* 101:31-46.
41. Davis, J. C., (2014) “Statistics and data analysis in Geology.” 3rd Edition. John Wiley & Sons, Inc. ISBN: 978-81-265-3008-3.



42. Drever, J. I., (2002) "The geochemistry of natural water." Third Edition. Prentice Hall (NJ). ISBN: 0-13-272790-0.
43. Domenico, A. P., Schwartz, W. F., (1997) "Physical and Chemical Hydrogeology." Second Edition. John Wiley & Sons, Inc. ISBN: 0-471-59762-7.
44. Dingman, S. L., (2002) "Physical Hydrology." Second Edition. Prentice Hall (NJ). ISBN: 0-13-099695-5.
45. Erez, J., Luz, B., (1983) "Experimental paleotemperature equation for planktonic foraminifera", *Geochim, Cosmochim. Acta*, 47, 1025-1031.
46. Epstein, S., Mayeda, T.K., (1953, a) "Variations of  $^{18}\text{O}$  content of waters from natural sources". *Geochim. Cosmochim. Acta*, 4, 213-224.
47. Epstein, S., Buchsbaum, R., Lowenstam H. A., Urey H. C., (1953, b) "Revised carbonate-water isotopic temperatures scale", *Geol. Soc. An. Bull.*, 64, 1315-1325.
48. Friedman, I., O'Neil, J. R., (1977) "Compilation of stable isotope fractionation factors of geochemical interest. In *Data of Geochemistry*". Fleischer, H., ed. U.S. Geol. Survey Professional Paper, 440 KK.
49. Fetter, C. W., (2001) "Applied Hydrogeology". 4th Edition. Prentice Hall, Inc. Upper Saddle River, New Jersey 07458.
50. Freeze, R. A., Cherry, J. A., (1979) "Groundwater". Prentice Hall, NJ. ISBN: 0-13-365312-9.

51. Feder, H. M., Taube, H., (1952), "Ionic hydration, an isotopic fractionation technique" J. Chem. Phys. 20, 1335.
52. Fontes, J. Ch., (1981). Palaeowaters. Chapter 12, Stable Isotope Hydrology: Deuterium and Oxygen-18 in the Water Cycle (J. R. Gat and R. Gonfiantini, eds.), Technical Report Series No. 210, IAEA, Vienna, pp. 273–302.
53. Fournier, R.O., and Potter R. W.II, (1979): "Magnesium correction to Na-K-Ca geothermometer". Geochim. Cosmochim. Acta, 43, 1543-1550.
54. Fournier, R.O., and Potter, R.W. II, (1982): "A revised and expanded silica (quartz) geothermometer". Geoth. Res. Council Bull., 11-10, 3-12.
55. Fouillac, R., Michard, S. (1981): "Sodium/Lithium ratio in water applied to geothermometry of geothermal reservoirs". Geothermics, 10, 55-70.
56. Giggenbach W.F., (1988): "Geothermal solute equilibria". Geochimica. Cosmochim. Acta 52, 2749 - 2765.
57. Grew, K. E., Ibbs T. L., (1952) "Thermal diffusion of Gases". Cambridge Univ. Press.
58. Gat, J. R., Issar, A., (1974). "Desert Isotope Hydrology: water sources of the Sinai Desert". Geochim. Cosmochim. Acta 38: 1117–1131.
59. Gat, J. R., (1983). "Precipitation, groundwater and surface waters: Control of climate parameters on their isotope composition and their utilization as palaeoclimatic tools. Palaeoclimates and

- Palaeowaters”: Application of Environmental Isotope Studies, IAEA Vienna, pp. 3–12.
60. Gat, J. R., Matsui, E., (1991) “Atmospheric water balance in the Amazon basin: An isotopic evapotranspiration model”. *J. Geophys. Res.* 96, 13179–13188.
61. Gat, J. R., (2010) “Isotope hydrology, A Study of the Water Cycle”. Imperial College Press. ISBN-13 978-1-86094-035-4.
62. Goff, F., Gardner, J. N., (2000). “Encyclopedia of Volcanoes”. Edited by Sigurdsson, H. Academic Press.
63. Ganguly, S., Tiwari, S., Bhan, U., Mittal, S., Rai, S., et al. (2015) “Melting of Sea Ice Inexplicable for Recent Global Eustatic Sea Level Rise”. *J Earth Science & Climate Change Vol 6*: 245. doi:10.4172/2157-7617.1000245.
64. Googin, J. M., Smith, H. A., (1957) “Vapor pressure studies involving solutions in light and heavy waters. III. The separation factor for the isotopes of hydrogen during distillation from salt solutions in the mixed water at room temperature”. *J. Phy. Chem.* 61, 345.
65. Gregory, R. T., Criss, R.E., Taylor, H. P., Jr., (1981) “An oxygen isotope profile in a section of Cretaceous oceanic crust, Samail ophiolite, Oman: evidence for  $\delta^{18}\text{O}$  buffering of the oceans by deep (>5 km) seawater-hydrothermal circulation at mid-oceanic ridges”. *J. Geophys. Res.*, 86, 2737-2755.

66. Gregory, R. T., Criss, R.E., Taylor, H. P., Jr., (1989) "Oxygen isotope exchange kinetics of mineral pairs in closed and open systems: applications to problems of hydrothermal alteration of igneous rocks and Precambrian iron formations". *Chem. Geol.*, 75, 1-42.
67. Horita, J., Driesner, T., Cole, D. R., (1999) "Pressure effect on hydrogen isotope fractionation between brucite and water at elevated temperatures". *Science* 286: 1545–1547.
68. Horita, J., Cole, D.R., Polyakov, V. B., Driesner, T., (2002) "Experimental and theoretical study of pressure effects on hydrous isotope fractionation in the system brucite-water at elevated temperatures". *Geochim Cosmochim Acta* 66: 3769–3788.
69. Huber, K. P., Herzberg, G., (1979) "Molecular Spectra and Molecular Structure". IV. Constantans of Diatomic Molecules. Van Nostrand Reinhold, New York.
70. Hoefs, J., (2009) "Stable Isotope Geochemistry". 6th Edition. Springer-Verlag Berlin Heidelberg. ISBN: 978-3-540-70703-5. Library of Congress Control Number: 2008933507.
71. Issar, A., Bein, A., Michaeli, A., (1972). "On the ancient waters of the upper Nubian Sandstone aquifer in central Sinai and southern Israel". *J. Hydrology* 17: 353–374.
72. International Atomic Energy Agency, Vienna, 1981, Technical Reports Series No 210.

73. Jenne, E. A., (1990) "Aquifer thermal energy storage: The importance of geochemical reactions". In Hydrochemistry and energy storage in aquifers. Edited by J. C. Hooghart and C. W S. Posthumus. Proc. & Info. No. 43, pp. 19-36, Tech. Mtg. 48, Ede, The Hague, The Netherlands.
74. Kappelmeyer, O., Hänel, R., (1974) "Geothermics with special reference to application". Gebruder Borntrargen, Berlin, Stuttgart.
75. Kohn, M. J., Valley, J. W., (1998),(a) "Obtaining equilibrium oxygen isotope fractionations from rocks: theory and examples". Contr Miner Petrol 132: 209–224.
76. Kohn, M. J., Valley, J. W., (1998),(b) "Effects of cation substitutions in garnet and pyroxene on equilibrium oxygen isotope fractionations". J Metam Geol 16: 625–639.
77. Kestin, J. et. al., (1984) "Thermophysical properties of fluid H<sub>2</sub>O". J. Phys. Chem. Ref. Data, 13, 175.
78. Kitchen, N. E., Valley, J. W., (1995) "Carbon isotope thermometry in marbles of the Adirondack Mountains". New York. J metamorphic Geol 13: 577–594.
79. Kendall, C., Coplen, T. B., (2001). "Distribution of oxygen- 18 and deuterium in river waters across the United States". Hydrological Processes 15, 1363- 1393.
80. Lee, Y., Deming, D., (1998) "Evaluation of thermal conductivity temperature corrections applied in terrestrial heat flow studies". Journal of

- geophysical research, vol. 103, no. B2, pages 2447-2454,  
February 10, 1998.
81. Lide, D. R., (1991) "Handbook of Chemistry and Physics". 71st edition. CRC Press, Boston, Massachusetts.
  82. Langmuir, D., (1997) "Aqueous Environmental Geochemistry". Prentice Hall. ISBN 0-02-367412-1.
  83. Lowrie, W., (2007) "Fundamentals of Geophysics." Second Edition. Cambridge University Press. ISBN-13: 978-0-521-27038-0.
  84. Masters, G. M., Ela, W. P., (2008) "Introduction to Environmental Engineering and Science" Third Edition. Pearson Education-Prentice Hall. ISBN: 978-81-317-2326-5.
  85. McGuffie K, Henderson-Sellers A (2005) "A Climate Modeling Primer". [3rd edn] John Wiley & Sons, West Sussex, England. ISBN: 978-1-118-68785-7.
  86. McCrea, J. M., (1950) "On the isotope chemistry of carbonates and a paleotemperature scale". J. Chem. Phys., 18, 849-857.
  87. Mendenhall, W., Beaver, R J., Beaver, B., (2002) "A Brief Introduction to Probability and Statistics." Duxbury-Thomson Learning. ISBN: 0-534-38777-2.
  88. Mayo, A. L.; Loucks M. D., (1995) "Solute and isotopic geochemistry and groundwater flow in the central Wasatch Range, Utah" Journal of Hydrology 172 (1995) 31-59.

89. Maurya, A. S., Shah, M., Deshpande, R. D., Bhardwaj, R. M., Prasad, A., Gupta S., K., (2011) "Hydrograph separation and precipitation source identification using stable water isotopes and conductivity: River Ganga at Himalayan foothills". *Hydrological Process* 25:1521–1530.
90. McCray, A. W., Cole, F.W., (2005) "Oil well drilling technology". New India Publication. Library of Congress Catalog Number 59-7486.
91. Murphy, (ed.). (1955) "Production of heavy water" (National Nuclear Energy Series, III-4F), McGraw-Hill, New York.
92. Nier, A. O., (1947) "A mass spectrometer for isotope and gas analysis". *Rev. Sci. Instrum.*, 18, 398-411.
93. O'Neil, J. R., (1986) "Terminology and standards. In *Stable Isotopes in High Temperature Geological Processes,*" Valley, J.W., O'Neil, J.R. and Taylor, H.P., Jr., eds. Mineralogical Society of America, *Reviews of Mineralogy*, Vol. 16, pp. 561-570.
94. Parkhurst, D. L., (1990) "Ion-association models and mean activity coefficients of various salts. In *Chemical modeling of aqueous systems*" 2nd edition. D. C. Melchior and R. L. Bassett, Am. Chern. Soc. Symp. Ser. 416, pp. 30-43. Washington DC: Am. Chern. Soc.
95. Pryor, W. A., (1971) "Reservoir inhomogeneities of some recent sand bodies". SPE Paper No: 3607.

96. Polyakov, V. B., Horita, J., Cole, D. R., (2006) "Pressure effects on the reduced partition function ratio for hydrogen isotopes in water". *Geochim Cosmochim Acta* 70: 1904–1913.
97. Poirier, J .P., (1991) "Introduction to the Physics of the Earth's Interior". 264 pp., Cambridge Univ. Press, New York, 1991.
98. Rybach, L., (1976) "Radioactive heat production in rocks and its relation to other petrophysical parameters". *Pure Applied Geophysics*. 114, 309-318.
99. Rybach, L., (1988) "Determination of heat production rate". In *Handbook of Terrestrial Heat Flow Density Determination*, ed R.Haenel, L. Rybach and L. Stegena, Dordrecht: Kluwer Academic Publishers, p.486.
100. Rosenbaum, M. J., (1997) "Gaseous, liquid, and supercritical fluid H<sub>2</sub>O and CO<sub>2</sub>: Oxygen isotope fractionation behavior". *Geochimica et Cosmochimica Acta*, Vol. 61, No. 23, pp. 4993-5003, 1997.
101. Rai, S.P., Purushothaman, P., Kumar, B., Jacob, N., Rawat, Y.S., (2014). "Stable isotopic composition of precipitation in the River Bhagirathi Basin and identification of source vapor". *Environmental earth sciences*, 71(11), pp.4835-4847.
102. Rayleigh, L., (1902) "On the distillation of binary mixtures" *Phil. Mag.*, S.6, v 4, 521-537.



103. Rozanski, K., Araguas, A. L., and Gonfiantini, R., (1992). "Relation-between long-term trends of oxygen-18 isotope composition of precipitation and climate". *Science* 258, 981 -985.
104. Severinghaus, J.P., Bender, M.L., Keeling, R.F., Broecker, W.S. (1996) Fractionation of soil gases by diffusion of watervapor, gravitational settling, and thermal diffusion. *Geochimica et Cosmochimica Acta* 60, 1005-1018.
105. Sonntag, C., Klitsch, E., Lohnert, E. P., Muennich, K. O., Junghans, C., Thorweihe, U., Weistroffer, K., Swailem, F. M., (1978). "Paleoclimate information from D and 18O in 14C-dated North Saharian groundwaters; groundwater formation from the past". *Isotope Hydrology*, IAEA, Vienna, pp. 569–580.
106. Souchez, R., Jouzel J., Lorrain R., Sleewaegen S., Stie´venard M., Verbeke V., (2000)" A kinetic isotope effect during ice formation by water freezing." *Geophys. Res. Lett.* 27, 1923–1926.
107. Sharp, Z. D., (1995) "Oxygen isotope geochemistry of the Al<sub>2</sub>SiO<sub>5</sub> polymorphs". *Am J Sci* 295: 1058–1076.
108. Sengupta, S. M., (2013) "Introduction to sedimentology". 2nd Edition. CBS Publishers & Distributors Pvt. Ltd. ISBN: 81-239-1491-1.
109. Sharp, Z., (2007) "Principles of Stable Isotope Geochemistry". Pearson Prentice Hall Pearson Education, Inc. Upper Saddle River, NJ 07458. ISBN-13: 978-0-13-009139-0.

110. Shiklomanov, I. A., and Sokolov, A. A., (1983) "Methodological basis of world water balance investigation and computation. In New Approaches in Water Computations". International Association for Hydrological Sciences Publ. No. 148. (Proceedings of the Hamburg Symposium).
111. Sofer, Z., Gat, J.R., (1972) "Activities and concentrations of oxygen-18 in concentrated aqueous salt solutions. Analytical and geophysical implications". Earth Planet. Sci. Lett. 15, 232.
112. Sofer, Z., Gat, J.R., (1975) "The isotope composition of evaporating brines: Effect on the isotopic activity ratio in saline solutions". Earth Planet. Sci. Lett. 26, 179
113. Stewart, M.K., Fiedman, I., (1975) "Deuterium fractionation between aqueous salt solutions and water vapour". J. Geophys. Res. 80, 3812.
114. Sibbitt, W L., Dodson, J. G., Tester, J. W., (1979) "Thermal conductivity of crystalline rocks associated with energy extraction from hot dry rock geothermal systems". J. Geophys. Res., 84, 1117-1124, 1979.
115. Schatz, J. F., Simmons, G., (1972) "Thermal conductivity of Earth materials at high temperatures". J, Geophys Res., 77, 6966-6983.
116. Sharp, K. A., (2001) "Encyclopedia of Life Sciences", John Wiley & Sons, Ltd. [www.els.net](http://www.els.net).
117. Taylor, H. P. Jr., (1977) "Water/rock interactions and the origin of H<sub>2</sub>O granitic batholiths". J. Geol. Soc. London, 133, 509-558.

118. Turner, J. F., Verhoogen, J., (2004) "Igneous and Metamorphic Petrology."  
Second Edition. CBS Publishers & Distributors. New Delhi. India.  
ISBN: 81-239-1100-3.
119. Urey, H. C., Lowenstam, H. A., Epstein, S., McKinney, C. R., (1951)  
"Measurement of paleotemperatures and temperatures of the  
Upper Cretaceous of England, Denmark, and Southeastern United  
States". Bull. Geol. Soc. Am. 62, 399-416.
120. Urey, H. C., (1947) "The thermodynamic properties of isotopic substances".  
J. Chem. Soc. (London), 562-581.
121. Wood, J. R., Hewett, T.A., (1982) "Fluid convection and mass transfer in  
porous sandstone-a theoretical model." *Geochimica et  
Cosmochimica acta*. Vol: 46. Issue: 10. p 1707-1713.
122. Werner, R. A., Brand, W. A., (2001) "Referencing strategies and techniques  
in stable isotope ratio analysis". *Rapid communications in mass-  
spectrometry*. Vol: 15. pp. 501-519. DOI: 10.1002 rcm.258
123. Yeh, H. M., Yang, S. C., (1984) "The Enrichment of Heavy Water in a Batch-  
Type Thermal Diffusion Column," *Chem. Eng. Sci.*, Vol. 39, p.  
1277.
124. Yeh, H. M., (2009) "Separation of Heavy Water from Water-Isotopes Mixture  
in Flat-Plate Thermal Diffusion Columns with Transverse  
Sampling Streams and Optimal Plate Spacing". *Tamkang Journal  
of Science and Engineering*, Vol. 12, No. 2, pp. 129-134.

125. Zheng, Y. F., (2011) “On the theoretical calculations of oxygen isotope fractionation factors for carbonate-water systems”. *Geochemical Journal*, Vol. 45, pp. 341 to 354, 2011.
126. Zhang, C. L., Horita, J., Cole, D.R., Zhou, J., Derek, R., Lovle, D.R., Phelps. T.J., (2001) “Temperature-dependent oxygen and carbon isotope fractionations of biogenic siderite”. *Geochimica et Cosmochimica Acta*, Vol. 65, No. 14, pp. 2257–2271.
127. Zheng, Y. F., (1993) “Oxygen isotope fractionation in  $\text{SiO}_2$  and  $\text{Al}_2\text{SiO}_5$  polymorphs: effect of crystal structure”. *Eur J Miner* 5: 651–658.

## Appendices

### **A.1 Manual of Isotemp Freeware**

Isotemp is a freeware and is a courtesy of Mr. Somenath Ganguly who developed this freeware at the time of his PhD research. This freeware is developed in MS EXCEL [© Microsoft] that calculates absolute abundance of  $^{18}\text{O}$  in ppm from given mass spectrometer data having  $\delta\text{VSMOW}$  as standard for water sample analysis for a particular temperature. This freeware calculates  $^{18}\text{O}$  in ppm from mass spectrometer data [“experimentally derived”] as well as for the model [“model derived”] proposed by Mr. Somenath Ganguly in his research for a confined aquifer model where there is only temperature gradient exists and no physical phase change of the water involved. Remarkably, both the values of  $^{18}\text{O}$  in ppm for a particular temperature corresponds to very close to each other and within internationally acceptable standard deviation of VPDB standard that is  $\pm 2.1$  ppm. This unequivocally demonstrates the robustness of the temperature dependent stable isotope fractionation model for a confined aquifer system as proposed by Mr. Somenath Ganguly. To use this freeware user have to follow the following stapes.

1. Put the  $\delta\text{VSMOW}$  value in column “B”.
2. After putting the value to column “B”, it will automatically calculate its corresponding  $\delta\text{VPDB}$  value in column “D”.
3. Column “F” will report the absolute abundance of  $^{18}\text{O}$  in ppm, which will be corresponding to a particular experimental temperature [“experimentally derived”].
4. Now copy the value of column “F” and past it to column “K” by **past>past special>values**.

5. Column “O” will give the  $^{18}\text{O}$  value according to the model [“model derived”], which will correspond, to same temperature of “step 3”.

## A.2 Publication details

The research that has been documented in this thesis has been published in two separate manuscript with following reference;

1. Ganguly, S., Rai, S. K., Mittal, S., Bhan, U., Ahluwalia, R. S., (2019) “Estimation of groundwater temperature from  $^{18}\text{O}$  fractionation-a deterministic analytical model”. Groundwater for Sustainable Development. (Volume 9). 1000234. <https://doi.org/10.1016/j.gsd.2019.100234>.
2. Ganguly, S., Bhan, U., Rai, S. K., Mittal, S., Ahluwalia, R. S., Verma, A., (2019) “An experimental approach to estimate groundwater temperature from  $^{18}\text{O}$  fractionation”. Groundwater for Sustainable Development. (Volume 9). 100257. <https://doi.org/10.1016/j.gsd.2019.100257>.